BAY AREA AIR QUALITY MANAGEMENT DISTRICT
939 Ellis Street, San Francisco, CA 94109

Research and Modeling Section Publication No. 201101-008-TX

2015 Toxics Modeling to Support the Community Air Risk Evaluation (CARE) Program

January, 2011

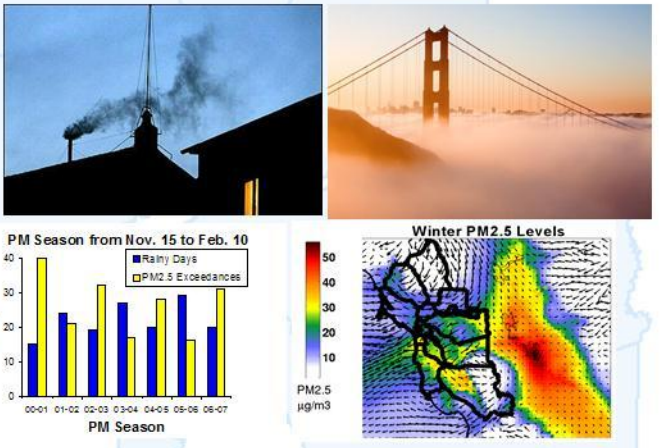

Prepared by:

Saffet Tanrikulu, Research and Modeling Manager
Phil Martien, Senior Advanced Project Advisor
Cuong Tran, Senior Atmospheric Modeler

Significant contributors:

Yiqin Jia, BAAQMD
Jeff Matsuoka, BAAQMD
Stephen B. Reid, Sonoma Technology, Inc.
James Cordova, BAAQMD
Amir Fanai, BAAQMD

Reviewed and approved by:

Henry Hilken, Director of Planning, Rules and Research Division

Executive Summary

Staff of the Bay Area Air Quality Management District (BAAQMD) previously conducted toxics modeling for 2005 and estimated health risks associated with exposure to outdoor toxic air contaminants (TAC) within the Bay Area in support of the Community Air Risk Evaluation (CARE) program. Results obtained from that effort were documented in a report by Tanrikulu et al., 2009. Recently, BAAQMD staff estimated TAC emissions for 2015, repeated the previous modeling effort with the new emissions estimates, and calculated the associated health risks.

This report presents the recent modeling effort, documents the estimated ambient levels of TAC for 2015 and the associated health risks, and discusses changes in emissions, ambient concentrations and health risks from 2005 to 2015.

As for the 2005 case, two sets of regional, grid-based, toxics simulations were performed using one square kilometer grid cells: 1) diesel particulate matter emissions (DPM) only and 2) reactive toxics species emissions.

The simulations with DPM only included emissions from all diesel sources in the Bay Area. Figure ES1 shows the distribution of simulated annual average DPM concentrations. The highest annual average DPM concentration was located over West Oakland (6-8 μg/m3), at the eastern end of the Bay Bridge, and along the Oakland Inner Harbor. Concentrations from 1-2 μg/m3 covered an area from Berkeley in the north to San Leandro in the south and from downtown San Francisco in the west to Piedmont in the east. This level was also estimated for a narrow strip next to Point Richmond. Concentrations from 0.6-1 μg/m3 covered an area from Richmond in the north to Hayward in the south and from San Francisco in the west to the East Bay Hills in the east. Downtown San Jose also had an annual average concentration of 0.6-1 μg/m3.

The full chemistry toxics simulation included many of the most important carcinogenic toxic air emissions in the Bay Area. Cancer risk from five toxics species (diesel PM, 1,3-butadiene, benzene, formaldehyde, and acetaldehyde) was calculated over the entire Bay Area. Other modeled carcinogenic toxic species were not included in this calculation because of their lower concentrations and smaller unit risk factors. The unit risk factors for the above species were 300, 170, 29, 6, and 2.7, respectively. They are expressed as expected excess cancer cases per million per μg/m3. These risk values assume a 70-year lifetime exposure (OEHHA, 2002).

Cancer risk for each species listed above was calculated by multiplying its respective annual average concentrations with the corresponding unit risk factor, and then the resulting values were summed across species. The results were expressed as the number of expected cancer incidents per million people and plotted in Figure ES2.

The Oakland Inner Harbor and West Oakland had grid cells with the highest cancer risks of around 2,000 per million. Emeryville and West Oakland both intersect grid cells with the second highest expected cancer risks of around 1,700 per million. There were several grid cells surrounding these regions and along the southbound I-880 corridor with cancer risks of around 1,400 in a million. Cancer risks in the range of 800 to 1100 per million were located over an area extending from Berkeley in the north to Alameda in the south and from downtown San Francisco in the west to Piedmont in the east. Expected risks in the range of 300-500 per million were found in downtown San Jose, around Point Richmond and at the San Francisco International Airport. Numbers ranging from 100 to 300 in a million covered an area from Vallejo in the north to San Jose in the south and from San Francisco in the west to the East Bay Hills in the east. Expected risks ranging from 100 to 300 in a million also covered Santa Rosa and Travis Air Force Base.

These cancer risks were used to estimate expected excess cancer cases from toxic air contaminants in 2015 Bay Area populations. This was done by multiplying the cancer risk in each grid cell by the actual population of that cell and dividing the result by one million. 2015 population estimates were developed by the Association of Bay Area Governments (ABAG). The expected excess cancer incidents, assuming a 70-year lifetime exposure, are shown in Figure ES3.

The spatial distribution of the population-adjusted expected incidences was similar to that of the cancer risk estimates (per million people). However, some shift in the distribution was evident, reflecting the Bay Area population densities. The highest population-adjusted incidence was around 15, occurring over a grid cell in downtown San Francisco. The second highest numbers of around 8 to 12 was also in downtown San Francisco, extending toward Civic Center. Population-adjusted expected incidences between 4 and 8 were found in east Oakland, along the I-880 corridor, and west and south of the San Francisco Civic Center. Expected incidences around 1-4 were found in much of Berkeley, Emeryville, Oakland, Alameda, San Francisco and San Jose. Incidences around 1 were found in Richmond and a number of isolated grid cells especially in the South Bay and along the I-880 corridor.

The estimated change in cancer risk between 2005 and 2015 from reductions in toxic air contaminants is shown in Figure ES4. Negative values indicate declining risks from 2005 to 2015. The largest reduction in cancer risk was found in downtown San Francisco (1900 per million). Reductions ranged from 600 to 900 per million over Emeryville, downtown Oakland and downtown San Francisco. Reductions between 300 and 600 per million were found over an area stretching from Berkeley in the north to Alameda to the south and downtown San Francisco in the west to Piedmont in the east. This level of reduction in cancer risk was also found along the I-880 corridor and over San Jose. Risk reductions on the order of 150 to 300 were found in an area from Richmond in the north to San Jose in the south and from San Francisco in the west to the Eastbay Hills in the east and along the I-580 corridor. There was a small increase in cancer risk of about 30 per million at the San Francisco International Airport from increased activity and emissions there.

Figure ES5 shows the estimated changes in the expected number of cancer cases based on reductions in toxic air contaminants and changes in population between 2005 and 2015. The largest reductions, between 10 to 25 cases per square kilometer (or cases per grid cell), were observed in downtown San Francisco. Reductions of 5 to 10 per grid cell were also found in San Francisco and downtown Oakland. Reductions of 1 to 5 cases per grid cell were found in Richmond, Berkeley, Emeryville, Oakland, eastern San Francisco and Alameda, along the I-880 corridor, and San Jose. There were small increases (1-3 per grid cell) along the Oakland Inner Harbor (near Jack London Square) and in two cells in eastern San Francisco. Note that these increases in the number of cancer incidents occurred despite the decrease in cancer risks in these areas. This is because the growth in population projected in these cells outpaces the reductions in emissions and risk.

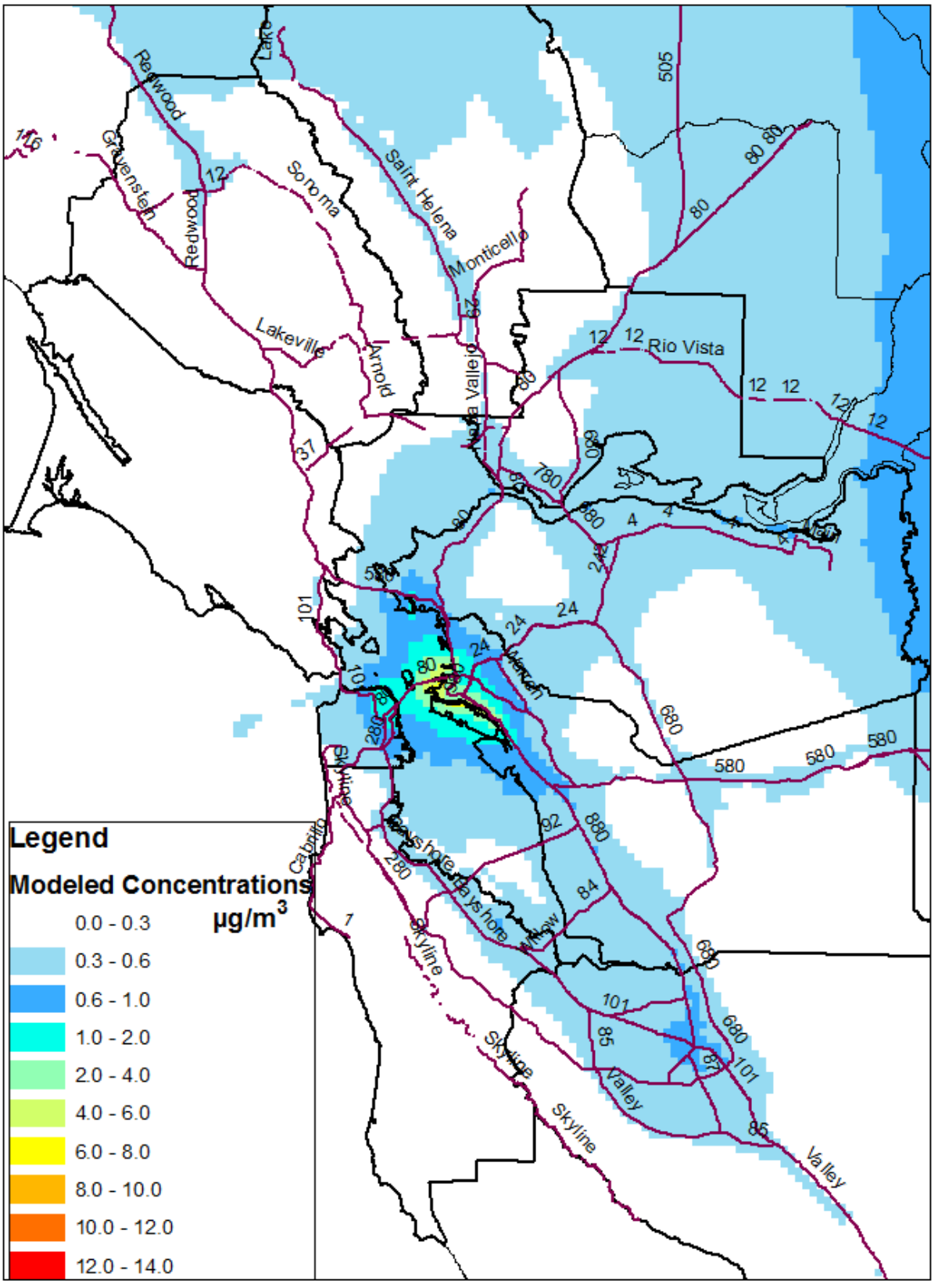

Figure ES1: Estimated annual average diesel PM concentrations in 2015.

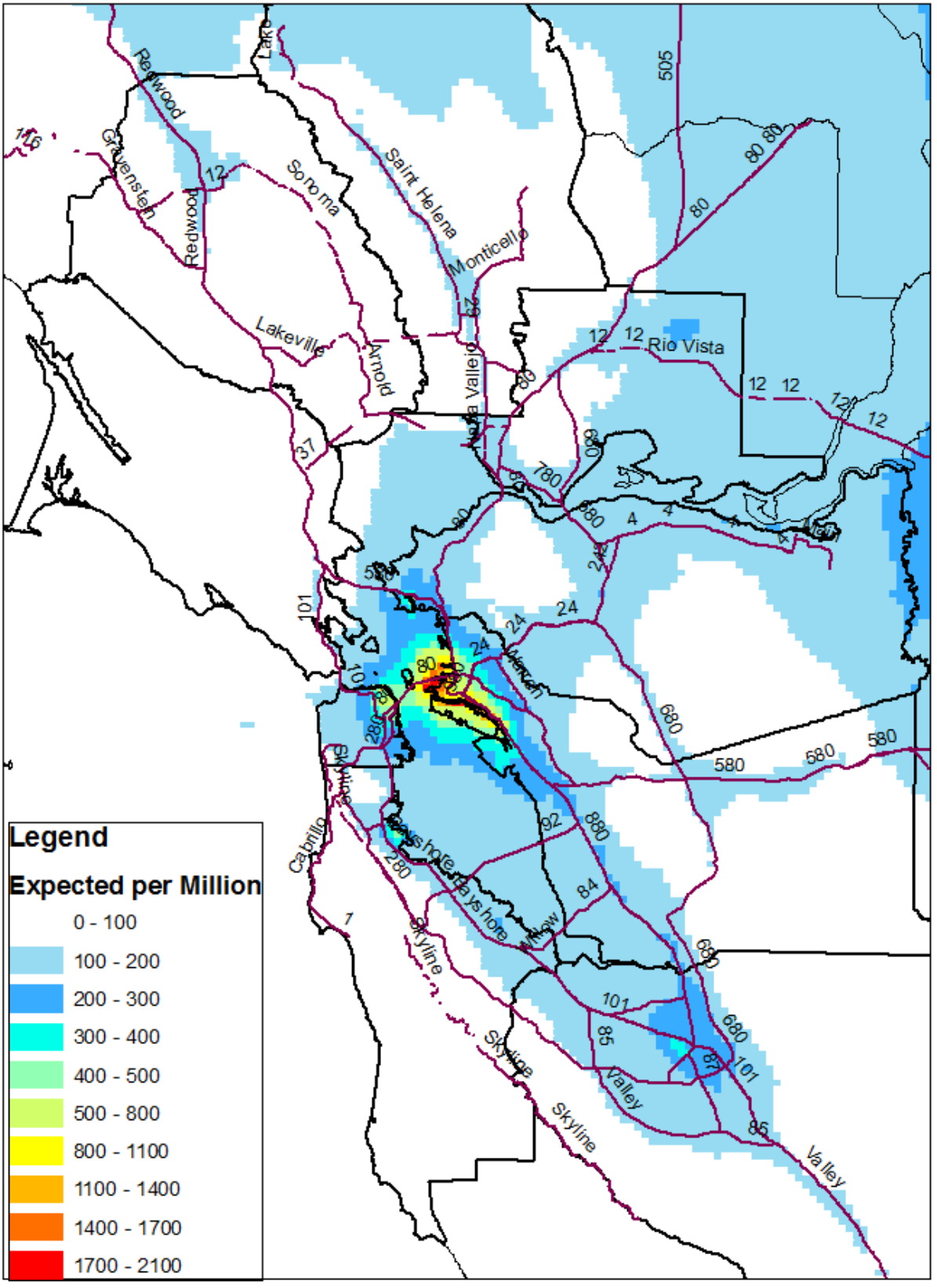

Figure ES2**:** Estimated cancer risk (number per million) in 2015 from toxic air contaminants. These risks are over an assumed 70-year lifetime of exposure.

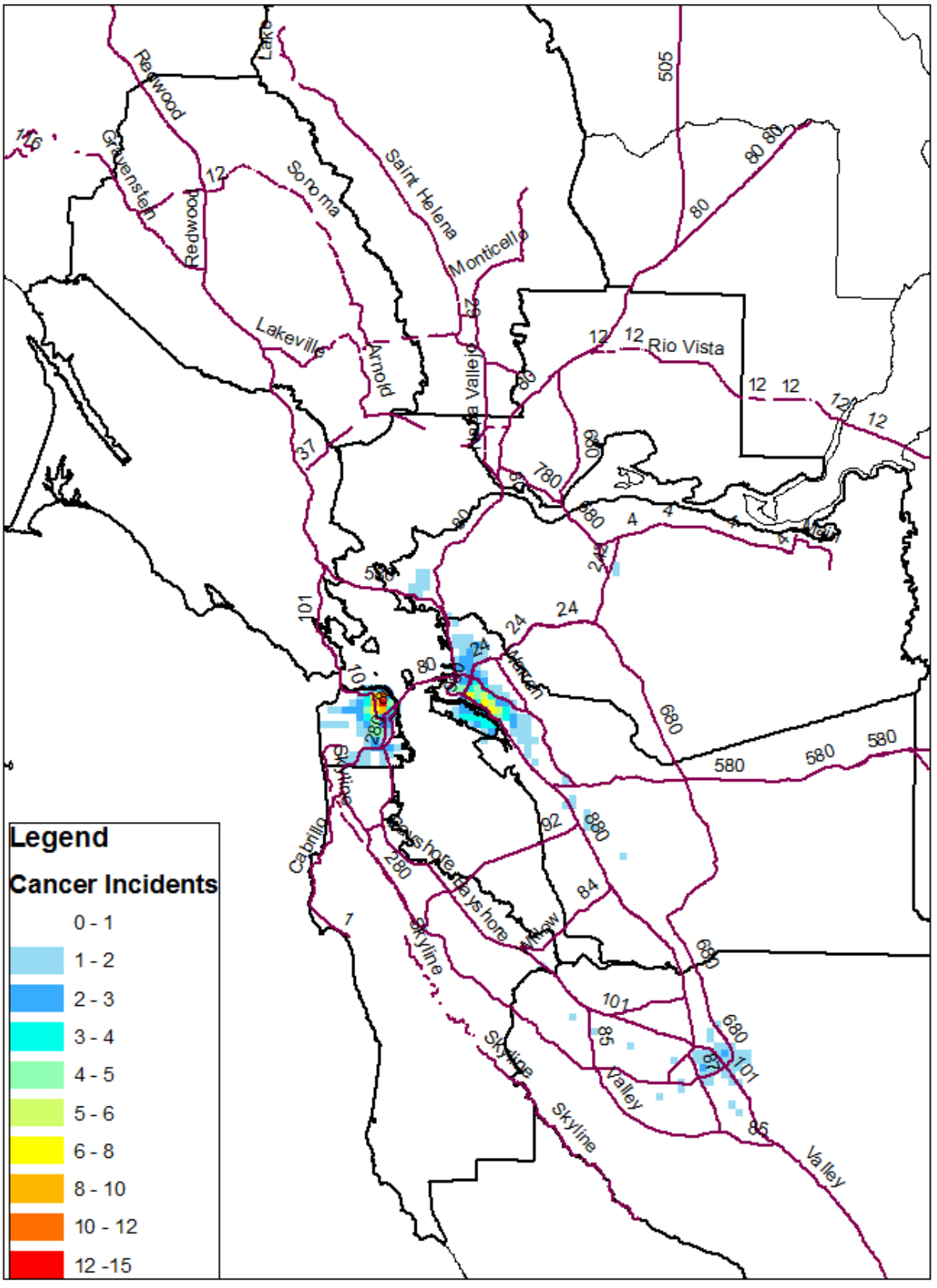

Figure ES3: Estimated number of Bay Area cancer incidents for concentration and population levels in 2015 from modeled toxic air contaminants.

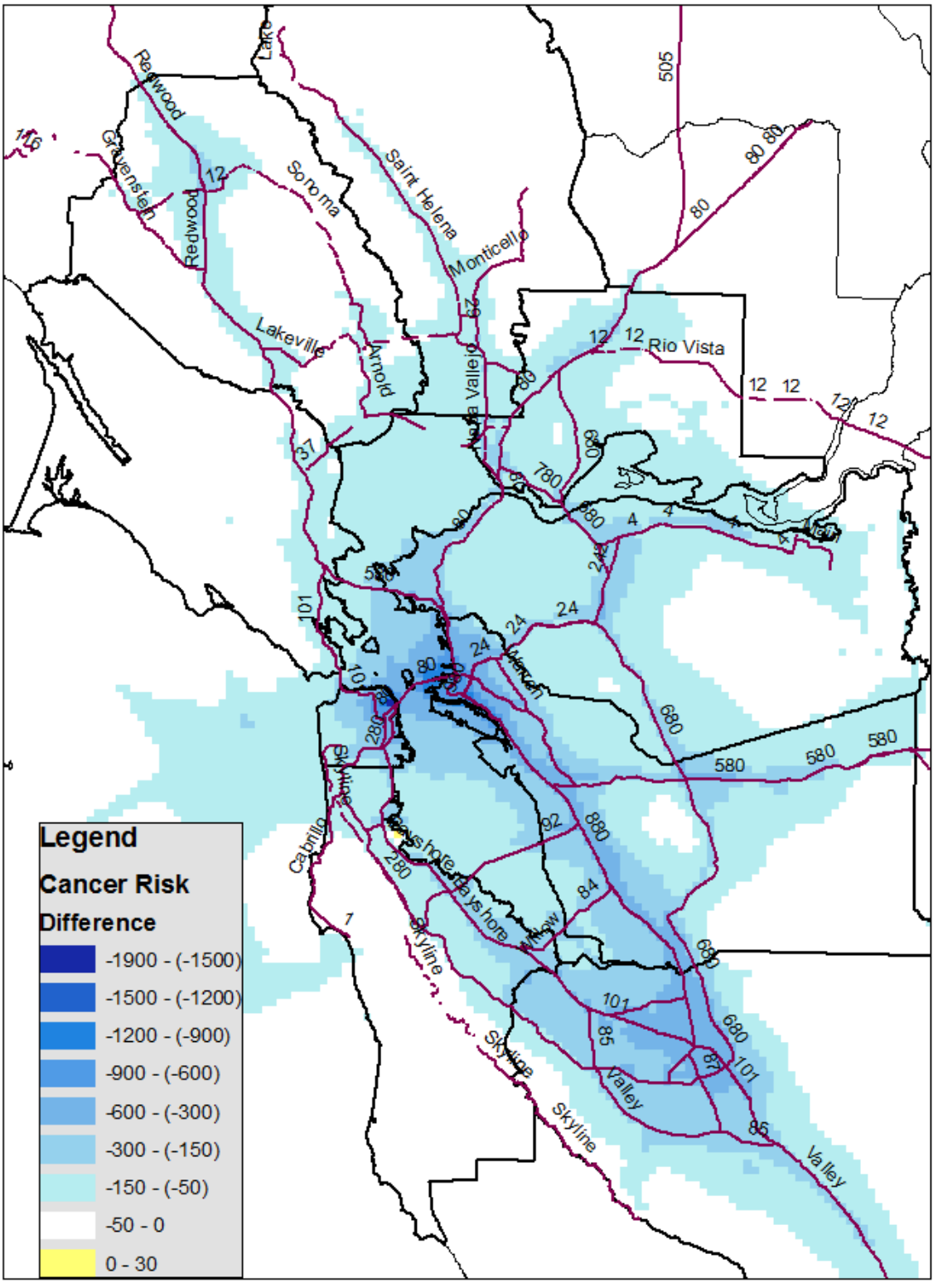

Figure ES4: Estimated change in cancer risk (number per million) between 2005 and 2015 from changes in toxic air contaminants.

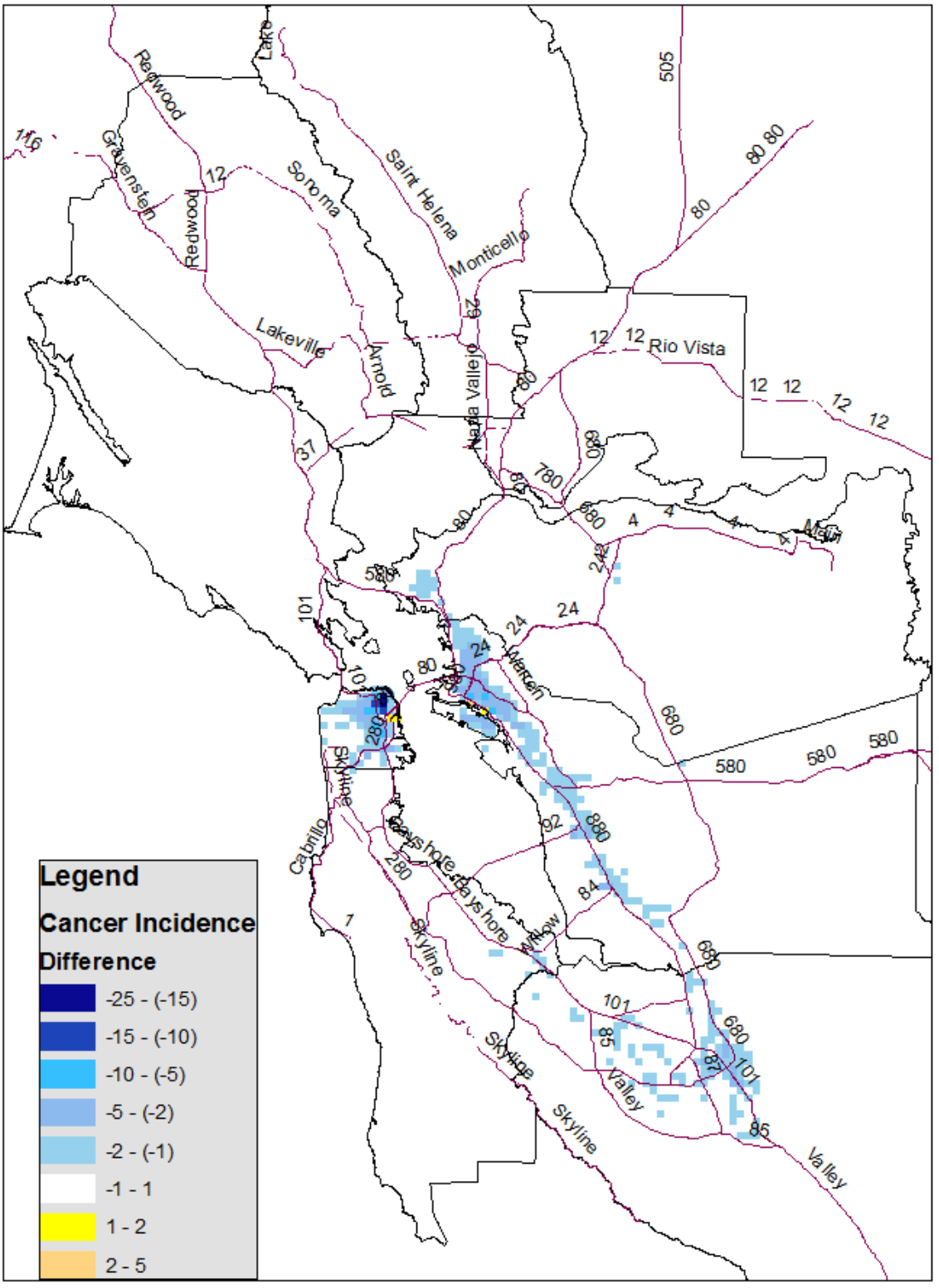

Figure ES5: Estimated change in Bay Area cancer incidents between 2005 and 2015. Differences reflect both changes in modeled concentrations of toxic air contaminants and changes in population.

2015 Toxics Modeling to Support the Community Air Risk Evaluation (CARE) Program

1. Introduction

This report presents technical details of 2015 toxics modeling conducted by staff of the Bay Area Air Quality Management District (BAAQMD) in support of the Community Air Risk Evaluation (CARE) program. Previously, BAAQMD staff conducted toxics modeling for 2005, also in support of the CARE program. Results obtained from the earlier effort along with model description, emissions inventory preparation, and ambient Toxic Air Contaminant (TAC) levels and the associated health risks were given in Tanrikulu et al., 2009. The only difference in inputs between the 2005 and 2015 simulations is the emissions inputs. All other model parameters did not change.

The rest of the report summarizes the emissions inventory preparation, modeling, and health risk evaluation for 2015. Additional information on emissions, and comparison of the 2015 and 2005 emissions, concentrations, and the expected cancer incidents are given in Appendices A-D, respectively.

2. Emissions Inventory Preparation

Emissions estimates of toxic pollutants and ozone precursors were prepared as inputs to the Comprehensive Air Quality Model with Extensions (CAMx). To ensure timely availability of the input files, the District obtained assistance from Sonoma Technology, Inc. (STI). STI processed the 2015 CARE emissions inventory (STI, 2010) for use in the U.S. EPA's Sparse Matrix Operator Kernel Emissions (SMOKE) computer program. SMOKE was then used by District staff to generate the CAMx inputs.

The 2015 toxics emissions database was supplemented with emissions of TOG and the criteria pollutants NOx, CO, SO_2, and PM_{10} to create a model-ready inventory. The addition of TOG and NOx emissions, in particular, was needed because they participate in photochemistry affecting the organic toxics' concentrations. Emissions from biogenic sources were prepared using a method developed by the California Air Resources Board (ARB). In this model application, anthropogenic emissions were limited to Bay Area sources while biogenic emissions included the Bay Area and portions of the northern San Joaquin Valley and the Sacramento area to carry out chemical reactions beyond the District boundaries.

The area and non-road mobile source data in the CARE inventory were given as annual average daily totals by county. First, these emissions were reformatted for input to SMOKE. Then using SMOKE, they were distributed spatially, temporally, and chemically to 1-km grid cells, using surrogates provided by STI. Since CAMx modeling was performed for July and

December, two separate emissions inventories were prepared for these two months. SMOKE was further applied to adjust the annual average emissions for seasonal effects. To prepare the CAMx-ready on-road mobile source emissions inventory, emissions from these sources were first gridded and temporally allocated using the California Department of Transportation's (CalTrans) Direct Travel Impact Model (DTIM). The rest of the processing and adjustments were made using SMOKE.

The CAMx-ready stationary point source emissions included emissions from all permitted sources as well as necessary stack parameters (height, diameter, exit velocity, etc…) for CAMx to estimate plume rise for each source.

After the base-case emissions were prepared as described briefly above, adjustment factors were then applied to model the impacts of diesel regulations on 2015 diesel PM emissions. These factors were developed by STI and District staff using information provided by ARB and are further documented in STI, 2010. The resulting 2015 controlled emissions inventory and changes from year 2005 are summarized in Appendices A and B.

Overall, between 2005 and 2015 there is a projected 71% reduction in DPM, the largest source of cancer risk. The largest absolute reductions in DPM are due to area and non-road categories. On a percentage basis, however, on-road vehicles show the highest emission reductions. These projected reductions were achieved in advance of ARB's on-road heavy duty diesel vehicle (in-use) regulation. The regulation was initially considered in 2008 and requires fleets that operate in California to reduce diesel truck and bus emissions by retrofitting or replacing existing engines. Amendments were considered in December 2010 to provide more time for fleets to comply. The amended regulation would require installation of PM retrofits beginning January 1, 2012 and replacement of older trucks starting January 1, 2015. By January 1, 2023, nearly all vehicles would need to have 2010 model year engines or equivalent. The fact that heavy-duty vehicles, even without the new State on-road regulations, are expected to emit less PM in 2015 than 2005 is due to fleet turnover to cleaner engines.

3. Modeling

3.1 Meteorological Modeling

Four nested domains were used for meteorological modeling. The outer domain covered the entire western U.S. with a 36-km horizontal grid resolution to capture synoptic flow features and the impact of these features on local meteorology. The second domain covered California and portions of Nevada with a 12-km horizontal resolution to capture mesoscale flow features and their impact on local meteorology. The third domain covered the Bay Area, northern San Joaquin Valley, and the Sacramento area as well as portions of the Pacific Ocean using a 4-km resolution to capture local air flow features. The innermost domain, which was used for CAMx simulations, covered just the Bay Area and had a 1-km resolution with 152 grid cells in the east-west direction and 208 grid cells in the north-south direction.

All four domains employed 50 vertical layers whose thicknesses expanded with height from the surface to the top of the modeling domain (about 16 km). In MM5, meteorological variables are estimated at the middle of the layers. The thickness of the first layer near the surface was about 22 m; thus meteorological variables near the surface were estimated 11 m above the ground level in this application. The physics options selected in MM5 were similar to those used by the National Oceanic and Atmospheric Administration (NOAA) for the Central California Ozone Study (CCOS) simulations. These options were well tested and proven to be the best choices to characterize meteorology in the region. The simulated winds were nudged toward surface observations obtained from National Weather Service stations.

Simulation periods were July 12-18 and December 12-18, 2000. The resulting meteorological fields were compared against observations. In general, MM5 replicated the observed meteorology well. Year 2000 was selected because rich surface and upper air meteorological data were available from the Central California Ozone Study and the California Regional Particulate Air Quality Study. Meteorological model performance for these periods is documented in Tanrikulu et al., 2009.

3.2 Toxics Modeling

The toxics modeling domain was centered in the innermost meteorological modeling domain with 140x196 horizontal grid cells and a 1-km grid resolution. Following this approach, the meteorological fields from six grid cells along the edges of the meteorological modeling domain were not used in order to minimize the impact of boundary conditions with the 4-km modeling domain on toxics modeling. In aloft layers, some meteorological model layers were combined in preparing meteorological inputs to CAMx to reduce computational time. This is a common practice in air quality modeling as pollutant concentrations in aloft layers are relatively low and do not significantly impact concentrations at the surface. The resulting number of vertical layers in CAMx was 20, with layer thicknesses also expanded with height from the surface to the top of the modeling domain (about 16 km). The thickness of the first layer of CAMx was kept the same as MM5's (about 22 m), estimating pollutant concentrations at 11 m above the surface.

Some toxics species, like formaldehyde and acetaldehyde, can undergo chemical reactions in the atmosphere and form secondary pollutants in addition to their direct emissions. Atmospheric oxidants play an important role in secondary toxics formation. These oxidants are essentially the products of ozone chemistry; therefore, it was necessary to carry out ozone-chemistry simulations during the toxics simulations. The ozone chemistry used in CAMx was the Statewide Air Pollution Research Center version 99 chemical mechanism (SAPRC99). The initial and boundary conditions for carrying out the ozone part of the simulation were taken from the 2000 CCOS modeling.

As done for the 2005 case, two sets of toxics simulations were performed: 1) diesel particulate matter emissions only and 2) full toxics species emissions.

3.2.1 Diesel Particulate Matter Modeling

Particulate matter emissions from all diesel sources in the Bay Area were included in this simulation. The eastern and northern boundary conditions from the surface to 500 m were set to 1 μg/m3 and 0.5 μg/m3 of PM concentrations, respectively; these were average concentrations estimated from observations. Above 500 m, the boundary conditions were set to zero. The western and southern boundary conditions were set to zero from the surface to the top of the modeling domain. The initial conditions for interior model cells were also zero. With these specifications, the non-zero boundary conditions allowed pollutant penetration to the modeling domain when winds were from the east or from the north along the eastern or northern boundaries, respectively.

July 12-18 and December 12-18, 2015 were simulated. First, average diesel PM concentrations were calculated separately for the selected July and December periods. Then an annual average concentration was calculated as 96% of the average of these two periods. The 96% factor was determined by comparing July and December observed CO average concentrations to annual average CO concentrations for several past years, Tanrikulu et al., 2009.

Figures 1-3 show the distribution of simulated annual average DPM concentrations as well as average concentrations for the simulated July and December periods. The highest annual average concentration was located over West Oakland (6-8 μg/m3), at the eastern end of the Bay Bridge, and along the Oakland Inner Harbor (Figure 1). The second and third highest concentrations (4-6 and 2-4 μg/m3) were narrow bands surrounding the areas with the highest concentrations. Concentrations from 1 to 2 μg/m3 covered an area from Berkeley in the north to San Leandro in the south and from downtown San Francisco in the west to Piedmont in the east. A narrow strip in Richmond adjacent to Point Richmond was also estimated to experience 1 to 2 μg/m3 levels of DPM. Concentrations from 0.6 to 1 μg/m3 covered an area from Richmond in the north to Hayward in the south and from San Francisco in the west to the East Bay Hills in the east. Downtown San Jose also had an annual average concentration of 0.6-1 μg/m3.

One grid cell in Emeryville and several over West Oakland and along the Oakland Inner Harbor exhibited the highest summertime concentration of 2 to 4 μg/m3. Concentrations ranging from 1 to 2 μg/m3 covered Emeryville and Oakland. Concentrations mainly to the east and to the north of these areas were ranging from 0.6 to 1 μg/m3. Outside of these areas, concentrations were below 0.6 μg/m3.

The reason summertime concentrations are significantly lower than the annual average is that during the afternoon hours of summer days, a strong sea breeze develops and allows pollutants to mix in the atmosphere (Figure 2). During the summer, the simulated high ambient toxics concentrations are, in general, east of high emission areas because of predominant westerly winds. Airflow also splits over West Oakland, with one branch heading toward Berkeley and the other toward San Leandro.

Wintertime concentrations, however, were generally larger than the annual average concentrations over the core Bay Area, mostly due to the stagnant meteorological conditions (Figure 3). The maximum wintertime concentrations reached 10.6 μg/m3 in West Oakland. Concentrations were 6 to 10 μg/m3 over much of West Oakland, the Oakland Inner Harbor, Emeryville, and along the eastern span of the Bay Bridge. Concentrations decreased sharply along the edges of the maximum area. Concentrations were 1 to 2 μg/m3 over an area from Richmond in the north to Hayward in the south and from San Francisco in the west to Piedmont in the east. They were also 1 to 2 μg/m3 over downtown San Jose.

3.2.2 Full Chemistry Toxics Modeling

The full chemistry toxics simulations included toxic compounds that were identified as significant contributors to the risk-weighted emissions in the Bay Area. The initial and boundary conditions were set to a small number, but greater than zero to avoid potential numerical problems. The full chemistry runs were conducted for the same July 12-18 and December 12-18 periods as were modeled for the diesel PM only runs. The selected days were average summer and winter days from the meteorological perspective; however, December 2000 was, in general, an above average PM month. Additionally, PM concentrations in mid-December are generally higher than other winter periods. Therefore, the simulated toxics concentrations were expected to represent high end winter concentrations.

Figures 4-18 show the annual average as well as monthly average concentrations for the simulated July and December periods for five toxics species (formaldehyde, acetaldehyde, benzene, 1,3-butadiene, acrolein). Again, the annual average concentrations are assumed to be 0.96 times the average of the July and December periods' concentrations. In the figures, the total concentrations are shown for species having both primary and secondary components.

The highest annual average formaldehyde concentrations were located at San Francisco International Airport, ranging from 6 to 12 μg/m3 (Figure 4). Several grid cells around San Francisco International Airport, at Travis Air Force Base in Fairfield, and at downtown San Jose had concentrations from 4 to 6 μg/m3. Near these three locations and Oakland International Airport, concentrations from 3 to 4.0 μg/m3 were also present. Concentrations in downtown San Francisco, West Oakland, downtown Oakland, surrounding areas of Travis Air Force Base and several grid cells surrounding areas of downtown San Jose ranged from 2 to 3 μg/m3.

During the summer, the highest formaldehyde concentration of 6 μg/m3 was located at San Francisco International Airport (Figure 5). Travis Air Force Base, downtown San Jose, and surrounding areas of San Francisco International Airport had concentrations ranging from 2 to 4 μg/m3.

The distribution of wintertime formaldehyde concentrations is shown in Figure 6. The magnitude of wintertime concentrations was higher than the annual average concentrations. The winter average concentrations reached 16.5 μg/m3 at San Francisco International Airport. The maximum concentration reached 9 μg/m3 at Travis Air Force Base and San Jose International Airport, and 6 μg/m3 at Oakland International Airport. In West Oakland, downtown San Francisco, downtown Oakland, surrounding areas of downtown San Jose, San Francisco International Airport and Travis Air Force Base, concentrations were 2-4 μg/m3. Concentrations immediately outside of these areas dropped below 1.5 μg/m3 quickly.

The highest annual average acetaldehyde concentrations (3-3.5 μg/m3), shown in Figure 7, were located in downtown and West Oakland, and near San Francisco International Airport. In downtown San Francisco, over downtown San Jose, at Travis Air Force Base, within the area from Berkeley in the north to Alameda in the south and the Bay Bridge in the west to Piedmont in the east, concentrations ranged from 1 to 3 μg/m3. Concentrations ranged from 0.25 to 1 μg/m3 over most of the Bay and its surrounding areas as well as at Santa Rosa, Travis Air Force Base, and portions of the SR-4, SR-24, I-80, US-101, I-580 and I-680 corridors.

The highest summertime acetaldehyde concentrations (1 to 2 μg/m3) were located in downtown San Francisco, West Oakland, Emeryville, Oakland, downtown San Jose and San Francisco International Airport (Figure 8). Concentrations ranging from 0.5 to 1 μg/m3 were located in the area from Berkeley in the north to San Leandro in the south and from West Oakland to Piedmont. Similar concentrations were present at downtown San Jose and San Francisco, as well as at San Francisco International Airport and Travis Air Force Base. These regions were surrounded by concentrations around 0.25 to 0.5 μg/m3.

Acetaldehyde concentrations for winter (Figure 9) were between 4 and 9 μg/m3 at San Francisco International Airport, West Oakland and along the Oakland Inner Harbor. Concentrations ranging from 1.5 to 4 μg/m3 covered an area surrounding these regions as well as San Jose, Travis Air Force Base and downtown San Francisco. Concentrations ranging from 0.5 to 1.5 μg/m3 covered an area from Vallejo in the north to San Jose in the south and from San Francisco in the west to the East Bay Hills in the east. Concentrations up to 2 μg/m3 were found in Santa Rosa.

The simulated annual average as well as average summer and winter concentrations for benzene are shown in Figures 10-12, for 1,3-butadiene in Figures 13-15, and for acrolein in Figures 16-18.

4. Risk Evaluation

Cancer risk from five toxics species (diesel PM, 1,3-butadiene, benzene, formaldehyde, and acetaldehyde) was calculated for each grid cell over the entire modeling domain. Other modeled carcinogenic toxics species were not included in this calculation because of their

lower concentrations and smaller unit risk factors. The unit risk factors for the above species were 300, 170, 29, 6, and 2.7, respectively. They are expressed as expected excess cancer cases per million per $\mu g/m^3$. These risk values assume a 70-year lifetime exposure (OEHHA, 2002).

Cancer risk for each species above was calculated by multiplying its respective annual average concentrations with the corresponding unit risk factor, and then the resulting values were summed across species. The results were expressed as the number of expected cancer incidents per million people and plotted in Figure 19.

The Oakland Inner Harbor and West Oakland had grid cells with the highest cancer risks of around 2,000 per million. Emeryville and West Oakland both intersect grid cells with the second highest expected cancer risks of around 1,700 per million. There were several grid cells surrounding these regions and along the southbound I-880 corridor with cancer risks of around 1,400. Cancer risks in the range of 300 to 1100 per million were located over an area extending from Berkeley in the north to Alameda in the south and from downtown San Francisco in the west to Piedmont in the east. Risks in the range of 300 to 500 per million were found in downtown San Jose, around Point Richmond and at the San Francisco International Airport. Numbers ranging from 100 to 300 in a million covered an area from Vallejo in the north to San Jose in the south and from San Francisco in the west to the East Bay Hills in the east. Expected risks ranging from 100 to 300 in a million also covered Santa Rosa and Travis Air Force Base.

These cancer risks were used to estimate expected excess cancer cases from toxic air contaminants in Bay Area populations. This was done by multiplying the cancer risk in each grid cell by the estimated 2015 population of that cell and dividing the result by one million. Population data were obtained from the Association of Bay Area Governments (ABAG). The expected excess cancer incidents, assuming a 70-year lifetime exposure, are shown in Figure 20.

The spatial distribution of the population-adjusted expected incidences was similar to that of the cancer risk estimates (per million people). However, some shift in the distribution was evident, reflecting the Bay Area population densities. The highest population-adjusted incidence was around 12, occurring over a grid cell in downtown San Francisco. The next highest numbers, between 8 and 12, were also in downtown San Francisco, extending toward Civic Center. Population-adjusted expected incidences around 4-8 were found in east Oakland, along I-880 corridor, and west and south of the San Francisco Civic Center. Expected incidences around 1-4 were found in much of Oakland, Berkeley/Emeryville, the eastside of San Francisco and downtown San Jose. Incidences around 1 to 2 were found in Richmond and a number of isolated grid cells especially in the South Bay and along the I-880 corridor.

The population-adjusted cancer incidence numbers were also calculated using only “sensitive populations” defined as people over 63 and under 20. The resulting distribution of

expected number of incidents is displayed in Figure 21. The highest expected incident number was around 5, located over downtown San Francisco. One cell each in downtown Oakland and San Francisco showed a value between 3 and 4. A value of around 1 to 3 covered much of Oakland and several grid cells in downtown San Francisco.

5. Comparison of 2005 and 2015 Results

BAAQMD staff previously conducted toxics modeling for 2005, also in support of the CARE program. Results obtained from the previous effort along with model description, emissions inventory, and health risk evaluation are given in Tanrikulu et al., 2009. The only difference between the 2005 and 2015 simulations is the emissions inventory. All other model parameters did not change. Both meteorological and air quality model performance was evaluated for the 2005 case by comparing simulations against observations. Since observations are unavailable for the 2015 case, an air quality model performance evaluation is omitted in the current effort. Appendix C contains detailed discussions of the resulting differences in modeled concentrations and health risks. Since differences in health impacts stem both from changing TAC concentrations and population, the effects of changes in the latter alone are also examined.

The estimated change in cancer risk between 2005 and 2015 from reductions in toxic air contaminants is shown in Figure 22. Negative values indicate declining risks from 2005 to 2015. The largest reduction in cancer risk was found in downtown San Francisco (1900 per million). Reductions ranged from 600 to 900 per million over Emeryville, downtown Oakland and downtown San Francisco. Reductions between 300 and 600 per million were found over an area stretching from Berkeley in the north to Alameda to the south and downtown San Francisco in the west to Piedmont in the east. This level of reduction in cancer risk was also found along the I-880 corridor and over San Jose. Risk reductions on the order of 150 to 300 were found in an area from Richmond in the north to San Jose in the south and from San Francisco in the west to the Eastbay Hills in the east and along the I-580 corridor. There was a small increase in cancer risk of about 30 per million at the San Francisco International Airport from increased activity and emissions there.

Figure 23 shows the estimated changes in the expected number of cancer cases based on reductions in toxic air contaminants and changes in population between 2005 and 2015. The largest reductions, between 10 to 25 cases per square kilometer (or cases per grid cell), were observed in downtown San Francisco. Reductions of 5 to 10 per grid cell were also found in San Francisco and downtown Oakland. Reductions of 1 to 5 cases per grid cell were found in Richmond, Berkeley, Emeryville, Oakland, eastern San Francisco and Alameda, along the I-880 corridor, and San Jose. There were small increases (1-3 per grid cell) along the Oakland Inner Harbor (near Jack London Square) and in two cells in eastern San Francisco. It is interesting to note that these increases in the number of cancer incidents occurred despite the decrease in cancer risks in these areas. This is because the growth in population projected in these cells outpaces the reductions in emissions and risk.

6. Conclusion and Further Study

This report summarizes the District's modeling and analysis of toxic air contaminants (TAC) for 2015 with 1 km grid resolution. This effort is essentially a repeat of previous modeling and analysis work for 2005 with the 2015 emissions inventory. Simulations were conducted for a summer and a winter period, and annual average concentrations of five major toxics compounds (diesel particulate matter [diesel PM], benzene, 1,3-butadiene, formaldehyde, and acetaldehyde) were estimated and their combined cancer risk was calculated. These five compounds account for more than ninety percent of TACs in the Bay Area. Seasonal and annual concentrations of acrolein, a non-carcinogenic toxic compound, were also estimated.

Emissions and modeling results obtained for 2015 were compared against emissions and modeling results from 2005 and major changes from 2005 to 2015 were documented and discussed.

One of the important findings of this study was that, many areas of the Bay Area have a cancer risk level of between 100 and 300 per million, based on unit cancer risk factors from the Office of Environmental Health Hazard Assessment (OEHHA; OEHHA, 2002). Highest risk areas in the District have risk levels greater than 2000.

A second important finding is that, like risk-weighted TAC emissions, risks from TAC exposures are focused in several core urban areas of the region near major freeways, ports, and areas with high levels of construction.

In this work, as for all modeling studies, there was a trade-off between spatial resolution and the length of the simulations. In future work it would be useful to consider longer simulations, to include multiple weeks in a season and, perhaps, additional seasons to help refine the estimate of annual concentrations and estimated lifetime risks.

A major decline in diesel PM emissions and ambient TAC concentrations from 2005 to 2015 is evident. The ARB adopted several major rules in 2010 and plans to continue adopting new rules in 2011 to reduce emissions. The amount of emission reductions due to these new rules was unavailable from ARB when emissions for 2015 were prepared. As additional information becomes available from ARB, the 2015 inventory will be updated and the simulations will be repeated to determine the benefit of the new rules in the Bay Area.

7. References

(OEHHA, 2002). "Air Toxics Hot Spots Program Risk Assessment Guidelines, Part II, Technical Support Document for Describing Available Cancer Potency Factors," Office of Environmental Health Hazard Assessment. Available on-line at http://oehha.ca.gov/air/cancer_guide/TSD2.html. December 2002.

(STI, 2010). "Draft documentation of the preparation of future-year emissions inventories of toxic air contaminants for the San Francisco Bay Area," Memorandum prepared by

Sonoma Technology, Inc. for the Bay Area Air Quality Management District. STI-909034-3859. April, 2010.

(Tanrikulu et al., 2009). “Toxics Modeling to Support the Community Air Risk Evaluation (CARE) Program,” [Available from Bay Area Air Quality Management District]. June, 2009.

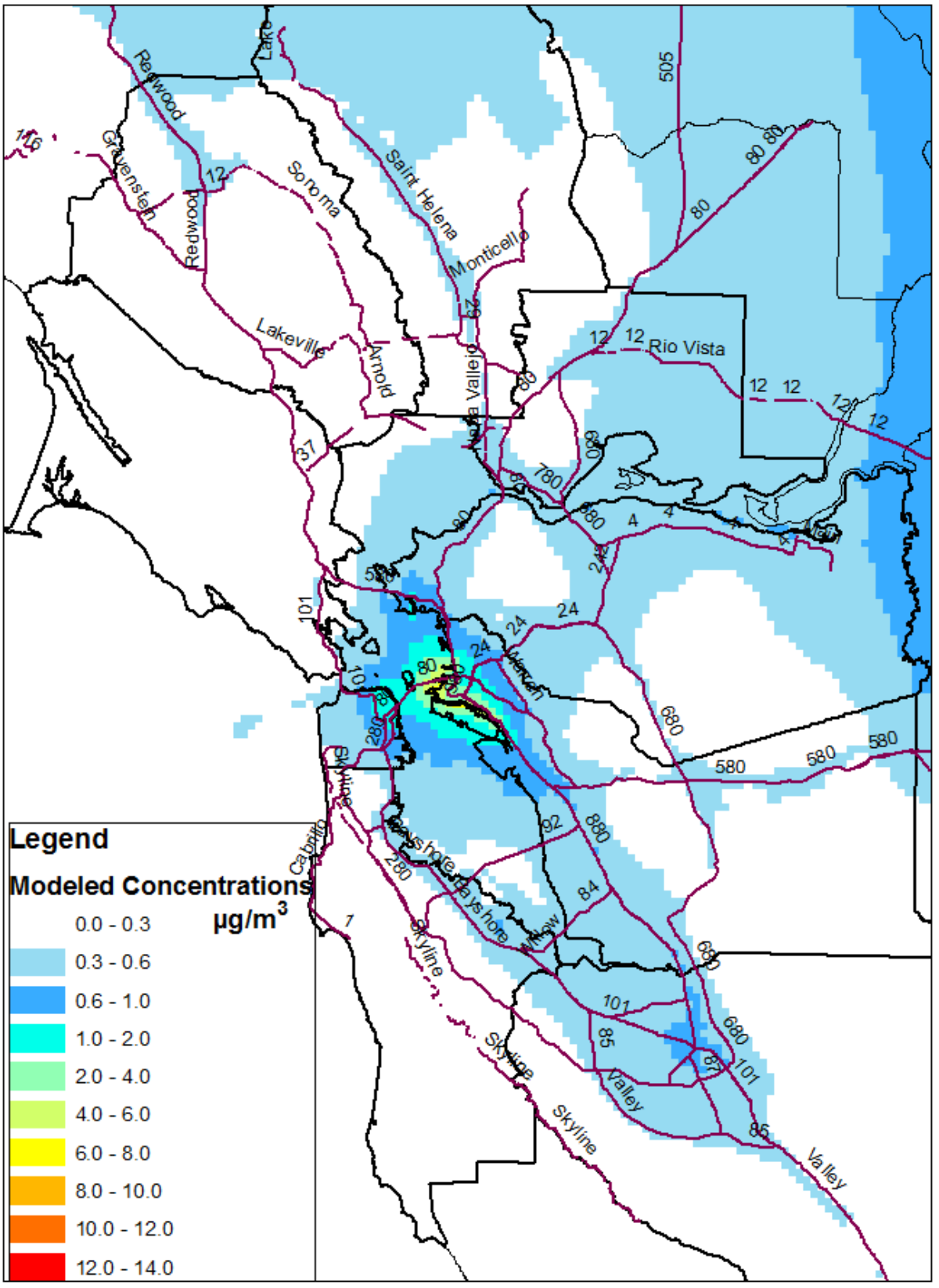

Figure 1: Annual average diesel PM concentrations, 2015.

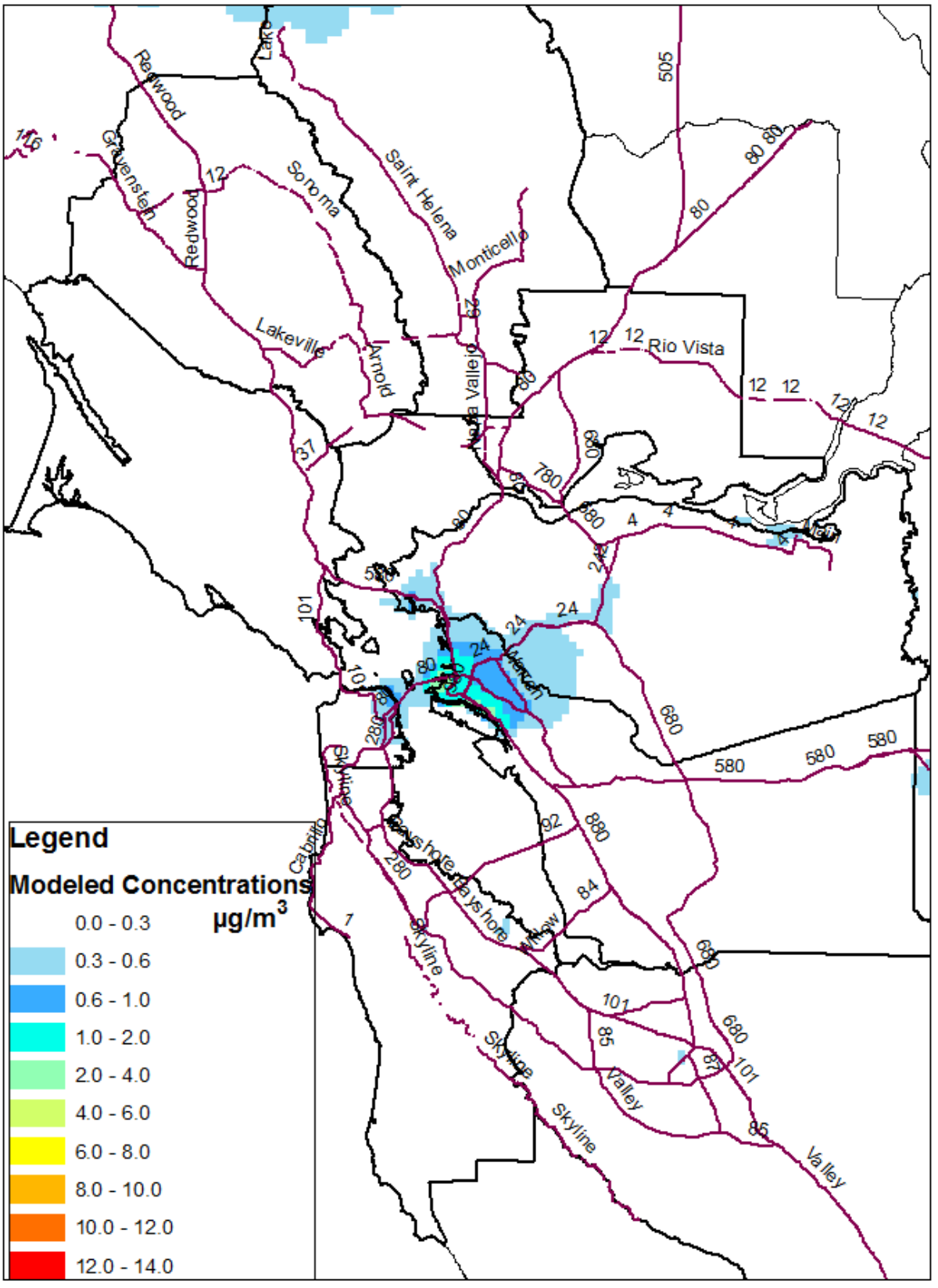

Figure 2: Diesel PM concentrations for July, 2015.

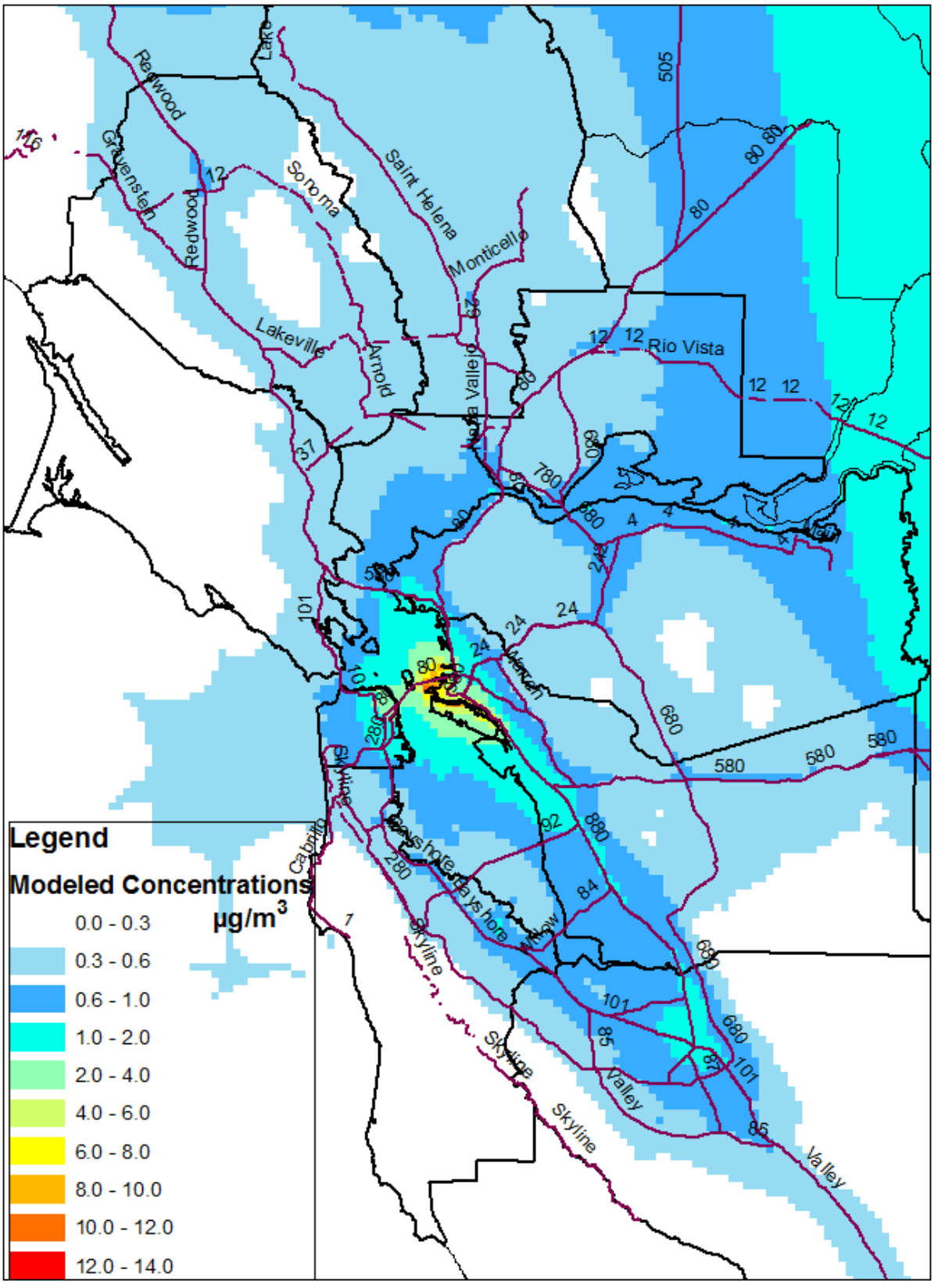

Figure 3: Diesel PM concentrations for December, 2015.

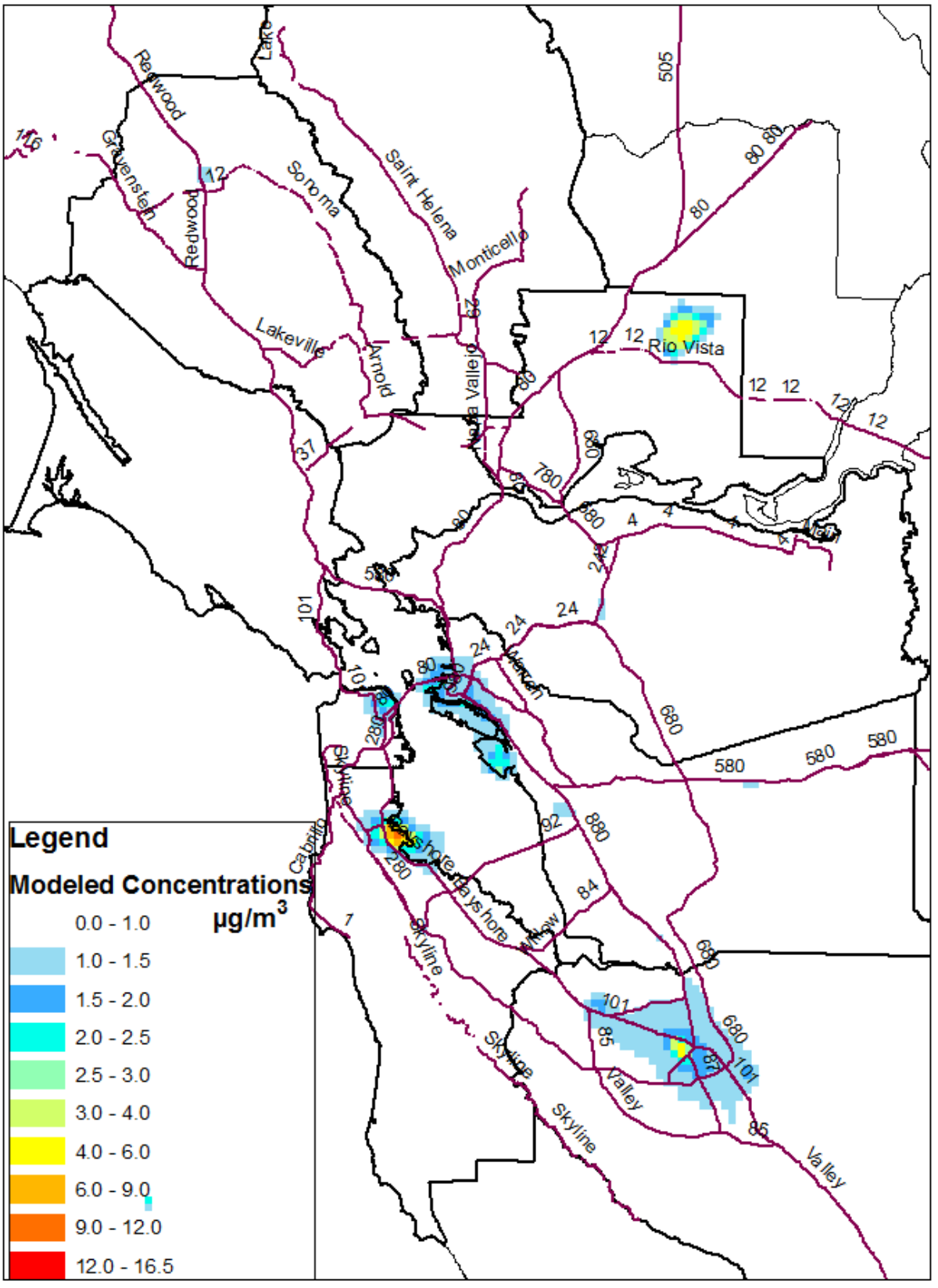

Figure 4: Annual average formaldehyde concentrations, 2015.

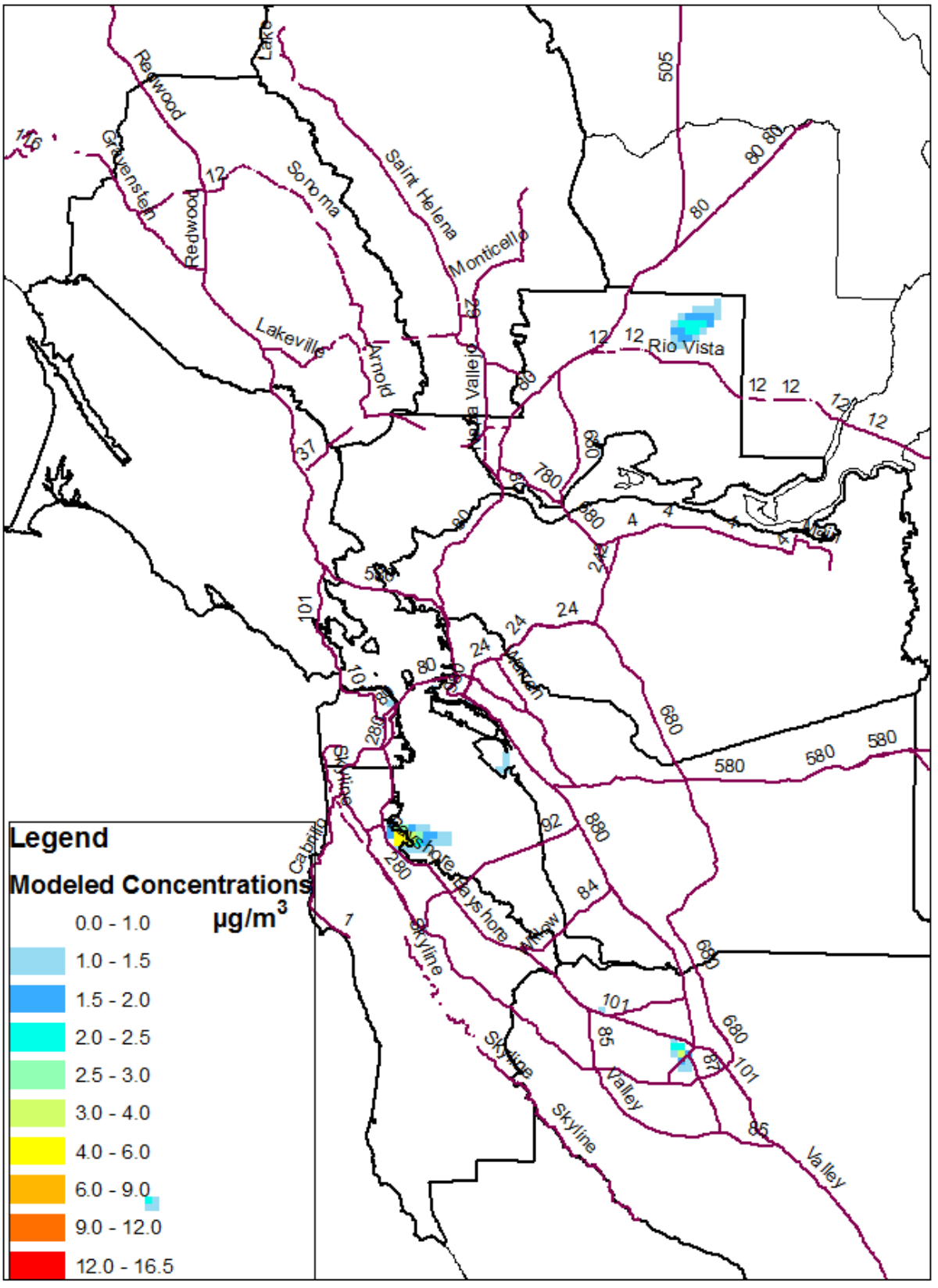

Figure 5: Formaldehyde concentrations for July, 2015.

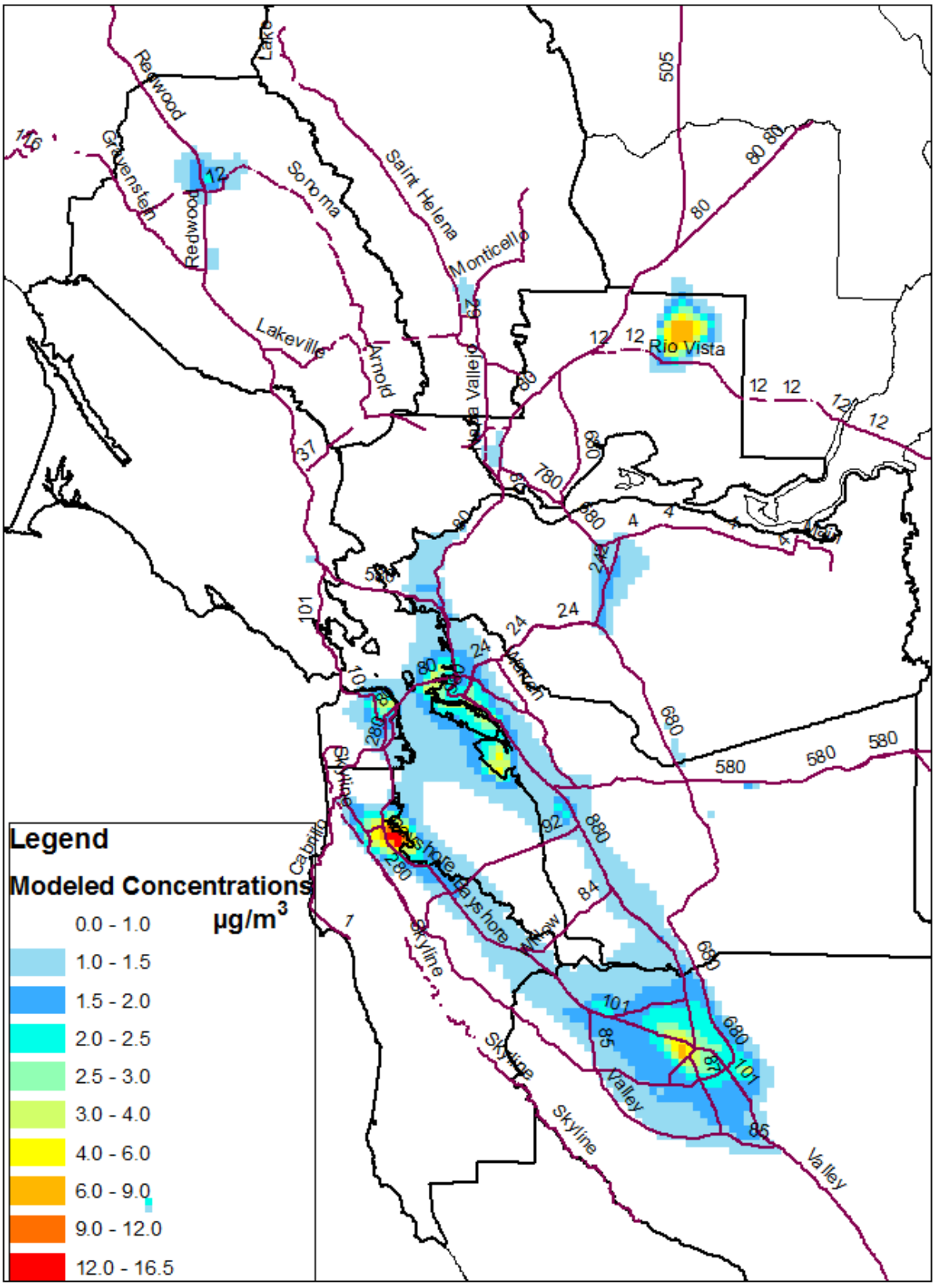

Figure 6: Formaldehyde concentrations for December. 2015.

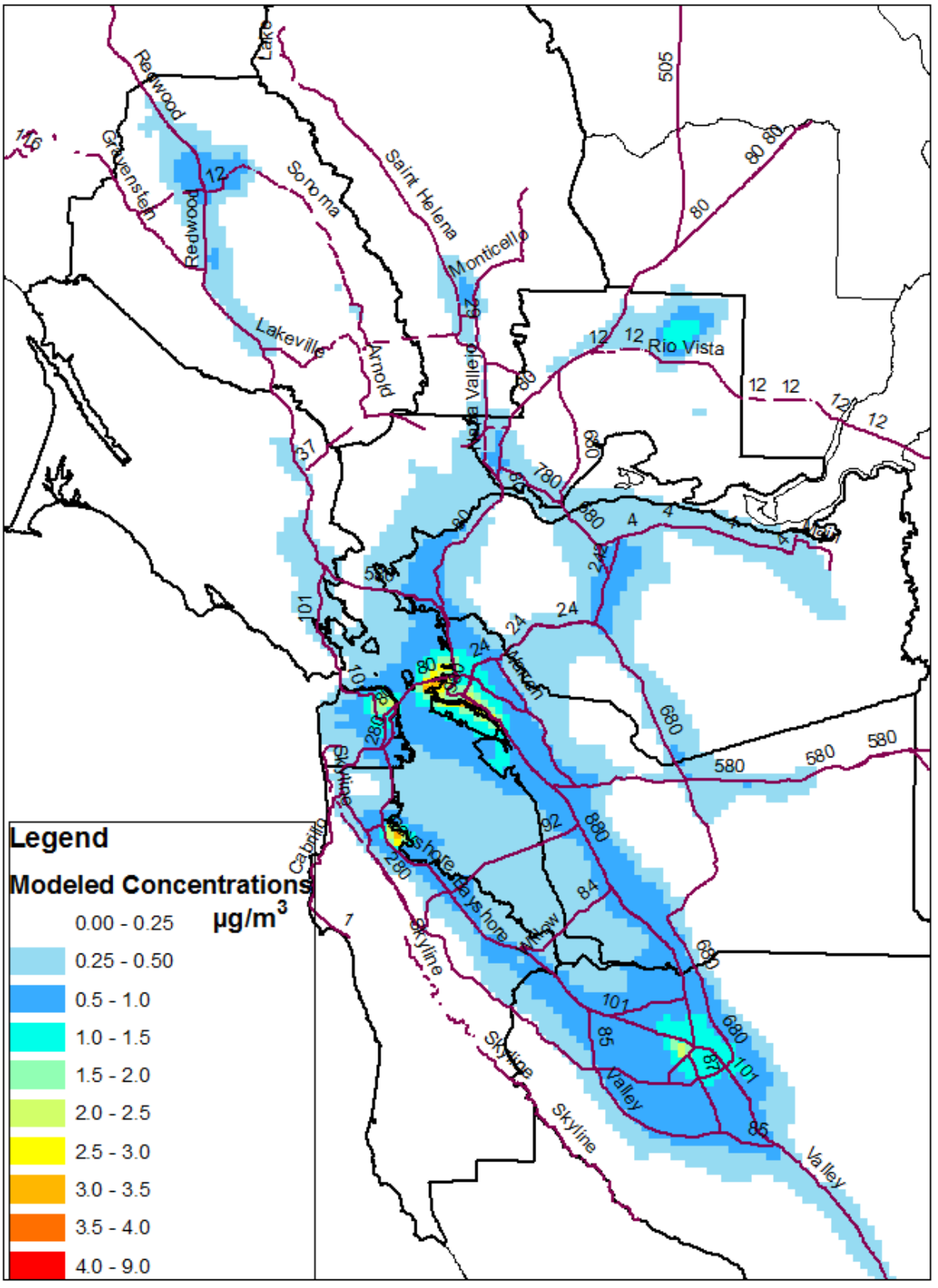

Figure 7: Annual average acetaldehyde concentrations, 2015.

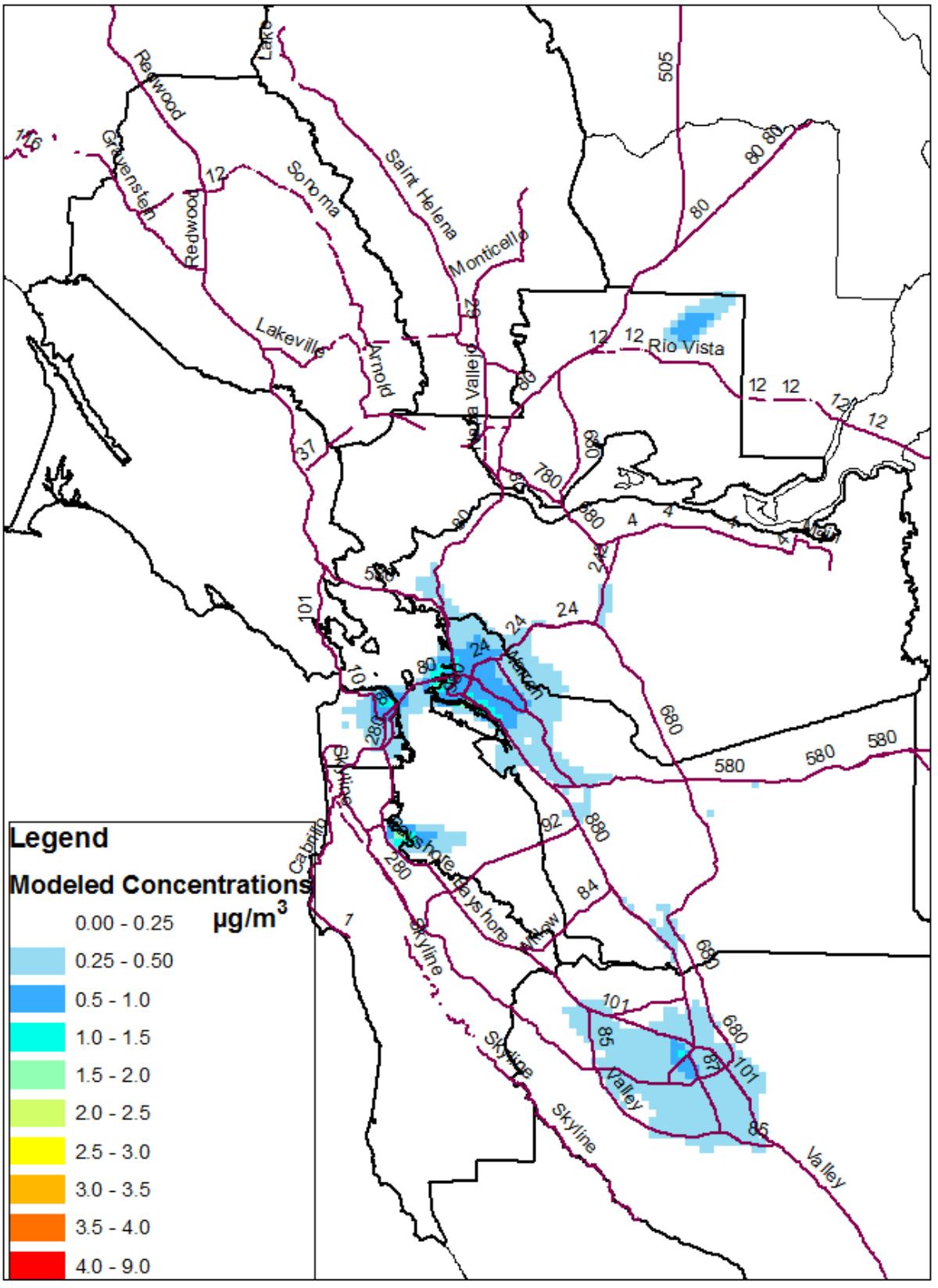

Figure 8: Acetaldehyde concentrations for July, 2015.

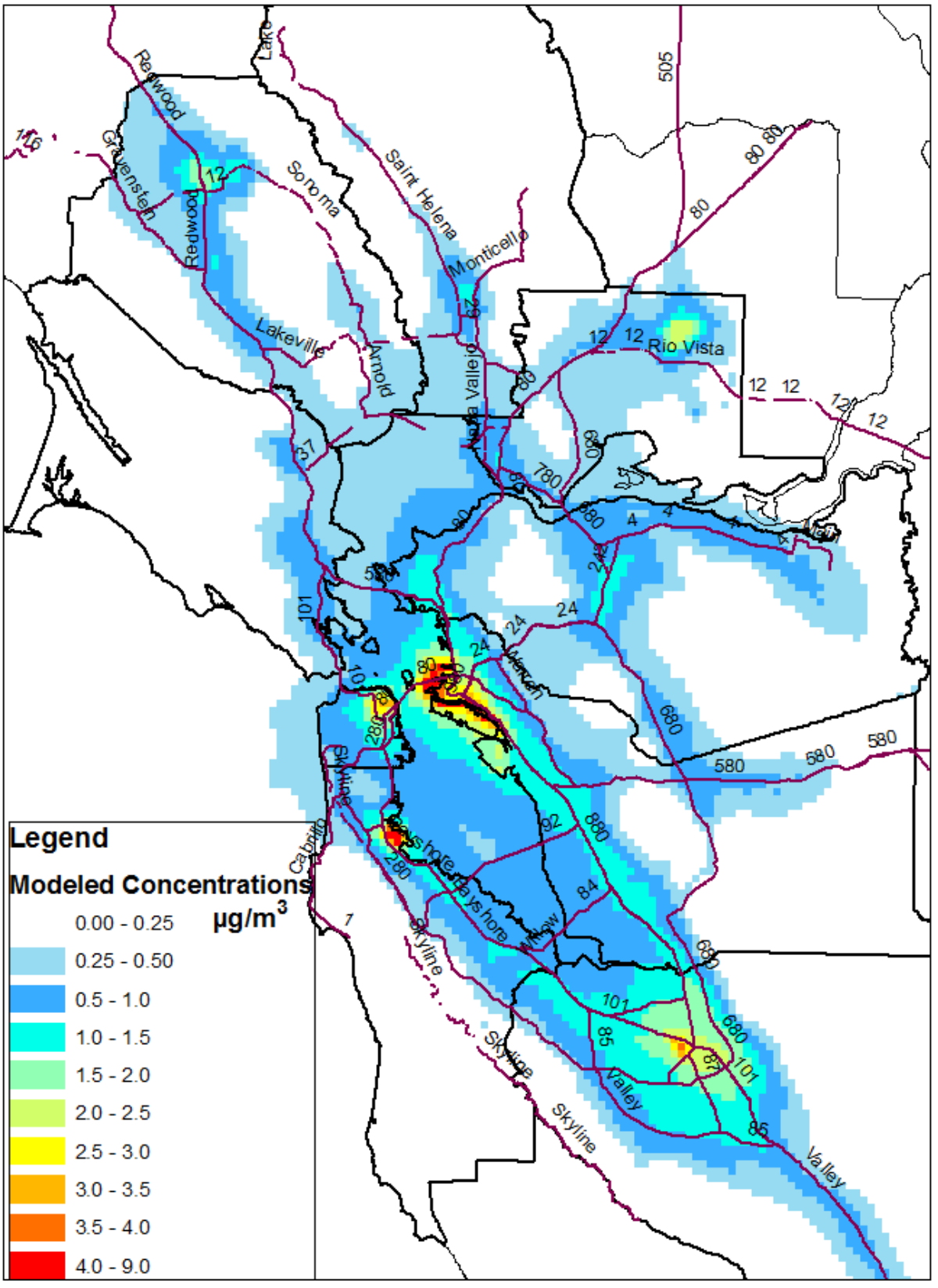

Figure 9: Acetaldehyde concentrations for December, 2015.

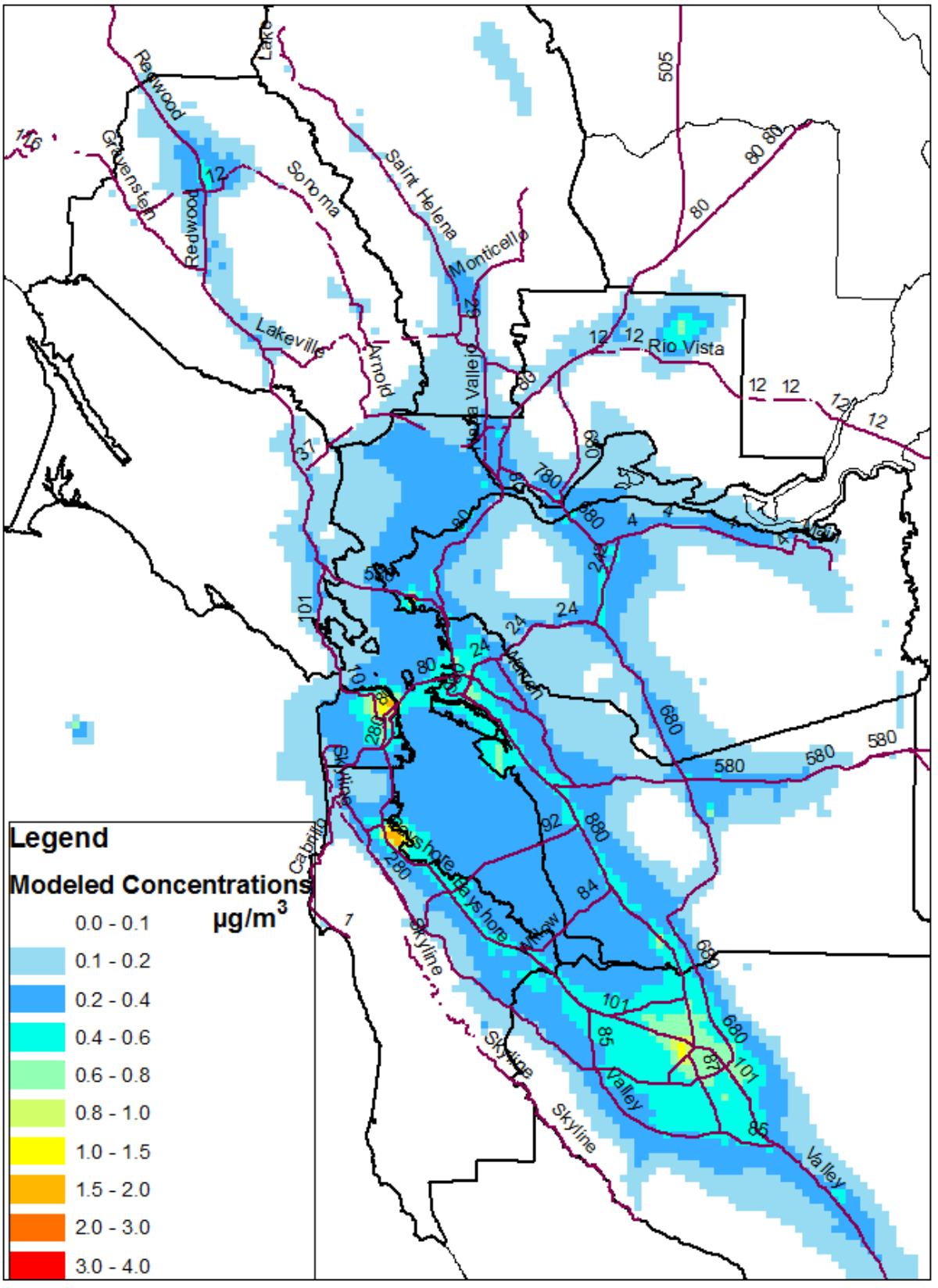

Figure 10: Annual average benzene concentrations, 2015.

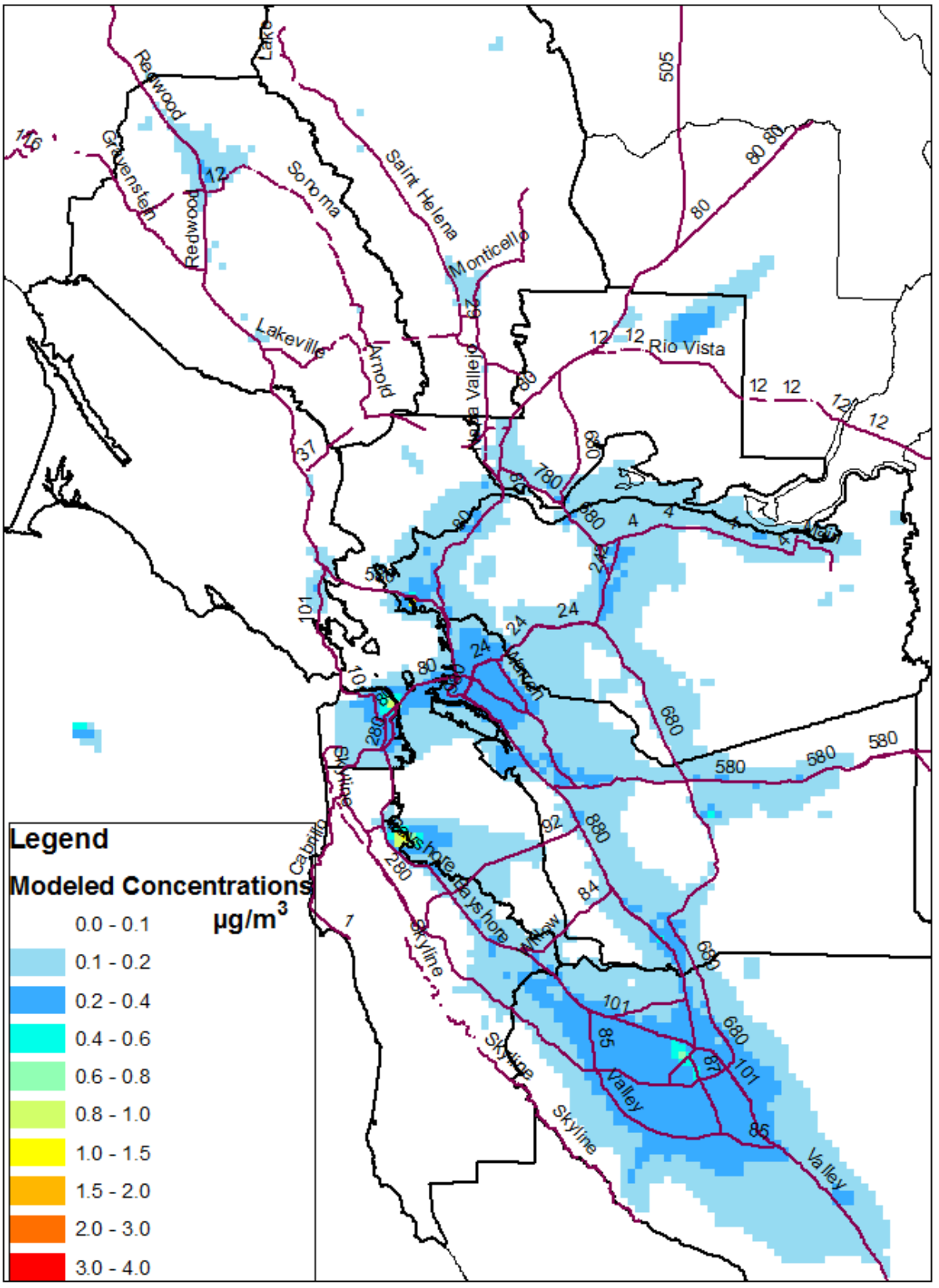

Figure 11: Benzene concentrations for July, 2015.

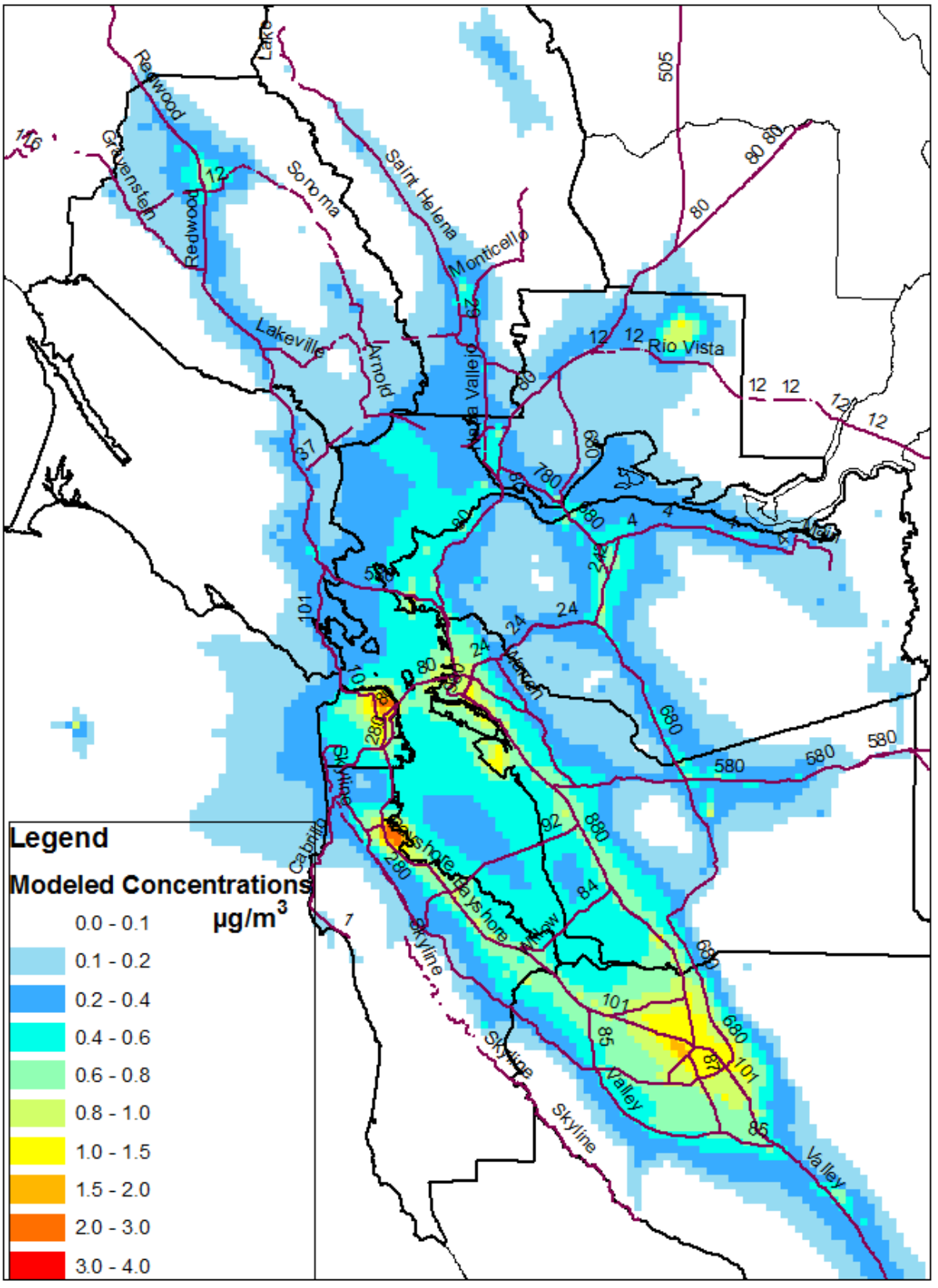

Figure 12: Benzene concentrations for December, 2015.

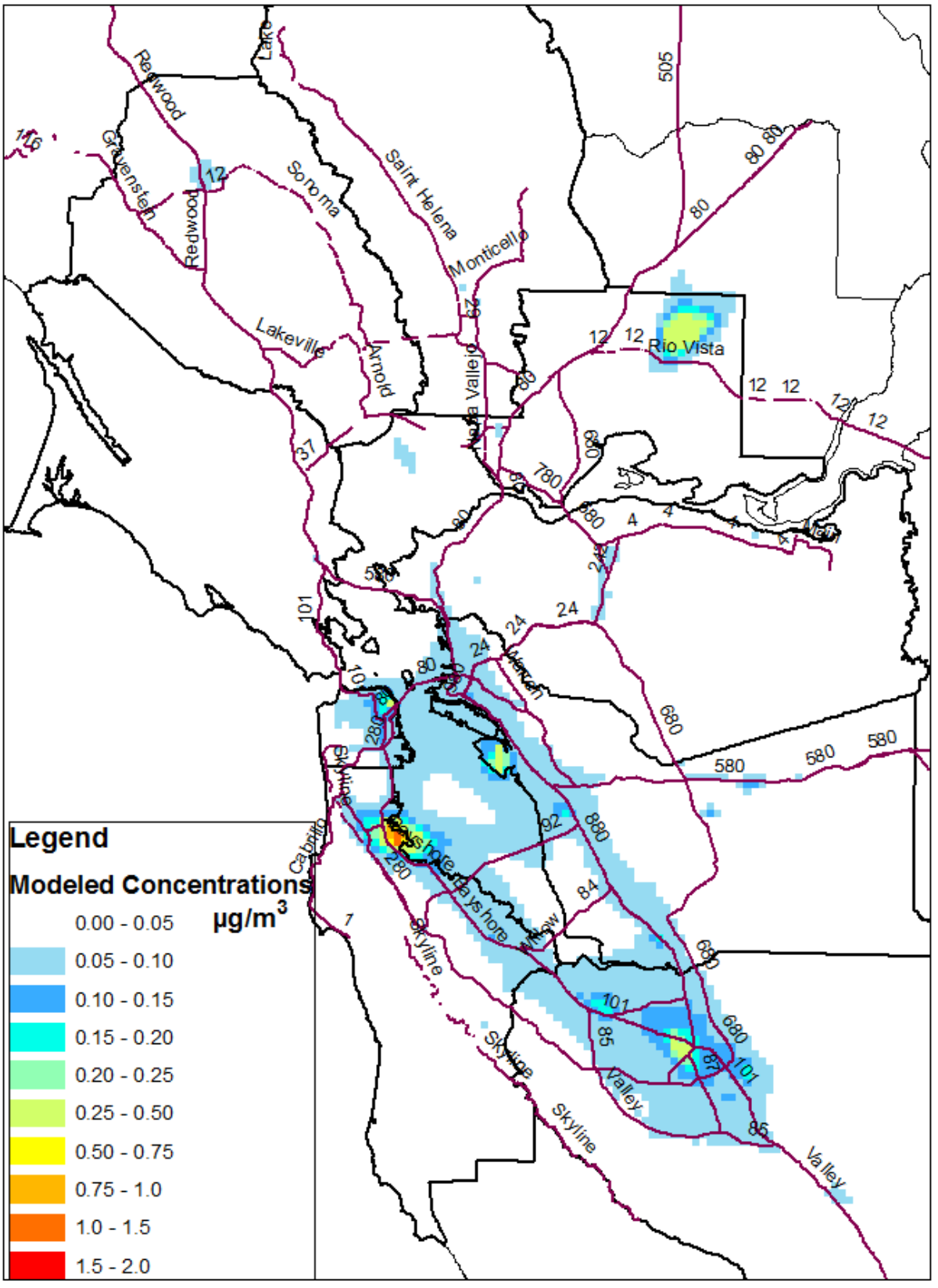

Figure 13: Annual average 1,3-butadiene concentrations, 2015.

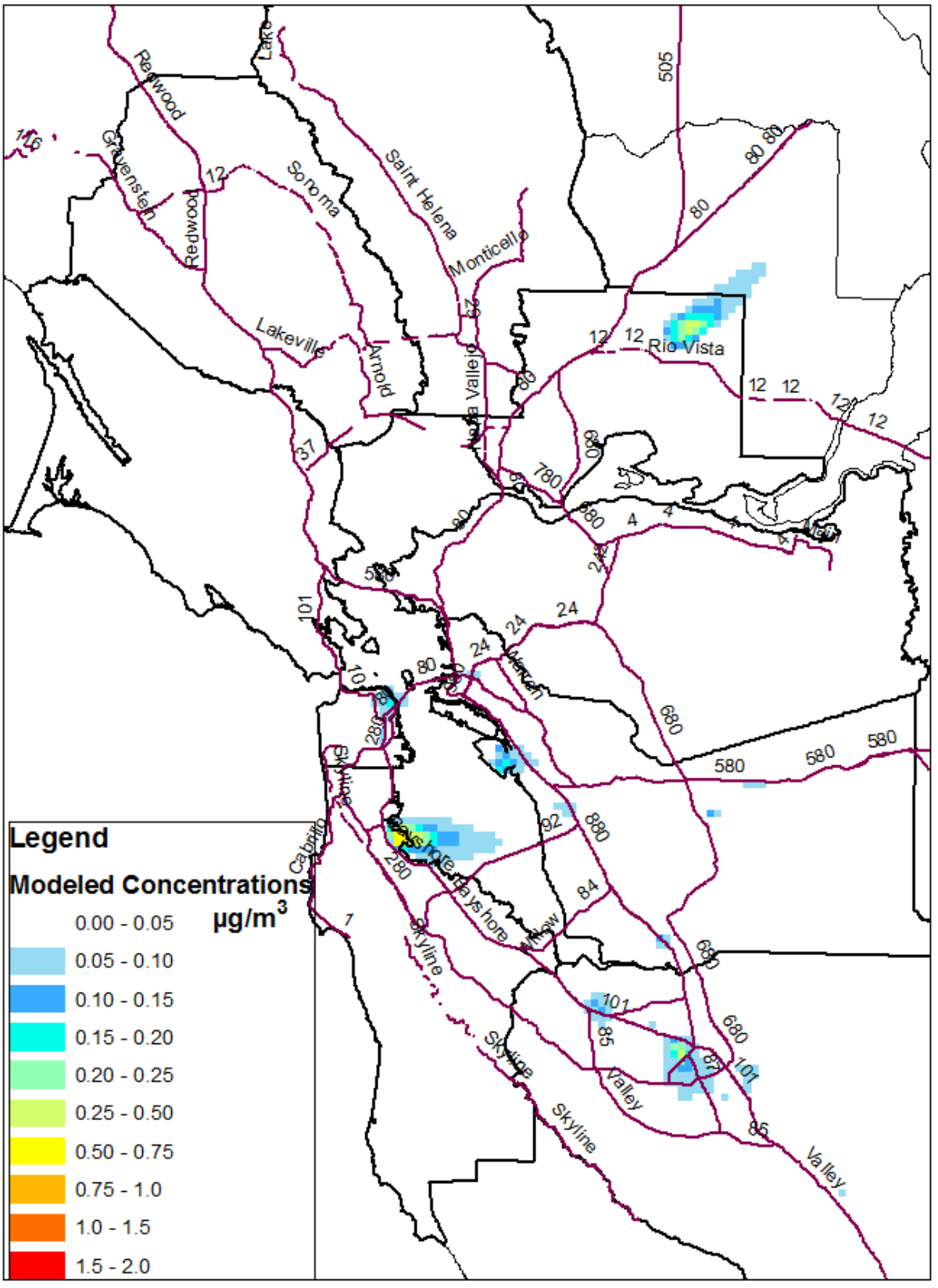

Figure 14: 1,3-butadiene concentrations for July, 2015.

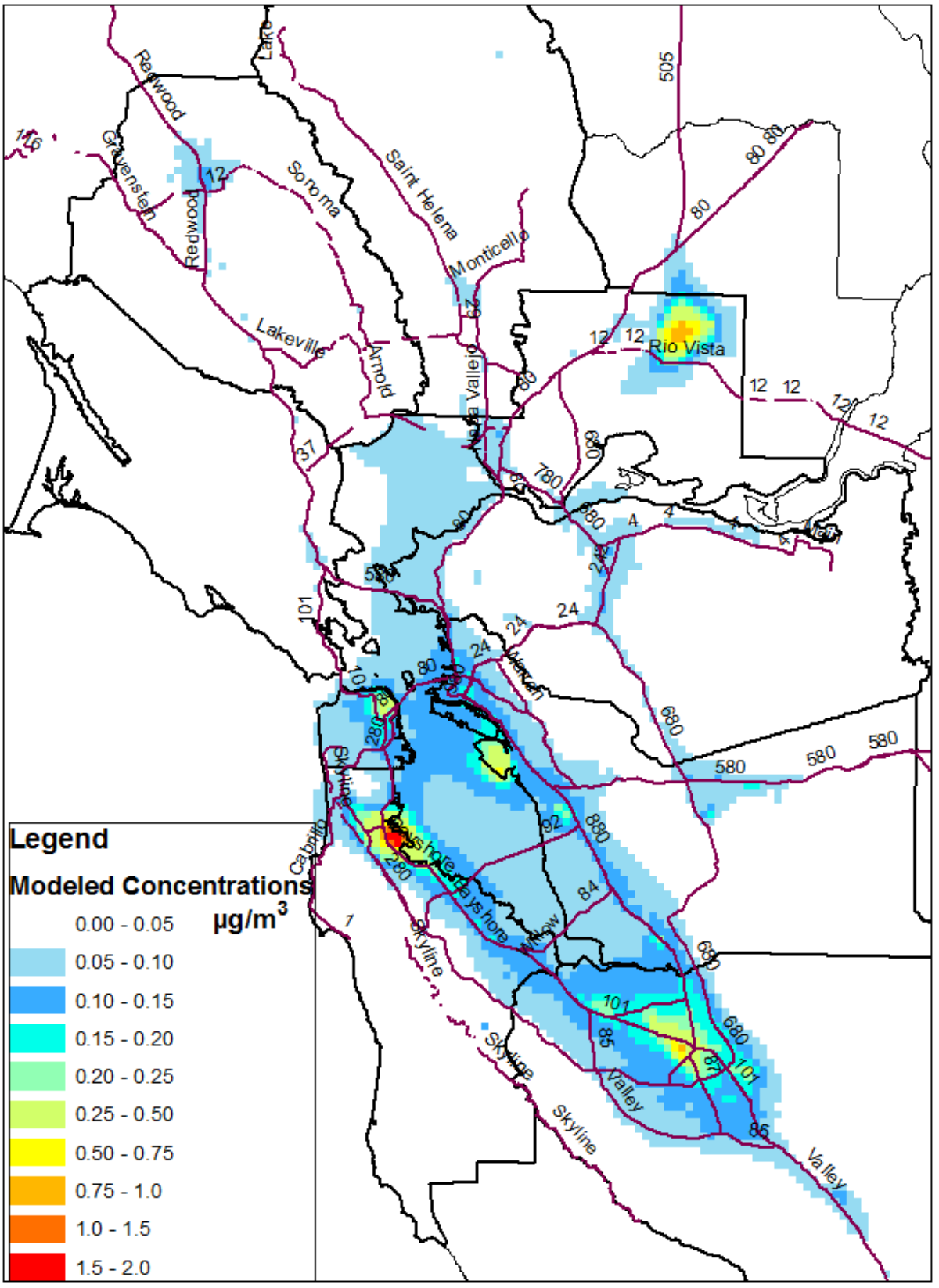

Figure 15: 1,3-butadiene concentrations for December, 2015.

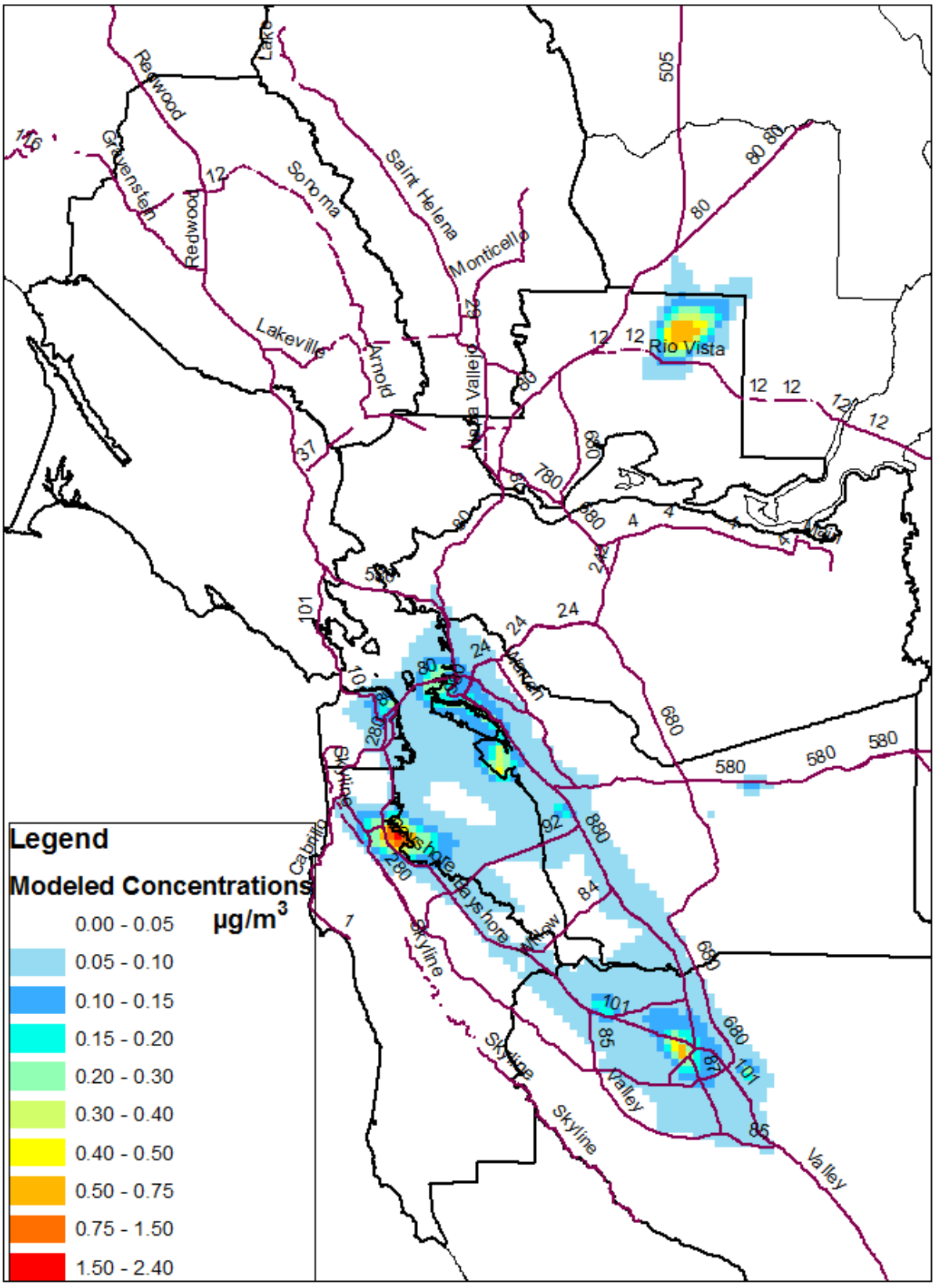

Figure 16: Annual average acrolein concentrations, 2015.

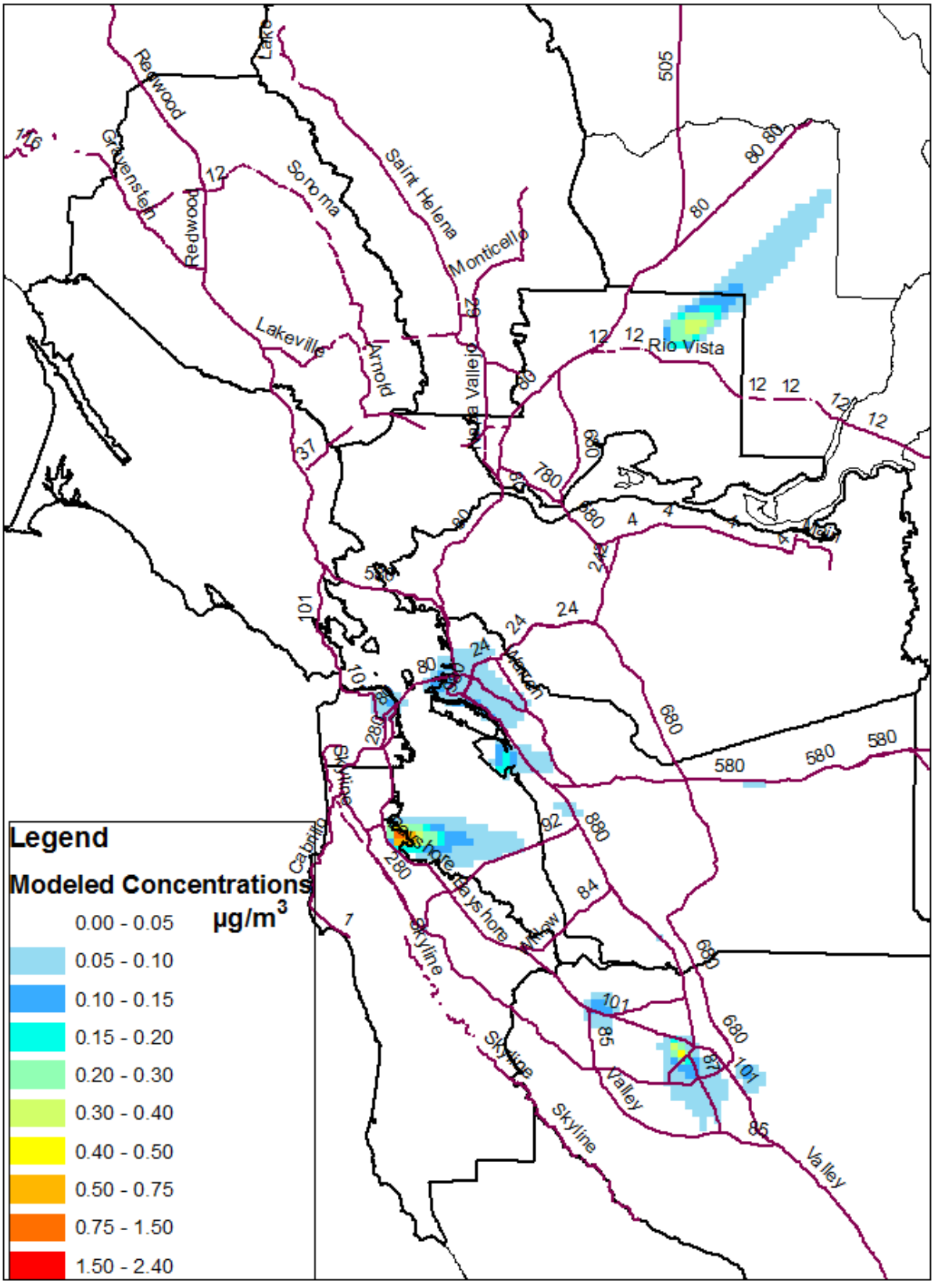

Figure 17: Acrolein concentrations for July, 2015.

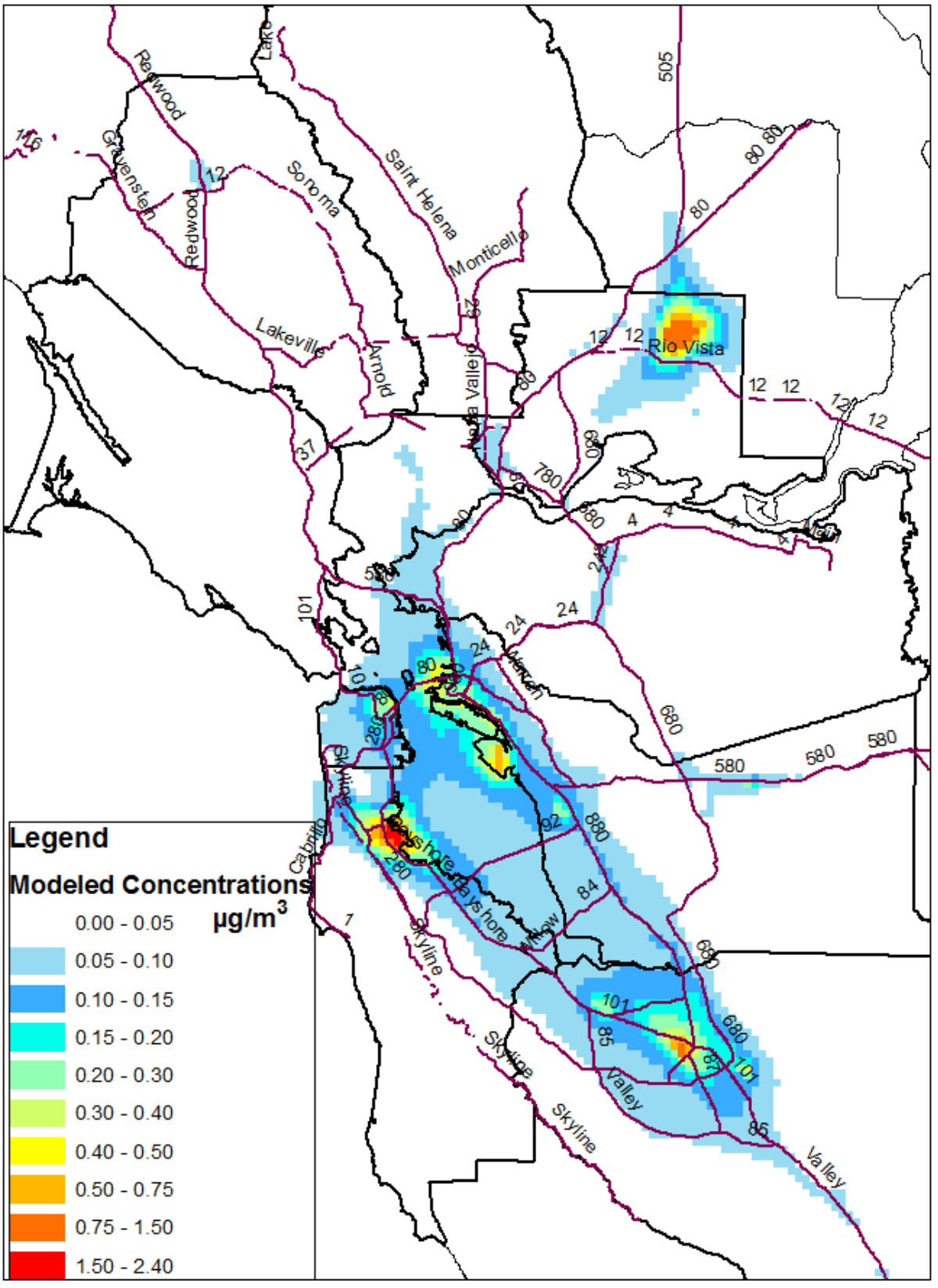

Figure 18: Acrolein concentrations for December, 2015.

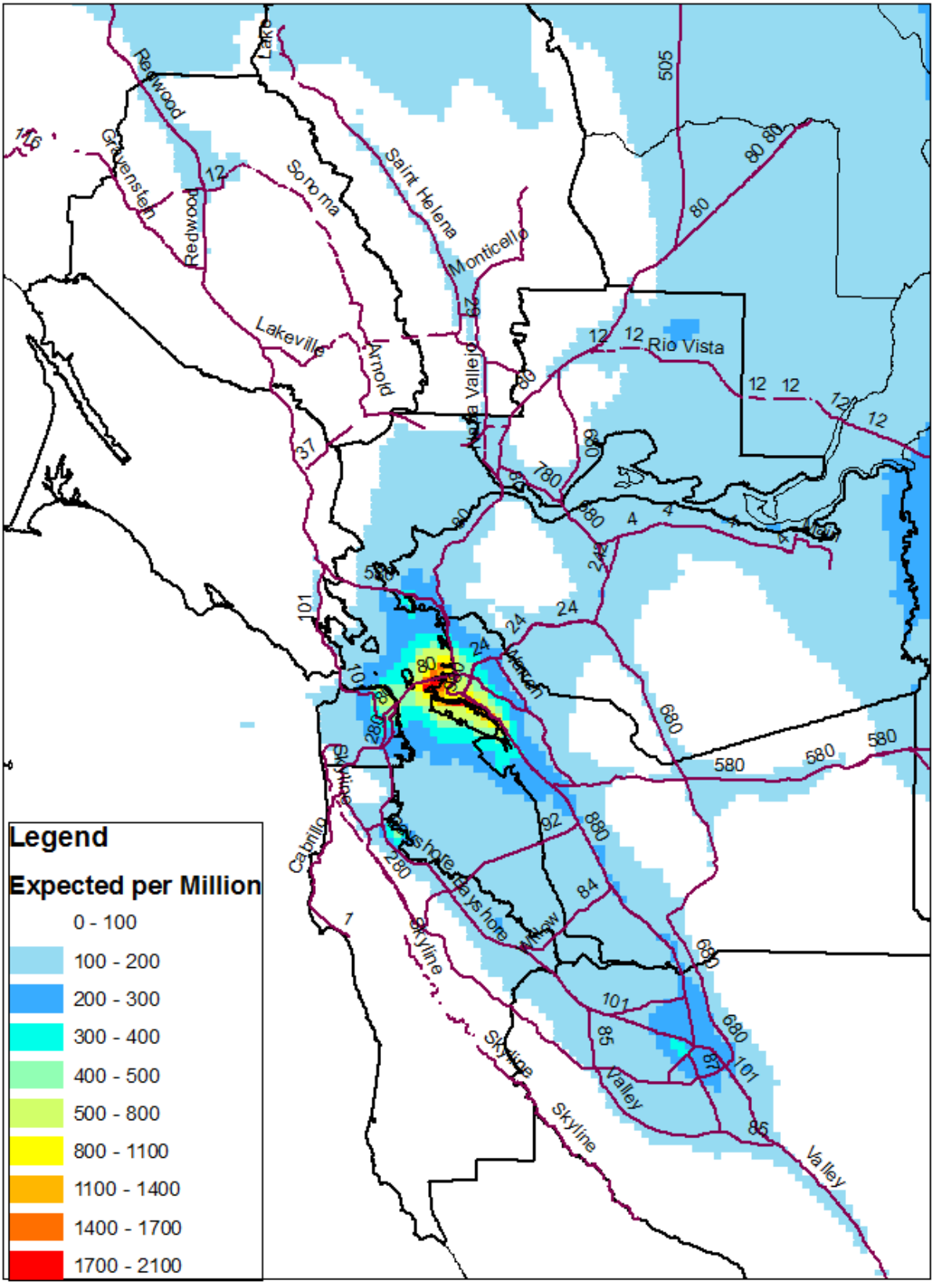

Figure 19: Estimated cancer risk (number per million) in 2015 from toxic air contaminants. These risks are over an assumed 70-year lifetime of exposure.

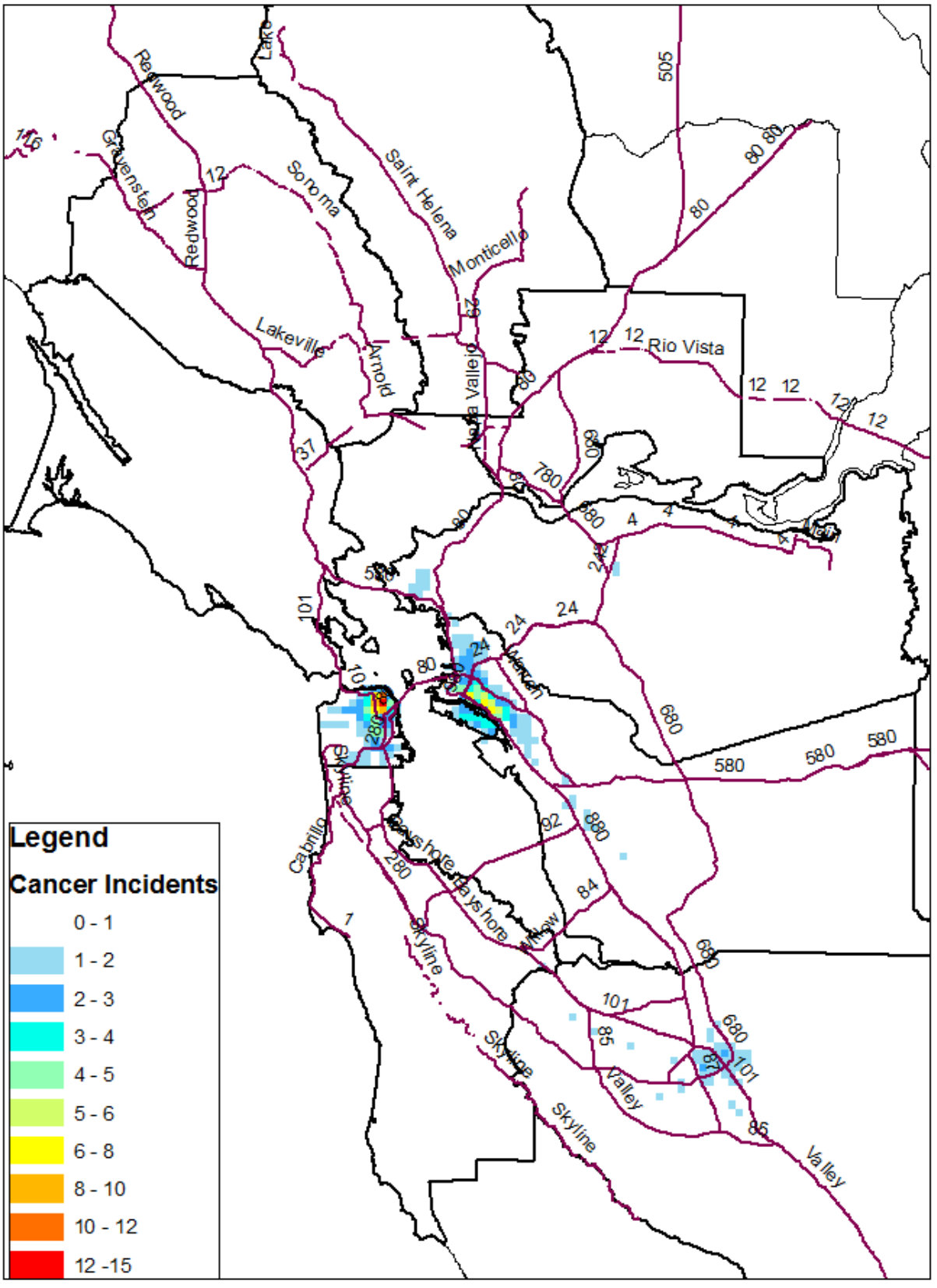

Figure 20: Estimated number of Bay Area cancer incidents from modeled toxic air contaminants for concentration and population levels in 2015.

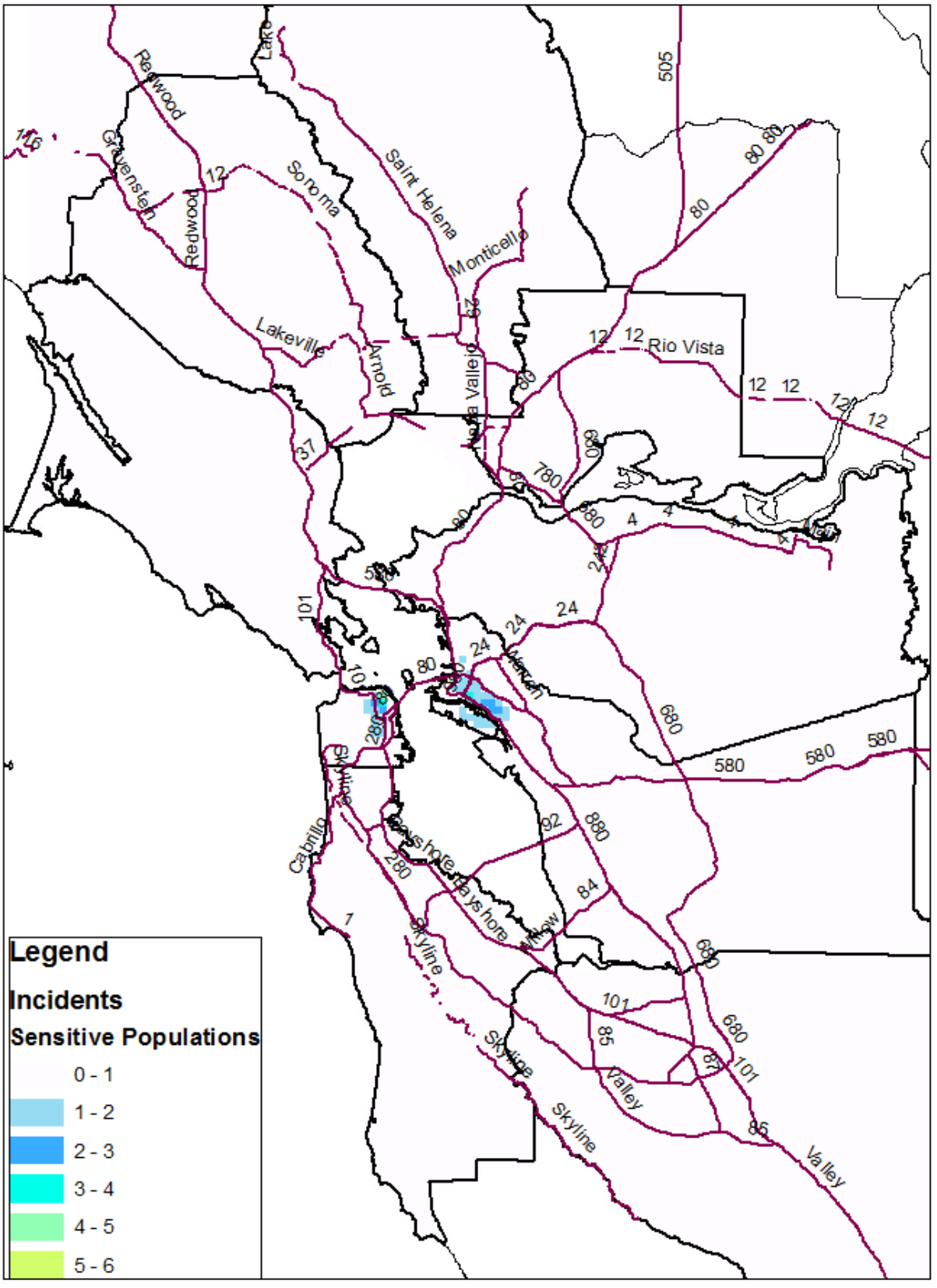

Figure 21: Estimated number of Bay Area cancer incidents from modeled toxic air contaminants for concentration levels and sensitive populations in 2015.

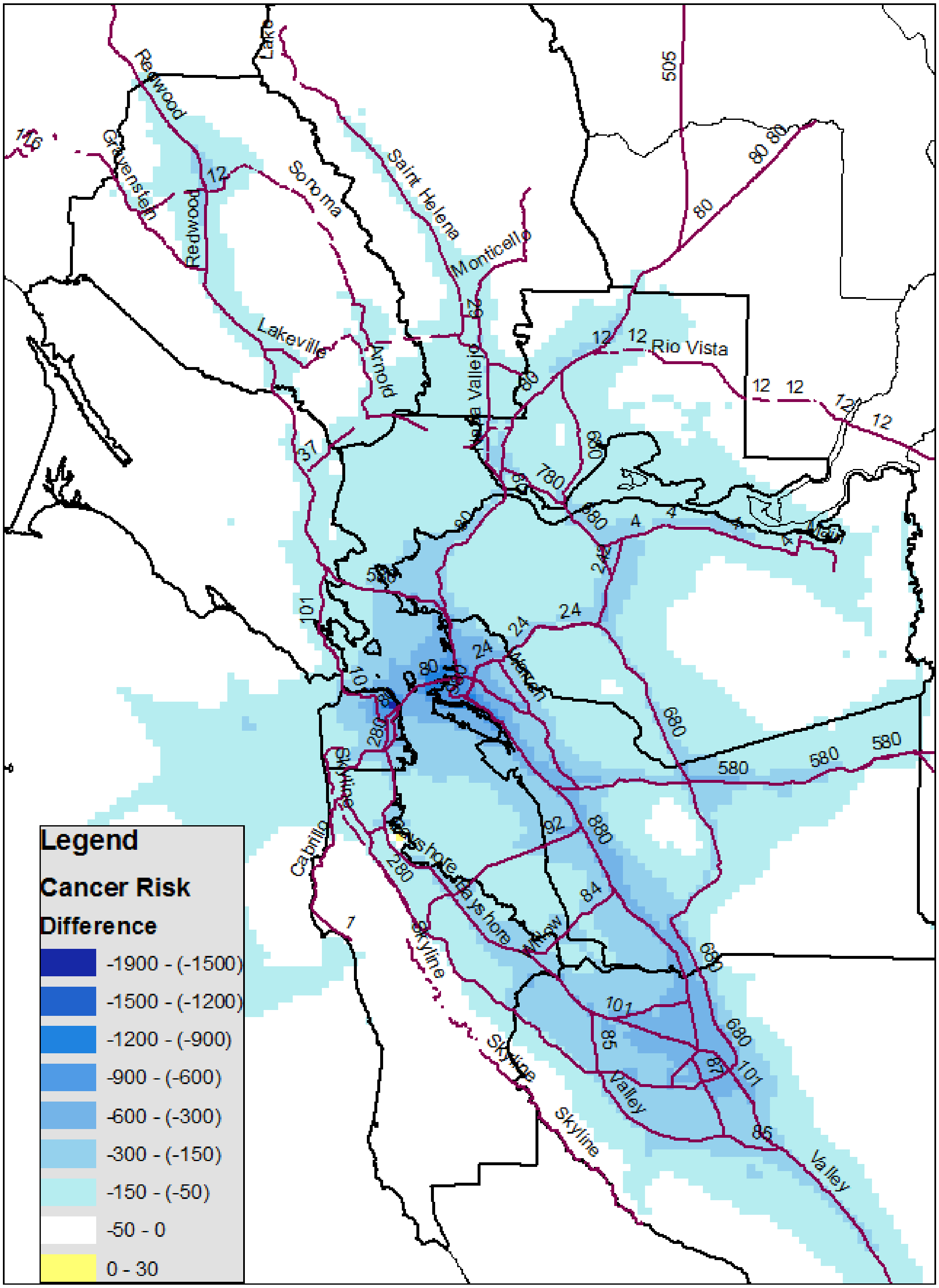

Figure 22: Estimated change in cancer risk (number per million) between 2005 and 2015 from changes in toxic air contaminants.

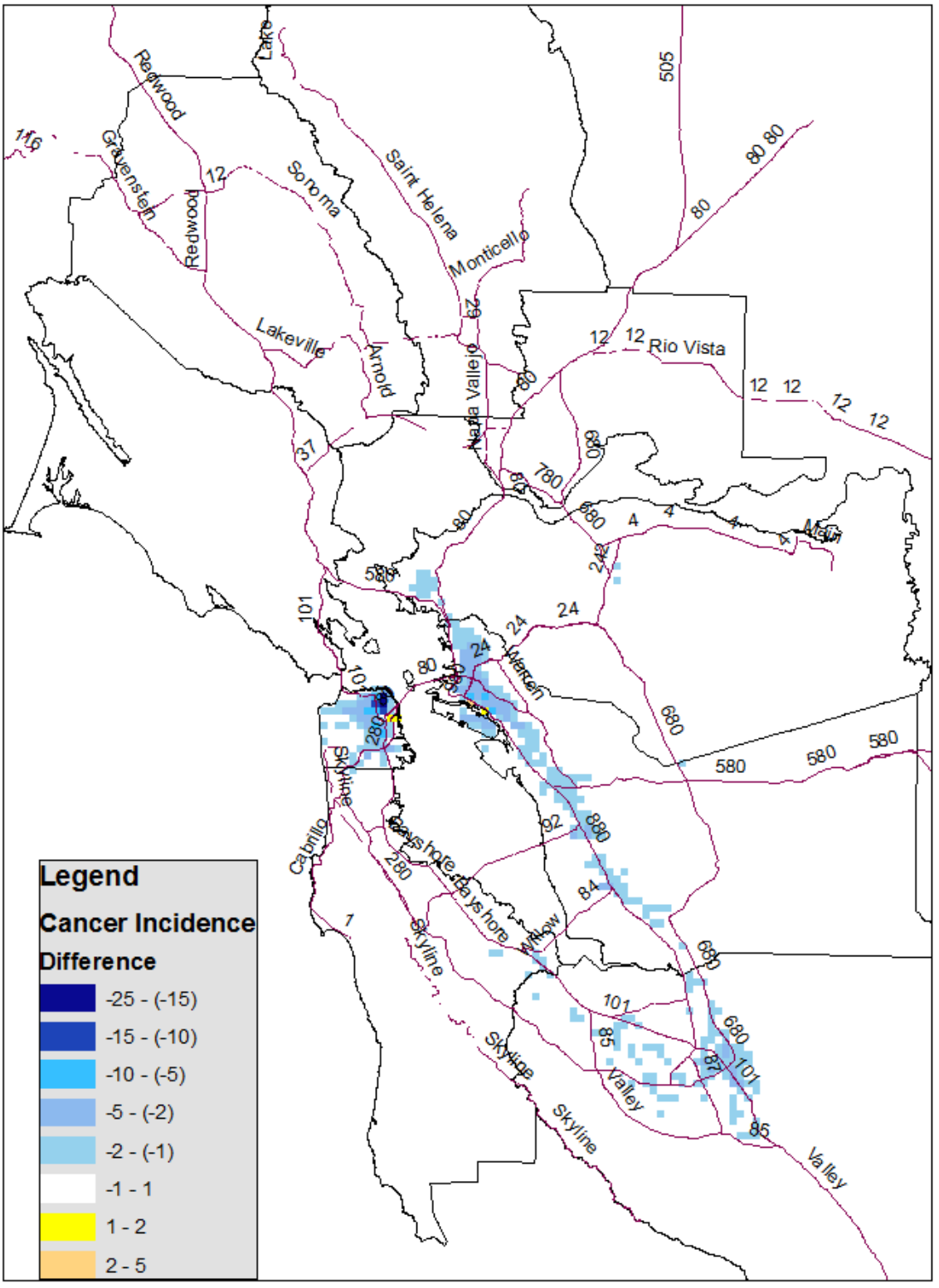

Figure 23: Estimated change in Bay Area cancer incidents between 2005 and 2015. Differences reflect both changes in modeled concentrations of toxic air contaminants and changes in population.

APPENDIX A

Toxics Emissions Inventory

The following tables and figures give information on the magnitude and spatial distributions of emissions of key toxics species.

Table A1 summarizes 2015 diesel particulate matter of less than ten microns (DPM10) emissions by Bay Area county and major source category. Overall, area and non-road equipment emissions dominate, with Alameda and San Mateo Counties showing the two highest emission estimates.

Table A1**:** DPM10 emissions by county and major source category (tons/day).

County	Area/Non-road	On-road	Stationary Point	Total
Alameda	1.02	0.20	0.01	1.23
Contra Costa	0.30	0.10	0.03	0.43
Marin	0.09	0.02	0.00	0.11
Napa	0.04	0.01	0.00	0.05
San Francisco	0.36	0.05	0.01	0.42
San Mateo	0.49	0.04	0.01	0.54
Santa Clara	0.25	0.13	0.02	0.40
Solano	0.10	0.03	0.00	0.13
Sonoma	0.08	0.04	0.00	0.12
Grand Total	2.73	0.62	0.08	3.45

Notes: Emissions from diesel off-road categories estimated in ARB's OFFROAD model have been halved based on District's fuel-based analysis. The effects of promulgated controls have also been included.

Table A2 shows detailed contributions to the area/non-road DPM10 emissions by county from Table A1. These two tables show that ship emissions are the largest source of DPM10 for Alameda, Contra Costa, Marin, San Francisco, and San Mateo Counties, while they are equivalent to on-road sources in Solano County. Note, however, that the bulk of shipping emissions associated with Marin, San Francisco, and San Mateo Counties are intransit emissions which may occur as far out as tens of nautical miles. Construction equipment (included under off-road equipment in Table A2) is a significant source for the majority of counties.

Tables A3-A7 show 2015 county-level emissions of acetaldehyde, acrolein, 1,3-butadiene, formaldehyde and benzene, respectively. Emissions are broken out by major source category.

Table A2**:** Area and non-road DPM10 emissions by county (tons/day).

COUNTY	FARM EQUIPMENT	MANUFACTURING AND INDUSTRIAL	OFF-ROAD EQUIPMENT	RECREATIONAL BOATS	SHIPS AND COMMERCIAL BOATS	TRAINS	Grand Total
Alameda	0.01	0.01	0.13	0.0003	0.81	0.06	1.02
Contra Costa	0.01	0.00	0.10	0.0010	0. 13	0.06	0.17
Marin	0.00	0.00	0.02	0.0003	0.06	0.00	*0.08*
Napa	0.02	0.00	0.01	0.0005		0.01	0.04
San Francisco	0.00	0.01	0.10	0.0003	0.23	0.03	*0.37*
San Mateo	0.01	0.00	0.06	0.0001	0.40	0.02	*0.49*
Santa Clara	0.02	0.01	0.16	0.0005		0.06	0.25
Solano	0.02	0.00	0.04	0.0002	0.03	0.01	0.10
Sonoma	0.02	0.00	0.04	0.0003	0.00	0.01	0.07
Grand Total	0.11	0.03	0.66	0.0035	1.53	0.26	2.59

Table A3**:** Acetaldehyde emissions by county and major source category (lbs/day).

County	Area/Non-road	On-road	Point	Total
Alameda	1929	518	1.6	2449
Contra Costa	1224	218	3.5	1446
Marin	355	51	0.0	406
Napa	230	46	0.0	276
San Francisco	679	108	0.0	787
San Mateo	876	105	0.0	981
Santa Clara	1480	340	19.1	1839
Solano	687	193	0.9	881
Sonoma	589	92	11.1	692
Grand Total	8049	1671	36.2	9756

Note: Emissions from diesel off-road categories estimated in ARB's OFFROAD model have been halved based on District's fuel-based analysis. The effects of promulgated controls have also been included.

Table A4**:** Acrolein emissions by county and major source category (lbs/day).

County	Area/Non-road	On-road	Point	Total
Alameda	189	58	0.7	248
Contra Costa	73	29	0.0	102
Marin	22	7	0.0	29
Napa	20	6	0.0	26
San Francisco	58	15	0.0	73
San Mateo	201	16	0.0	217
Santa Clara	148	45	0.0	193
Solano	198	20	0.0	218
Sonoma	32	13	0.0	45
Grand Total	941	209	0.7	1151

Note: Emissions from diesel off-road categories estimated in ARB's OFFROAD model have been halved based on District's fuel-based analysis. The effects of promulgated controls have also been included.

Table A5: 1,3-butadiene emissions by county and major source category (lbs/day).

County	Area/Non-road	On-road	Point	Total
Alameda	207	117	0.0	324
Contra Costa	82	81	2.0	165
Marin	45	20	0.0	65
Napa	30	18	0.0	48
San Francisco	46	43	0.0	89
San Mateo	178	54	0.0	232
Santa Clara	116	128	0.2	244
Solano	161	28	0.3	189
Sonoma	31	44	0.0	75
Grand Total	896	533	2.5	1432

Note: Emissions from diesel off-road categories estimated in ARB's OFFROAD model have been halved based on District's fuel-based analysis. The effects of promulgated controls have also been included.

Table A6: Formaldehyde emissions by county and major source category (lbs/day).

County	Area/Non-road	On-road	Point	Total
Alameda	1697	514	36	2247
Contra Costa	1330	285	430	2044
Marin	435	68	0	503
Napa	261	63	9	333
San Francisco	566	146	52	764
San Mateo	1614	169	16	1799
Santa Clara	1614	446	294	2354
Solano	1458	162	18	1638
Sonoma	587	140	1	728
Grand Total	9562	1993	856	12411

Note: Emissions from diesel off-road categories estimated in ARB's OFFROAD model have been halved based on District's fuel-based analysis. The effects of promulgated controls have also been included.

Table A7: Benzene emissions by county and major source category (lbs/day).

County	Area/Non-road	On-road	Point	Total
Alameda	531	625	10	1166
Contra Costa	550	423	96	1069
Marin	214	108	1	323
Napa	139	94	1	234
San Francisco	288	225	2	515
San Mateo	469	282	5	756
Santa Clara	527	696	53	1276
Solano	305	143	9	457
Sonoma	159	228	4	391
Grand Total	3182	2824	181	6187

Note: Emissions from diesel off-road categories estimated in ARB's OFFROAD model have been halved based on District's fuel-based analysis. The effects of promulgated controls have also been included.

Table A8 shows Bay Area county-level total organic gas (TOG) and nitrogen oxides (NOx) by major source category.

Table A8**:** 2015 Bay Area annual average TOG and NOx emissions by county and major source category (tons/day).

	TOG						NOx					
County	Point	Area	On-road	Non-road	Natural	Total	Point	Area	On-road	Non-road	Natural	Total
Alameda	46.2	63.2	18.3	11.7	12.2	151.6	4.4	5.8	36.4	34.9	0.1	81.6
Contra Costa	27.4	72.9	12.1	8.4	12.1	132.9	19.9	6.7	17.9	11.8	0.0	56.3
Marin	10.8	19.5	3.2	4.3	7.7	45.5	0.2	1.1	4.8	5.7	0.1	11.9
Napa	6.3	15.1	2.6	3.2	31.4	58.6	0.4	0.6	3.6	2.1	1.2	7.9
San Francisco	1.6	23.3	6.3	5.6	1.0	37.8	2.1	2.5	9.4	17.5	0.0	31.5
San Mateo	30.3	25.4	7.6	9.2	7.4	79.9	0.8	2.5	9.8	46.5	0.0	59.6
Santa Clara	43.3	72.7	20.2	10.2	31.1	177.5	5.7	5.7	27.0	17.5	0.2	56.1
Solano	6.7	12.5	3.5	6.1	2.7	31.5	6.6	1.0	5.9	9.4	0.0	22.9
Sonoma	16.1	31.4	6.1	3.4	10.6	67.6	0.4	1.4	7.3	3.5	0.0	12.6
Grand Total	188.7	336.0	79.9	62.1	116.2	782.9	40.5	27.3	122.1	148.9	1.6	340.4

Notes: Natural source emissions taken from ARB's online Almanac at http://www.arb.ca.gov/app/emsinv/emssumcat.php. Emissions from diesel off-road categories estimated in ARB's OFFROAD model have been halved based on District's fuel-based analysis. The effects of promulgated controls have also been included.

Figure A1 illustrates the Bay Area-wide hourly distribution of DPM10 emissions for a weekday and weekend day. It clearly shows a drop in overall activity on weekend days. Since ship, construction equipment, and heavy-duty truck emissions dominate for this pollutant, most of the emissions occur during daylight hours. Note that stationary point source emissions are not included in the figure. Overall, these are small contributions that tend to be flat throughout the day.

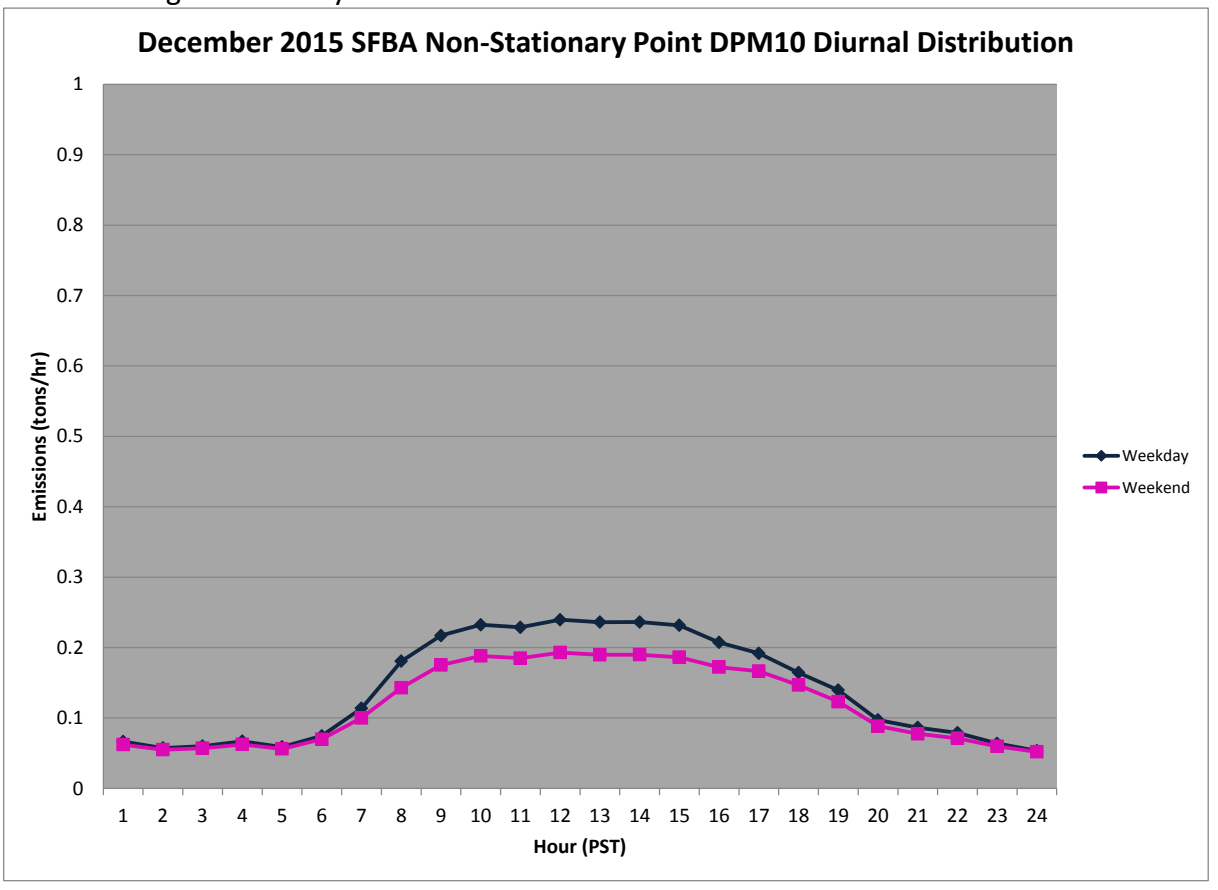

Figure A1**:** December weekday and weekend day diurnal distributions of DPM10 emissions (emissions from stationary point sources are not included).

The following plots give spatial distributions of DPM10, formaldehyde, acetaldehyde, 1,3-butadiene, acrolein and benzene emissions. As discussed above, DPM10 originates mostly from ships, construction equipment, and heavy-duty trucks and is shown below to be concentrated in areas where these activities occur (shipping lanes, populated areas, and major highways) (Figure A2). Formaldehyde, acetaldehyde, 1,3-butadiene, acrolein and benzene are generally combustion byproducts (Figures A3 through A7, respectively). In particular, aircraft are a significant source of acrolein so that emissions of acrolein are concentrated around large airfields. Benzene is emitted primarily in the exhaust of combustion engines and through gasoline evaporation; therefore, its emissions follow the major roadways and are found in the populated areas.

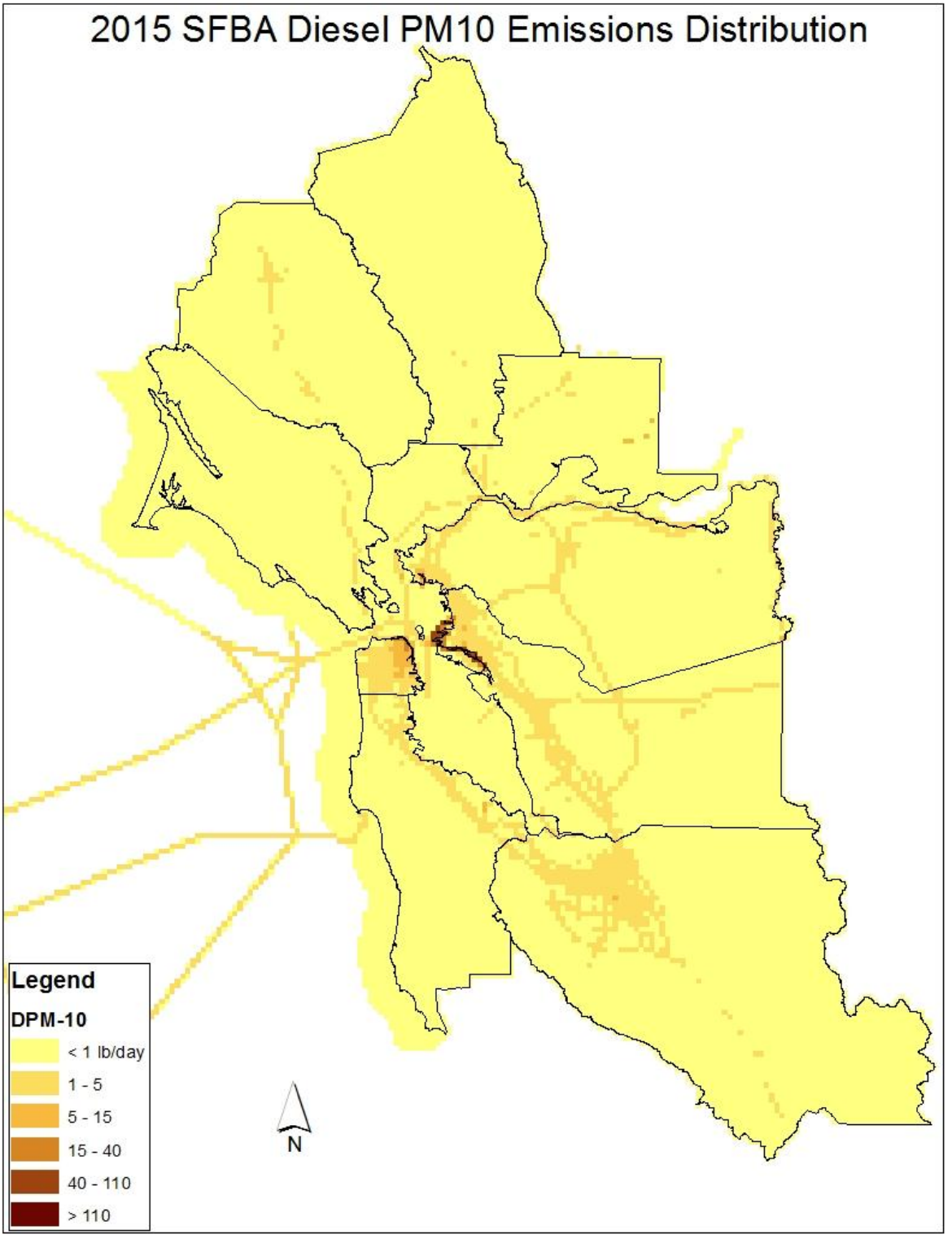

Figure A2: Spatial distribution of DPM10 emissions in the Bay Area.

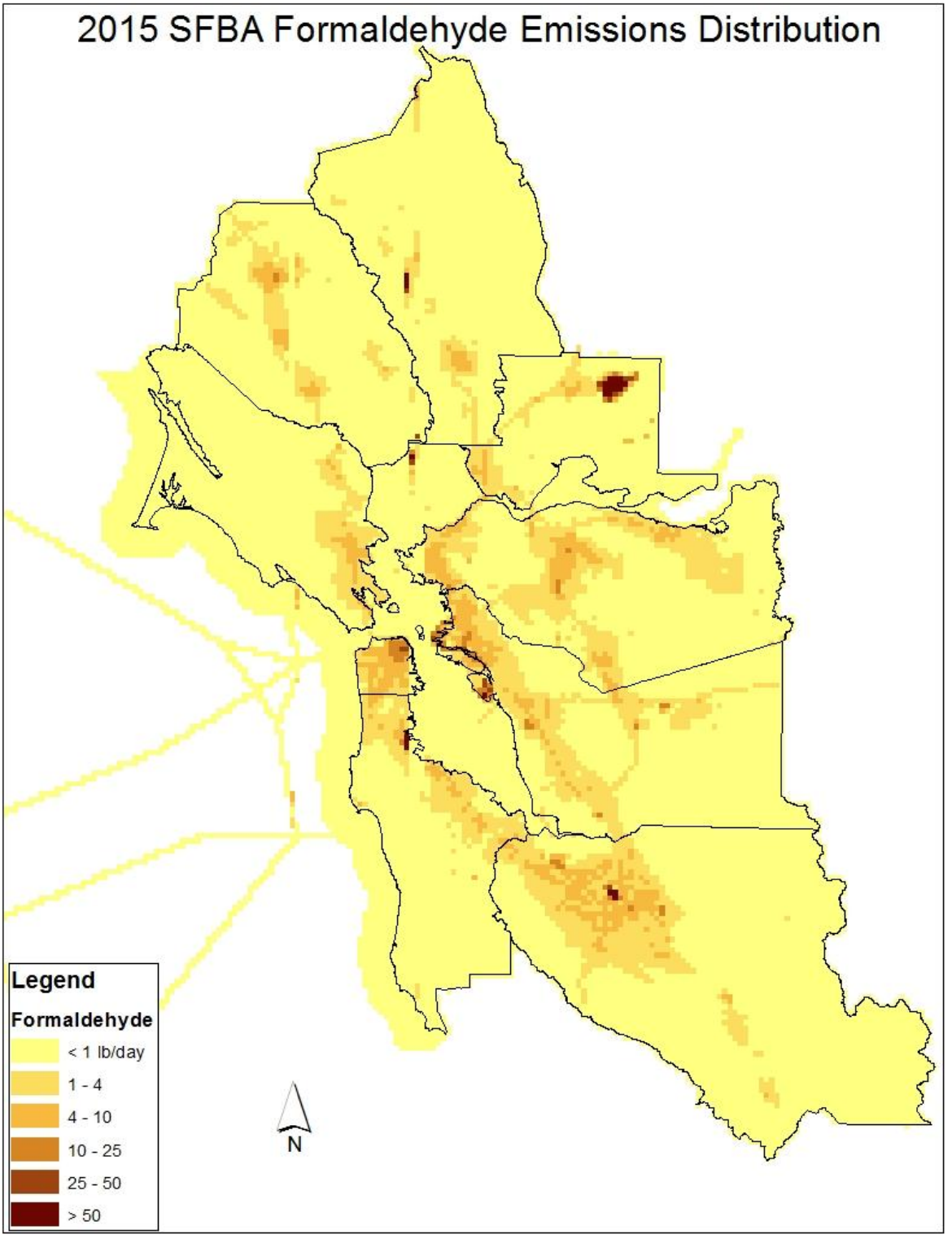

Figure A3**:** Spatial distribution of formaldehyde emissions in the Bay Area.

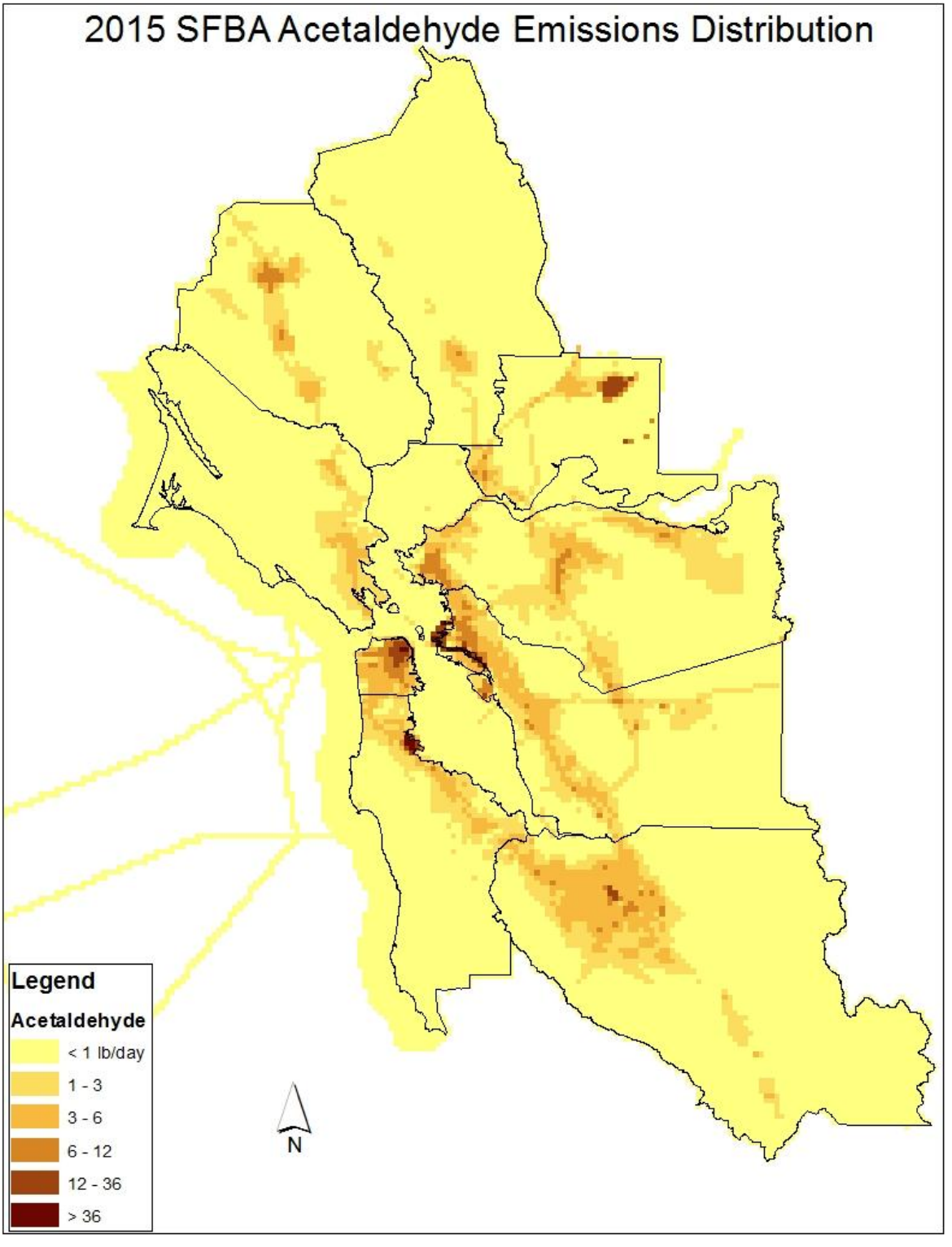

Figure A4**:** Spatial distribution of acetaldehyde emissions in the Bay Area.

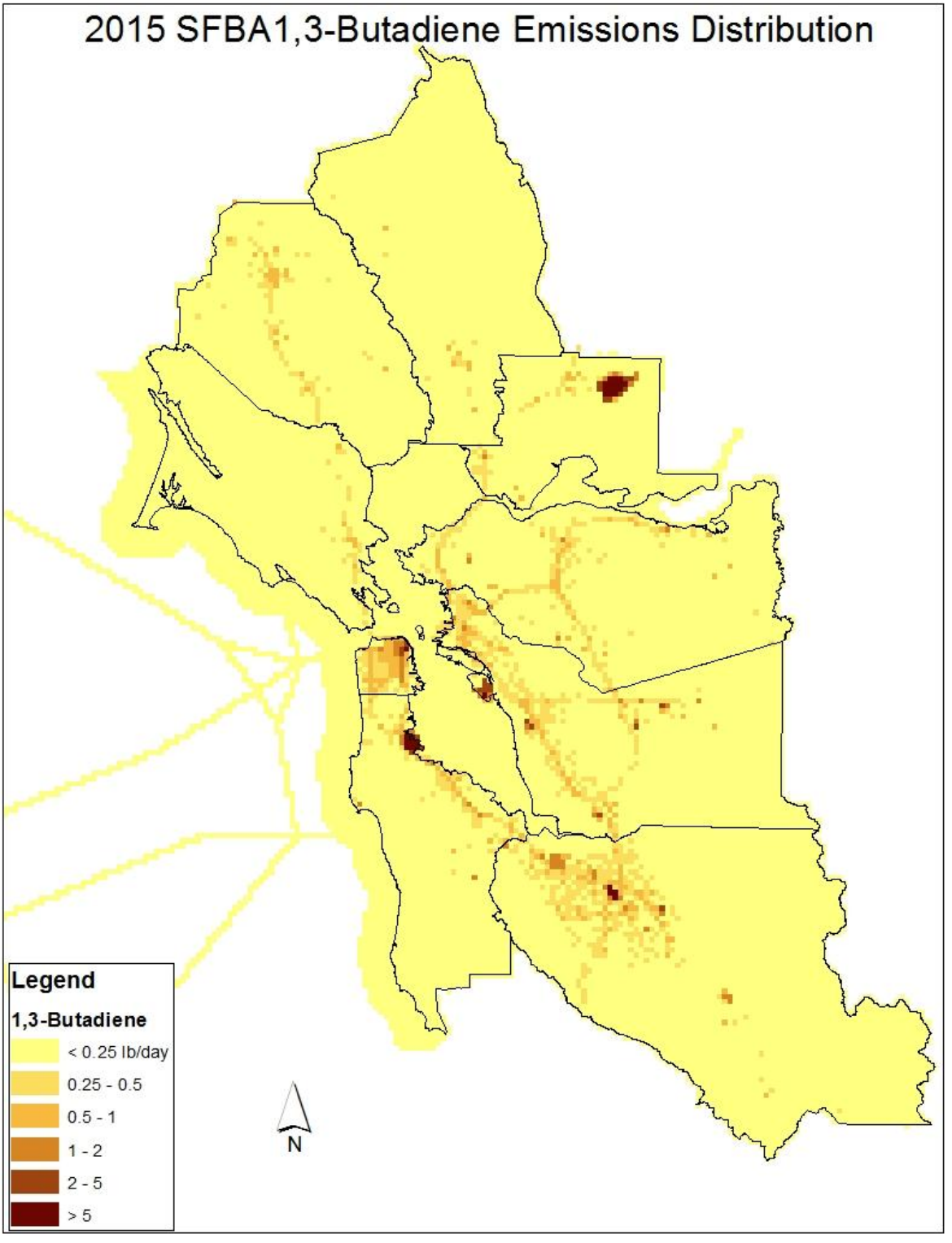

Figure A5: Spatial distribution of 1,3-butadiene emissions in the Bay Area.

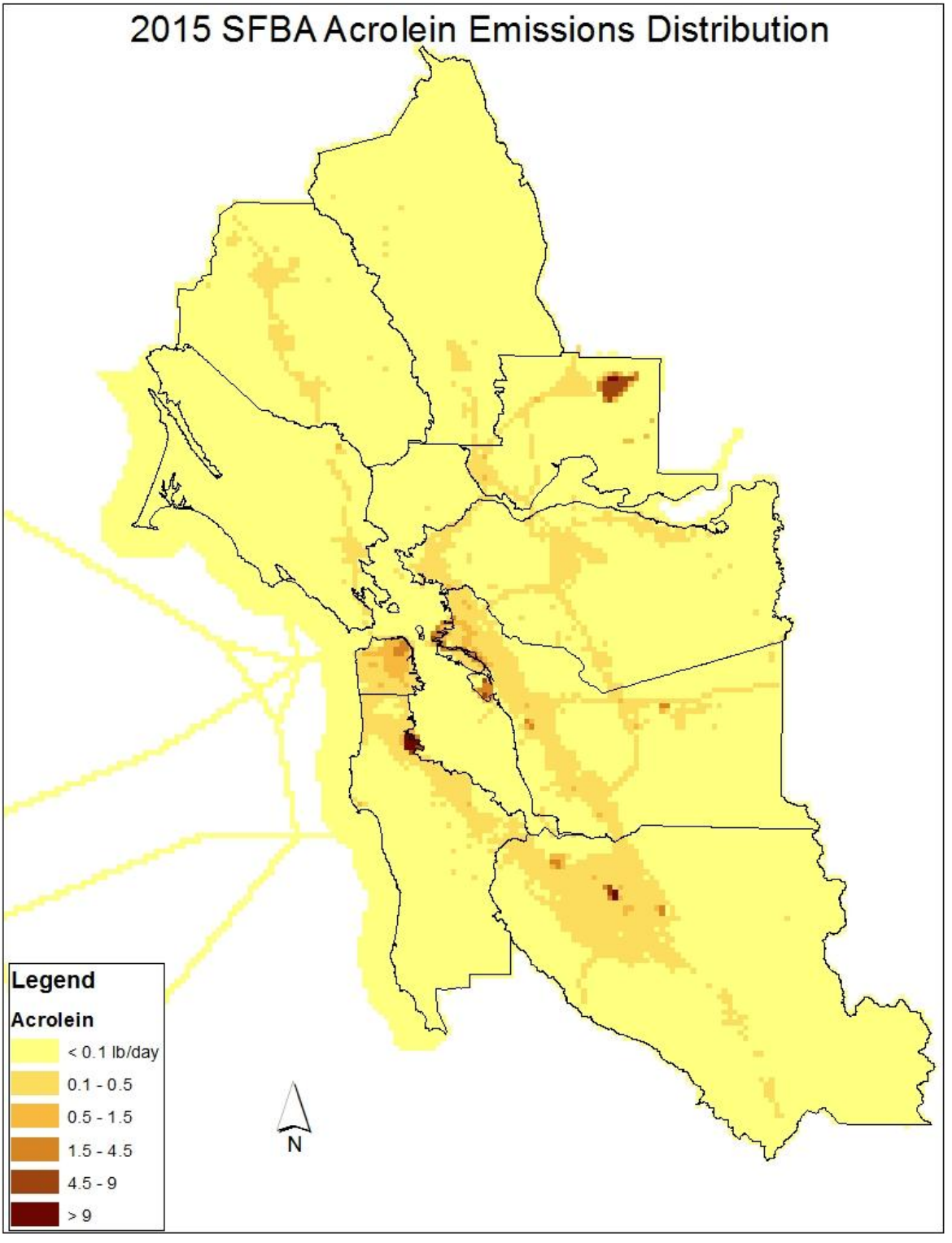

Figure A6**:** Spatial distribution of acrolein emissions in the Bay Area.

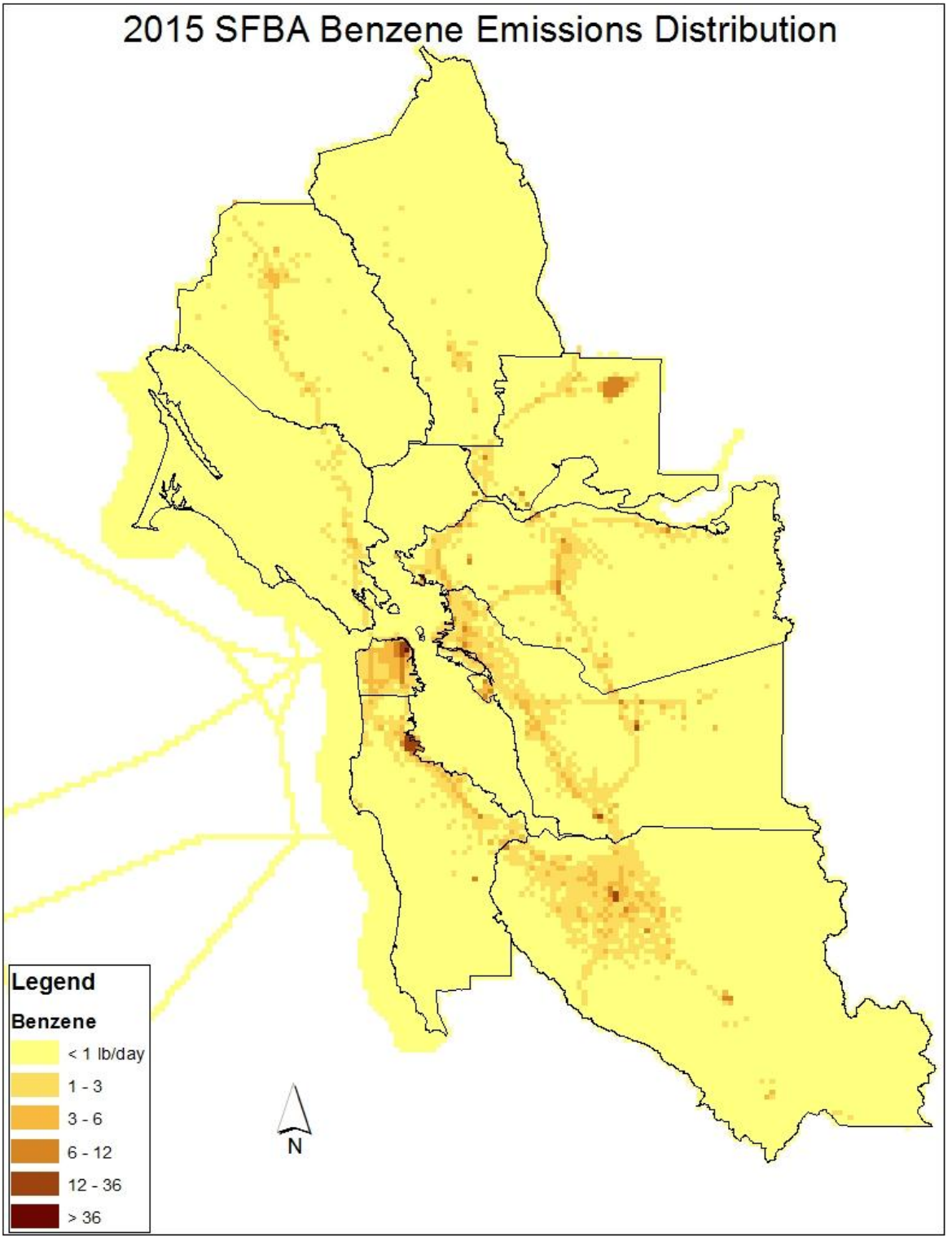

Figure A7: Spatial distribution of benzene emissions in the Bay Area.

APPENDIX B

Comparison of 2005 and 2015 Emissions

This appendix summarizes major changes in the toxics emissions inventory between 2005 and 2015. The 2015 scenario presented here reflects the effects of all promulgated controls and regulations based upon information available from the California Air Resources Board at the time this work was done. Since then, ARB has considered revising the implementation schedules of some regulations.

Tables B1 and B2 show absolute and percent changes in diesel particulate matter emissions from 2005 to 2015 by county and by major source category. Overall, there is a 71% reduction, with the largest absolute reductions occurring for area and non-road categories. On a percentage basis, however, on-road vehicles show the highest emission reductions. The fact that heavy-duty vehicles, even without the new regulations, are expected to emit less PM10 in 2015 than 2005 is due to fleet turnover to cleaner engines.

Table B1: Change in DPM10 from 2005 to 2015 (tons/day).

County	Area/Non-road	On-road	Point	Total
Alameda	-1.02	-1.20	-0.01	-2.23
Contra Costa	-0.51	-0.41	-0.02	-0.94
Marin	-0.27	-0.07	0.00	-0.34
Napa	-0.07	-0.09	0.00	-0.16
San Francisco	-0.86	-0.14	0.00	-1.00
San Mateo	-1.43	-0.16	0.00	-1.59
Santa Clara	-0.61	-0.63	-0.01	-1.25
Solano	-0.16	-0.23	-0.01	-0.40
Sonoma	-0.17	-0.15	-0.01	-0.33
Grand Total	-5.10	-3.08	-0.06	-8.24

Table B2: Percent change in DPM10 from 2005 to 2015.

County	Area/Non-road	On-road	Point	Total
Alameda	-50%	-86%	-39%	-65%
Contra Costa	-63%	-81%	-33%	-68%
Marin	-75%	-76%	0%	-75%
Napa	-60%	-89%	0%	-73%
San Francisco	-71%	-74%	-8%	-71%
San Mateo	-75%	-79%	-39%	-75%
Santa Clara	-71%	-82%	-36%	-76%
Solano	-61%	-88%	-61%	-74%
Sonoma	-69%	-80%	-59%	-74%
Grand Total	-65%	-83%	-35%	-71%

The following two tables give further insights into the DPM10 emission reductions for area and non-road source categories. As indicated, the bulk of the reductions come via shipping followed closely by off-road equipment (construction, industrial equipment, etc…). Note that while shipping emission reductions are the largest, the associated percentage decrease is not. This is because the new controls do not affect intransit emissions, which comprise a large part of the inventory for this category. Nevertheless, the reductions that are achieved are likely to be in the vicinity of populated places so that population exposure will be affected.

Table B3**:** Change in area and non-road DPM10 from 2005 to 2015 (tons/day).

COUNTY	FARM EQUIPMENT	MANUFACTURING AND INDUSTRIAL	OFF-ROAD EQUIPMENT	RECREATIONAL BOATS	SHIPS AND COMMERCIAL BOATS	TRAINS	Grand Total
Alameda	-0.01	-0.01	-0.5	0.0001	-0.47	-0.03	-1.02
Contra Costa	-0.01	-0.01	-0.37	0.0003	-0.08	-0.03	-0.50
Marin	-0.01	0	-0.08	0.0001	-0.18	0	-0.27
Napa	-0.02	0	-0.04	0.0001	0	-0.01	-0.07
San Francisco	0	-0.01	-0.34	0.0001	-0.5	0	-0.85
San Mateo	0	-0.01	-0.22	0	-1.19	-0.01	-1.43
Santa Clara	-0.02	-0.02	-0.54	0.0001	0	-0.02	-0.60
Solano	-0.02	0	-0.08	0.0001	-0.04	-0.01	-0.15
Sonoma	-0.02	-0.01	-0.14	0.0001	-0.01	-0.01	-0.19
Grand Total	-0.11	-0.07	-2.31	0.001	-2.47	-0.12	-5.08

Table B4: Percent change in area and non-road DPM10 from 2005 to 2015.

COUNTY	FARM EQUIPMENT	MANUFACTURING AND INDUSTRIAL	OFF-ROAD EQUIPMENT	RECREATIONAL BOATS	SHIPS AND COMMERCIAL BOATS	TRAINS	Grand Total
Alameda	-50%	-50%	-79%	50%	-37%	-33%	-50%
Contra Costa	-50%	-100%	-79%	43%	-38%	-33%	-62%
Marin	-100%	0%	-80%	50%	-75%	0%	-77%
Napa	-50%	0%	-80%	25%	0%	-50%	-63%
San Francisco	0%	-50%	-77%	50%	-68%	0%	-70%
San Mateo	0%	-100%	-79%	0%	-75%	-33%	-74%
Santa Clara	-50%	-67%	-77%	25%	0%	-25%	-71%
Solano	-50%	0%	-67%	100%	-57%	-50%	-60%
Sonoma	-50%	-100%	-78%	50%	-100%	-50%	-73%
Grand Total	-50%	-70%	-78%	40%	-60%	-32%	-65%

Figure B1 shows the spatial distribution of the DPM10 emission changes. As indicated, the areas around northeastern San Francisco and the Port of Oakland have the greatest decrease in emissions and thus are expected to experience the largest reduction in ambient diesel PM concentrations. The reductions in San Francisco are driven mainly by on-road controls. This figure also shows small increases in recreational marine emissions around the bay and at Lake Berryessa in Napa County.

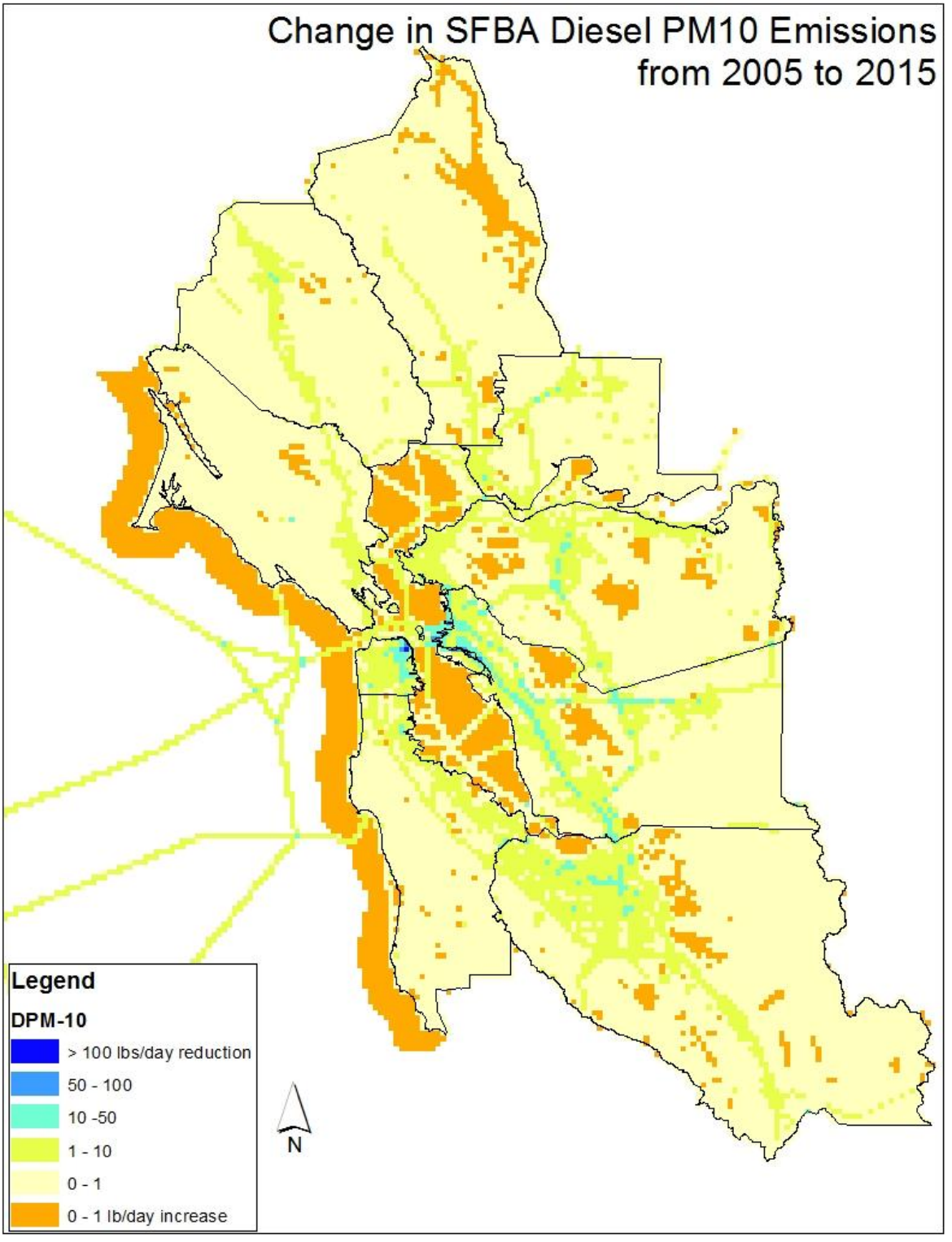

Figure B1**:** Spatial distribution of changes in Bay Area DPM10 emissions from 2005 to 2015.

Table B5 summarizes changes in 1,3-butadiene, acetaldehyde, acrolein, benzene, and formaldehyde emissions by county between 2005 and 2015.

Table B5: Changes in 1,3-butadiene, acetaldehyde, acrolein, benzene, and formaldehyde emissions from 2005 to 2015.

COUNTY	BUTD (lbs/day)	% Change	ACET (lbs/day)	% Change	ACR (lbs/day)	% Change	BENZ (lbs/day)	% Change	FORM (lbs/day)	% Change
Alameda	-183	-36%	-624	-20%	-60	-19%	-845	-42%	-646	-22%
Contra Costa	-142	-46%	-218	-13%	-38	-27%	-633	-37%	-331	-14%
Marin	-51	-44%	-44	-10%	-10	-26%	-223	-41%	-137	-21%
Napa	-34	-41%	-52	-16%	-10	-26%	-145	-38%	-109	-25%
San Francisco	-80	-47%	-51	-6%	-15	-17%	-358	-41%	-208	-21%
San Mateo	-31	-12%	94	11%	67	45%	-368	-33%	312	21%
Santa Clara	-201	-45%	-238	-11%	-36	-16%	-936	-42%	-404	-15%
Solano	-43	-18%	-166	-16%	-17	-7%	-186	-29%	-168	-9%
Sonoma	-78	-51%	-75	-10%	-18	-29%	-344	-47%	-211	-22%
Grand Total	-843	-37%	-1375	-12%	-137	-11%	-4039	-40%	-1901	-13%

Emissions decreased for most toxic air contaminants and in most counties. The most notable exceptions are formaldehyde, acetaldehyde and acrolein in San Mateo County, which significantly increased. These increases are associated with non-road sources, particularly activities at San Francisco International Airport, as depicted in Figure B2. It can therefore be expected that non-cancer (i.e. chronic) risks are increased in the surrounding areas since acrolein is a major driver for chronic risks. Oakland International and San Jose International Airports also show moderate increases (1 to 5 pounds a day).

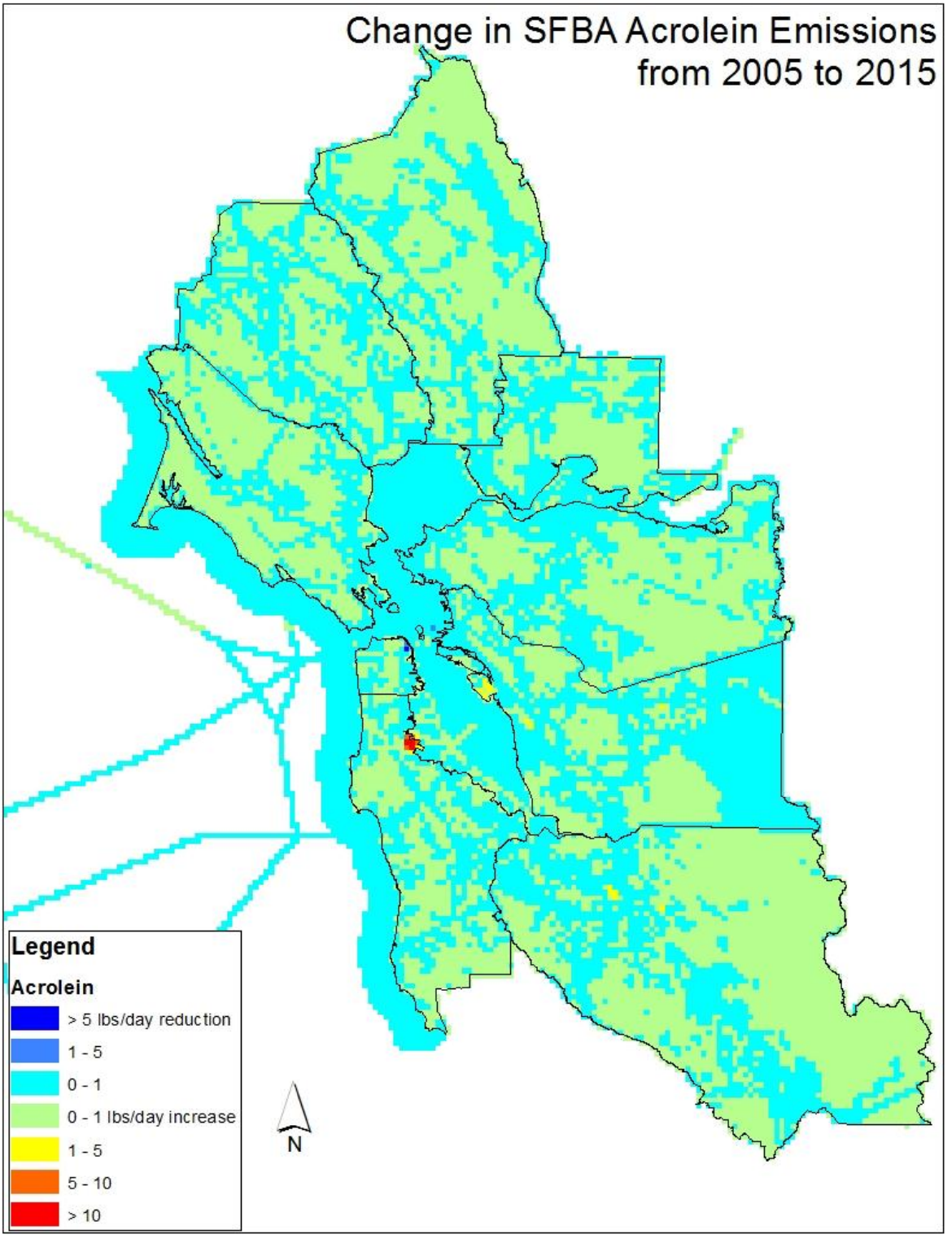

Figure B2: Spatial distribution of changes in Bay Area acrolein emissions from 2005 to 2015.

APPENDIX C

Comparison of 2015 and 2005 Concentrations and Risks

BAAQMD staff previously conducted toxics modeling for 2005, also in support of the CARE program. Results obtained from the previous effort along with model description, emissions inventory, and health risk evaluation are given in Tanrikulu et al., 2009. The only difference between the 2005 and 2015 simulations is the emissions inventory. All other model parameters did not change. Both meteorological and air quality model performance was evaluated for the 2005 case by comparing simulations against observations. Since observations are unavailable for the 2015 case, an air quality model performance evaluation is omitted in the current effort. This appendix contains discussions of the resulting differences in modeled concentrations and health risks. Since differences in health impacts stem both from changing TAC concentrations and population, the effects of changes in the latter alone are also examined.

Figures C1-C3 show differences in DPM concentrations between 2015 and 2005. Negative values depict reductions from 2005 to 2015. With respect to the annual average, the largest difference (a reduction of 6 μg/m3) was found in downtown San Francisco while reductions of 2.5 to 5 μg/m3 were estimated for downtown and West Oakland as well as Emeryville (Figure C1). Reductions of 1 to 2.5 μg/m3 were estimated for the area between Berkeley in the north and Alameda in the south and downtown San Francisco in the west and Piedmont in the east and San Jose. Similar reductions were also estimated along the I-880 corridor. Reductions between 0.25 and 1 μg/m3 were found throughout most of the Bay and along the interstate highways with the exception of a portion of I-280 in San Mateo County. Santa Rosa also saw estimated reductions around 0.25 to 1 μg/m3.

In July, a peak reduction of 3.7 μg/m3 was estimated for a grid cell in downtown San Francisco (Figure C2). Reductions of 1 to 2.5 μg/m3 were found in downtown San Francisco and throughout most of Oakland, Emeryville and Berkeley. Reductions of 0.5 to 1 μg/m3 were estimated for portions of the East Bay from Berkeley to East Oakland and West Oakland in the west to the East Bay Hills and downtown San Jose.

December modeling results showed larger ambient DPM reductions, with a peak reduction of 8.75 μg/m3 occurring within a grid cell in downtown San Francisco (Figure C3). Reductions in cells over West Oakland, Emeryville and downtown San Francisco also reached 7.5 μg/m3. Most of West and North Oakland, downtown San Francisco, and parts of San Jose are expected to experience reductions of 2.5 to 5 μg/m3 while reductions between 1 and 2.5 μg/m3 were found in the greater San Jose area, a strip running along I-880, and the area bounded by Richmond in the north to Hayward in the south and San Francisco in the west to Piedmont in the east. Reductions from 0.25 to 1 μg/m3 were estimated for most of the remaining portions around the bay and along the major interstate routes.

Figures C4-C18 show differences in modeled concentrations of formaldehyde, acetaldehyde, benzene, 1,3-butadiene, and acrolein between 2015 and 2005. Again, negative values mean reductions from 2005 to 2015. Annual formaldehyde showed both increases and reductions in ambient concentrations (Figure C4). The increases occurred at civilian airports, namely San Francisco International, San Jose International and Oakland International airports. The largest increase was found to be around 5 μg/m3 at San Francisco International Airport. Increases of 0.5 to 3 μg/m3 were estimated around San Jose International and Oakland International airports. On the other hand, reductions of 0.2 to 1 μg/m3 were estimated for downtown San Francisco, Emeryville, the area enveloping the eastern span of the Bay Bridge, and along the I-880 corridor in Union City and Fremont.

For July, the largest increases were around the three major airports, with the area around San Francisco International Airport experiencing a 3 μg/m3 increase in formaldehyde (Figure C5). The largest decrease (0.6 μg/m3) was found in the northeast corner of San Francisco while decreases between 0.2 and 0.5 μg/m3 were estimated for Emeryville.

The December scenario is similar to July but with higher magnitudes (Figure C6). The largest increase was 8.5 μg/m3 in the vicinity of San Francisco International Airport with increases of 3 μg/m3 or less at both San Jose International and Oakland International airports. There were also small (mainly 0.2 to 0.5 μg/m3) increases elsewhere, most notably in Marin County around San Rafael and in Santa Rosa. Decreases of more than 1 μg/m3 were present in a grid cell in downtown San Francisco and one in the bay just north of the Bay Bridge's eastern span. Reductions of 0.2 to 1 μg/m3 were estimated for downtown San Francisco, Emeryville, West and East Oakland, the area enveloping the eastern span of the Bay Bridge, and along the I-880 corridor in San Leandro, Union City and Fremont.

Figures C7-C9 show differences in modeled concentrations of acetaldehyde between 2015 and 2005. Again, negative values mean reductions from 2005 to 2015. Annual acetaldehyde showed both increases and reductions in ambient concentrations (Figure C7). The increases occurred at civilian airports, namely San Francisco International and San Jose International airports. The largest increase was found to be 1.7 μg/m3 at San Francisco International Airport. Increases of 0.25 to 1 μg/m3 were estimated around San Jose International Airport and Santa Rosa. One grid cell in downtown San Francisco saw a reduction of 1.6 μg/m3. Reductions of 0.25 to 1 μg/m3 were estimated for downtown San Francisco, West Oakland, Emeryville, the area enveloping the eastern span of the Bay Bridge, and Fremont.

For July, the largest increase was around San Francisco International Airport (0.9 μg/m3) with moderate increases of 0.1 to 0.5 μg/m3 around San Jose and Oakland International airports (Figure C8). The largest decrease (1 μg/m3) was found in the northeast corner of San Francisco while decreases between 0.1 and 0.5 μg/m3 were estimated for Berkeley, Emeryville, Oakland, Palo Alto and south Fremont.

The December scenario is similar to July, but with higher magnitudes (Figure C9). The largest increase was 2.7 μg/m3 in the vicinity of San Francisco International Airport. Other increases of up to 1 μg/m3 occurred at San Jose International Airport and Santa Rosa. There were also small (mainly 0.1 to 0.5 μg/m3) increases elsewhere, most notably in Marin County around San Rafael, around San Jose and Napa. A decrease of 2.3 μg/m3 was present in a grid cell in downtown San Francisco. Emeryville and the area enveloping the eastern span of the Bay Bridge are expected to see reductions of 0.5 to 1 μg/m3. Reductions of 0.1 to 0.5 μg/m3 were estimated for downtown San Francisco, Richmond, Martinez/Benicia, and along the I-880 and I-580 corridors.

The differences in simulated annual average as well as average summer and winter concentrations for benzene are shown in Figures C10-C12, for 1,3-butadiene in Figures C13-C15, and for acrolein in Figures C16-C18.

The difference in cancer risks between 2005 and 2015 is shown in Figure C19. Negative values indicate declining risks from 2005 to 2015. As indicated, the largest reduction in cancer risk was found in downtown San Francisco (1900 per million). Reductions ranged from 600 to 900 per million over Emeryville, downtown Oakland and downtown San Francisco. Reductions between 300 and 600 per million were found over an area stretching from Berkeley in the north to Alameda to the south and downtown San Francisco in the west to Piedmont in the east. This level of reduction in cancer risk was also found along the I-880 corridor and over San Jose. Risk reductions on the order of 150 to 300 were found in an area from Richmond in the north to San Jose in the south and from San Francisco in the west to the Eastbay Hills in the east and along the I-580 corridor. There was a small increase in cancer risk of about 30 per million at San Francisco International Airport.

Figure C20 shows the difference in the expected number of cancer cases based on 2005 and 2015 general populations. The results reflect the change in the expected number of cancer cases due to both concentration differences and population change (i.e., 2005 concentrations and population compared to 2015 concentrations and population). The largest reductions were observed in downtown San Francisco where values peaked between 10 and 25 cases per square kilometer. Reductions of 5 to 10 per grid cell were also found in downtown San Francisco and a few cells in Oakland including downtown. Reductions of 1 to 5 cases per grid cell were found in Richmond, Berkeley, Emeryville, Oakland, eastern San Francisco and Alameda, along the I-880 corridor, and San Jose. There were small increases (1-3 per grid cell) along the Oakland Inner Harbor (near Jack London Square) and in two cells in eastern San Francisco. It is interesting to note that these increases in the number of cancer incidents occurred despite the decrease in cancer risks in these areas. This is because the growth in population projected in these cells outpaces the reductions in emissions and risk.

Figure C21 shows the difference in the expected number of cancer cases between the 2005 and 2015 scenarios for sensitive populations (less than 20 years old and greater than 63 years old). The largest reductions were observed in downtown San Francisco where values

ranged between 5 and 10 cases per square kilometer. Reductions of 1 to 5 per grid cell were also found in downtown San Francisco and a few cells in Oakland, including downtown Oakland. The cell which showed an increase of about 3 in Oakland (for the general population) showed an increase of about 1 with respect to sensitive populations.

Figure C22 shows differences in the expected number of cancer cases between the 2005 and 2015 scenarios assuming 2005 general population for both years. This is an estimate of the change in health outcomes due to changes in concentrations/risks alone. As indicated the largest reductions (15 to 25) were found in downtown San Francisco. These are larger than the differences shown in Figure C20 for the same area. Also, the areas with increasing cancer incidence in Figure C20 did not exhibit appreciable increases in cancer incidence here. At the same time, the area around San Francisco International Airport did not experience appreciable increases in cancer incidence despite the risks being increased (see Figure C19). In summary, these observations illustrate the importance of both the magnitude and location of population growth in determining whether cancer incidence will increase despite the significant reductions in risks. At the projected population growth rate and pattern, it is possible to see increases in cancer incidence even in areas with the most significant reductions in risks. On the other hand, it is possible to avert observable increases in cancer incidence in areas with estimated increasing risks by not locating residential neighborhoods there.

Figure C23 shows differences in the expected number of cancer cases between the 2005 and 2015 scenarios using 2005 sensitive populations for both sets of concentrations. This is similar to the discussion above, particularly for the grid cell directly south of downtown Oakland.

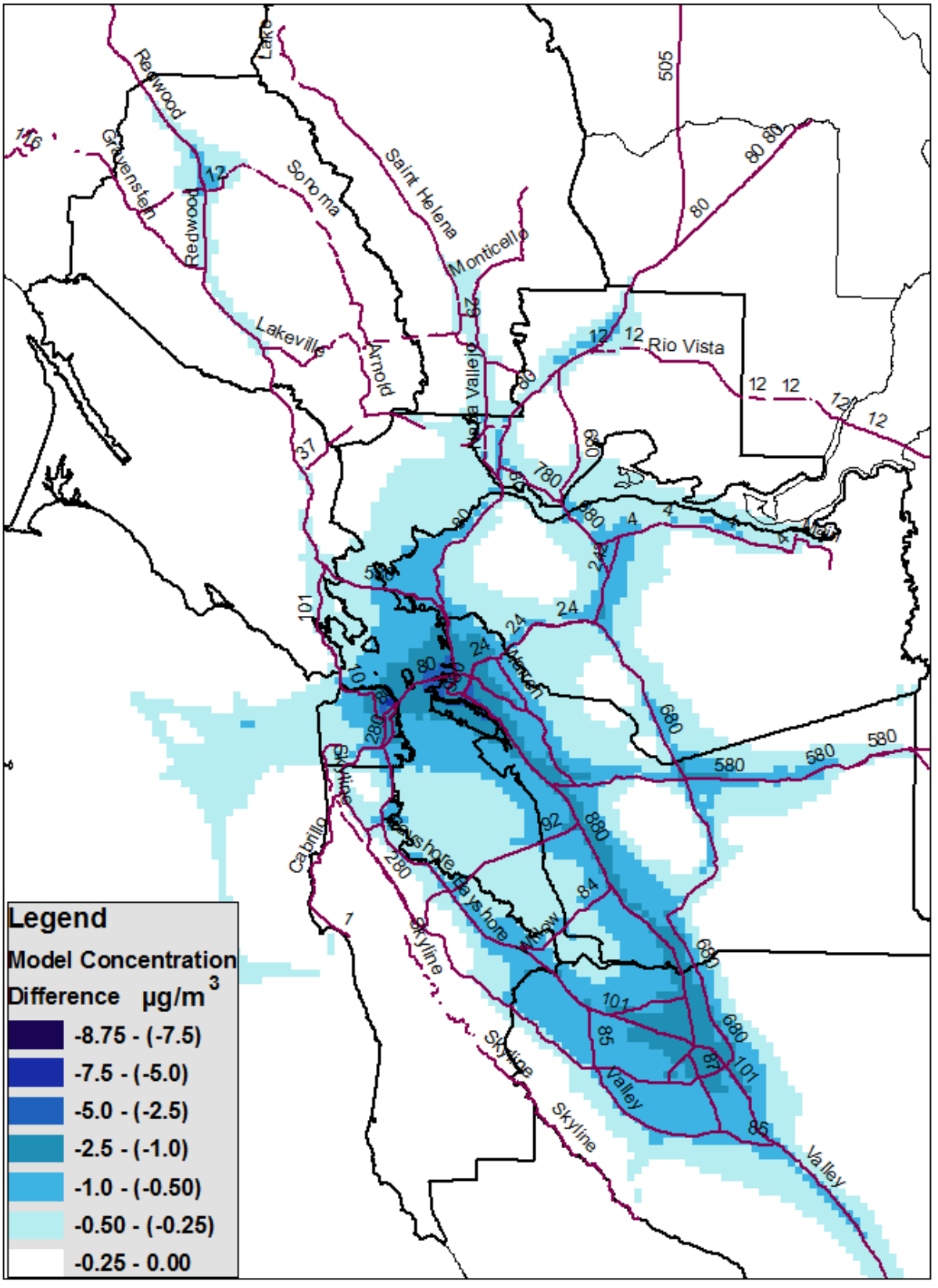

Figure C1: 2015-2005 annual average diesel PM concentration difference.

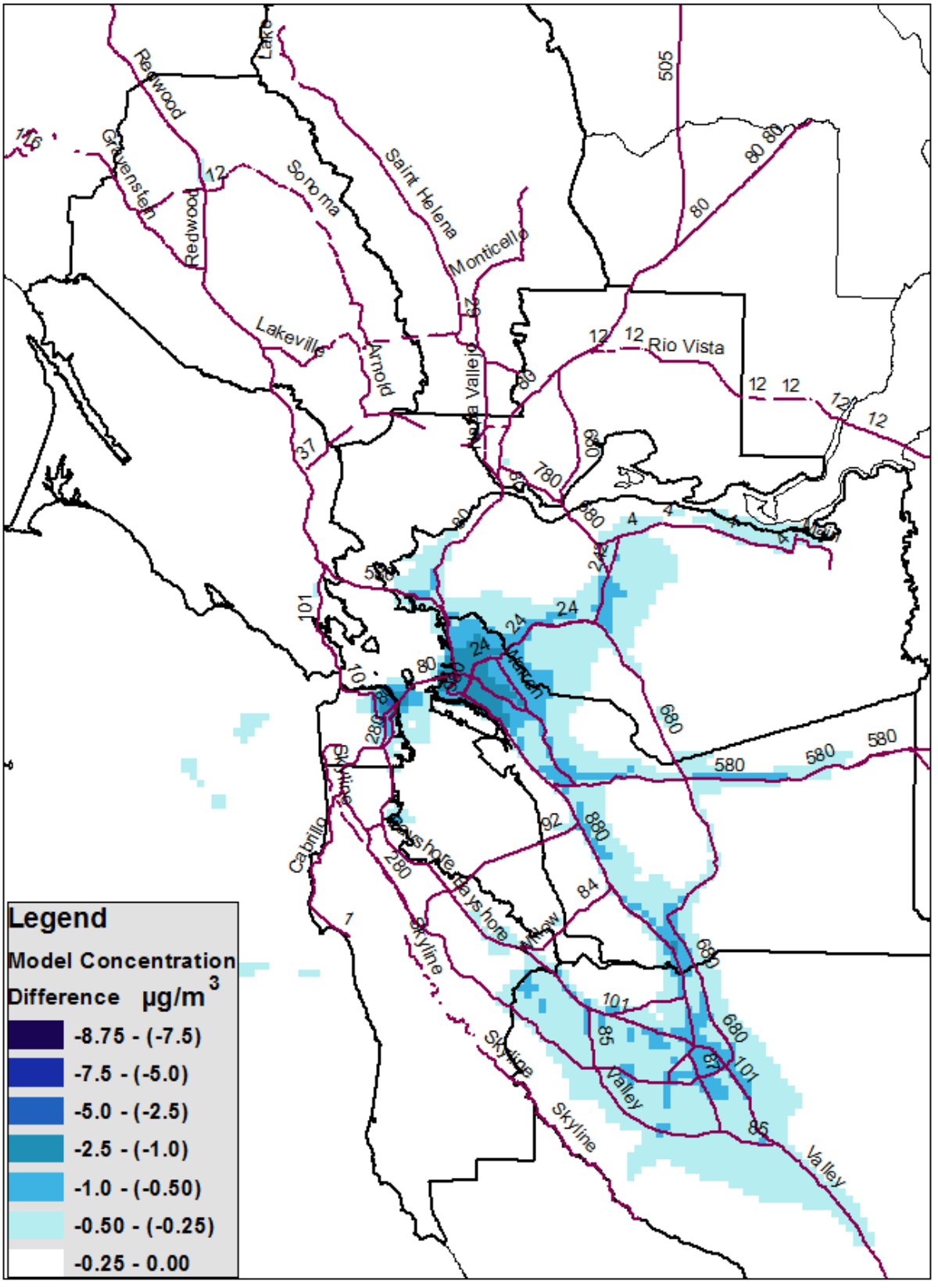

Figure C2: 2015-2005 diesel PM concentration difference for July.

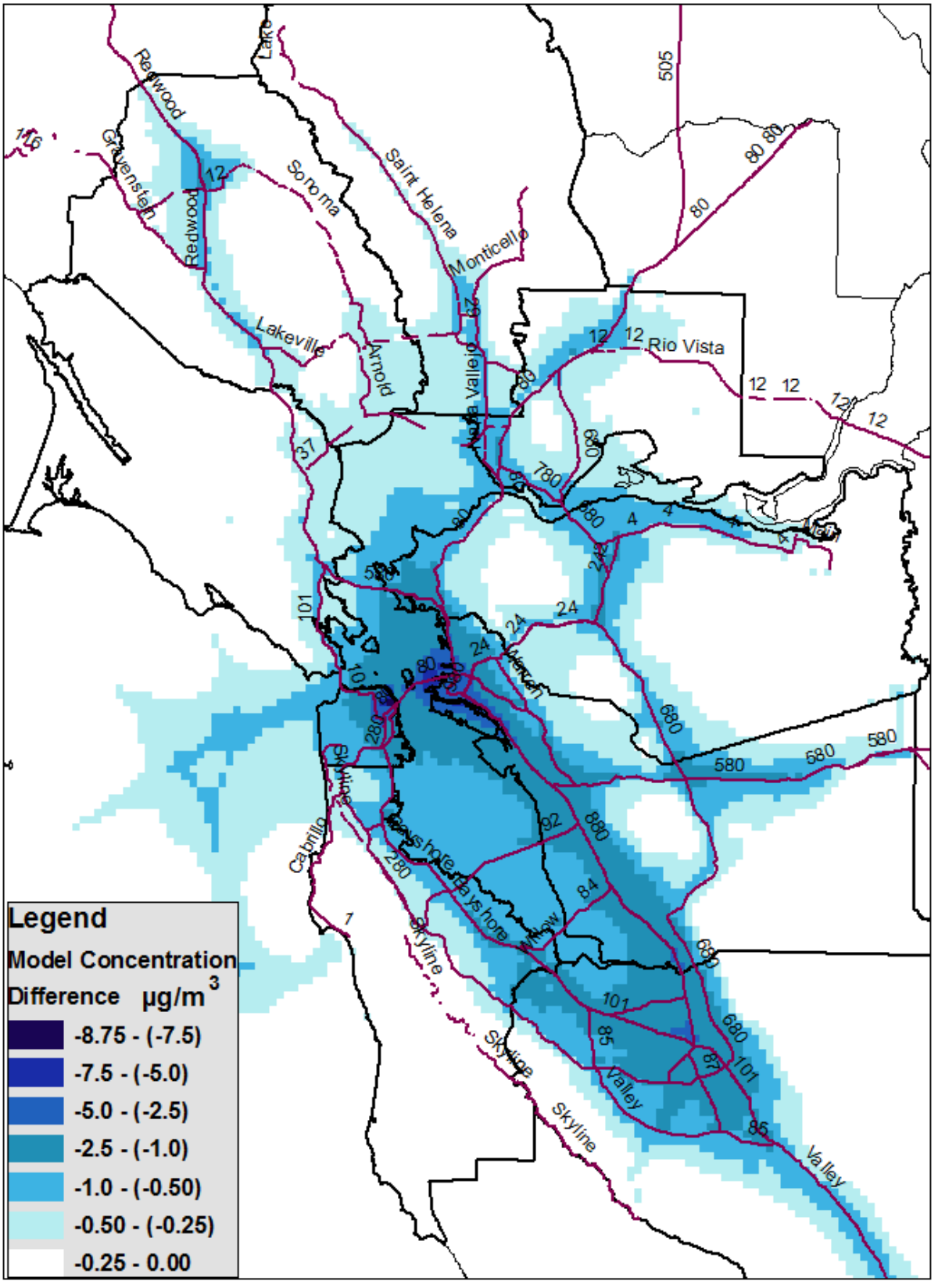

Figure C3: 2015-2005 diesel PM concentration difference for December.

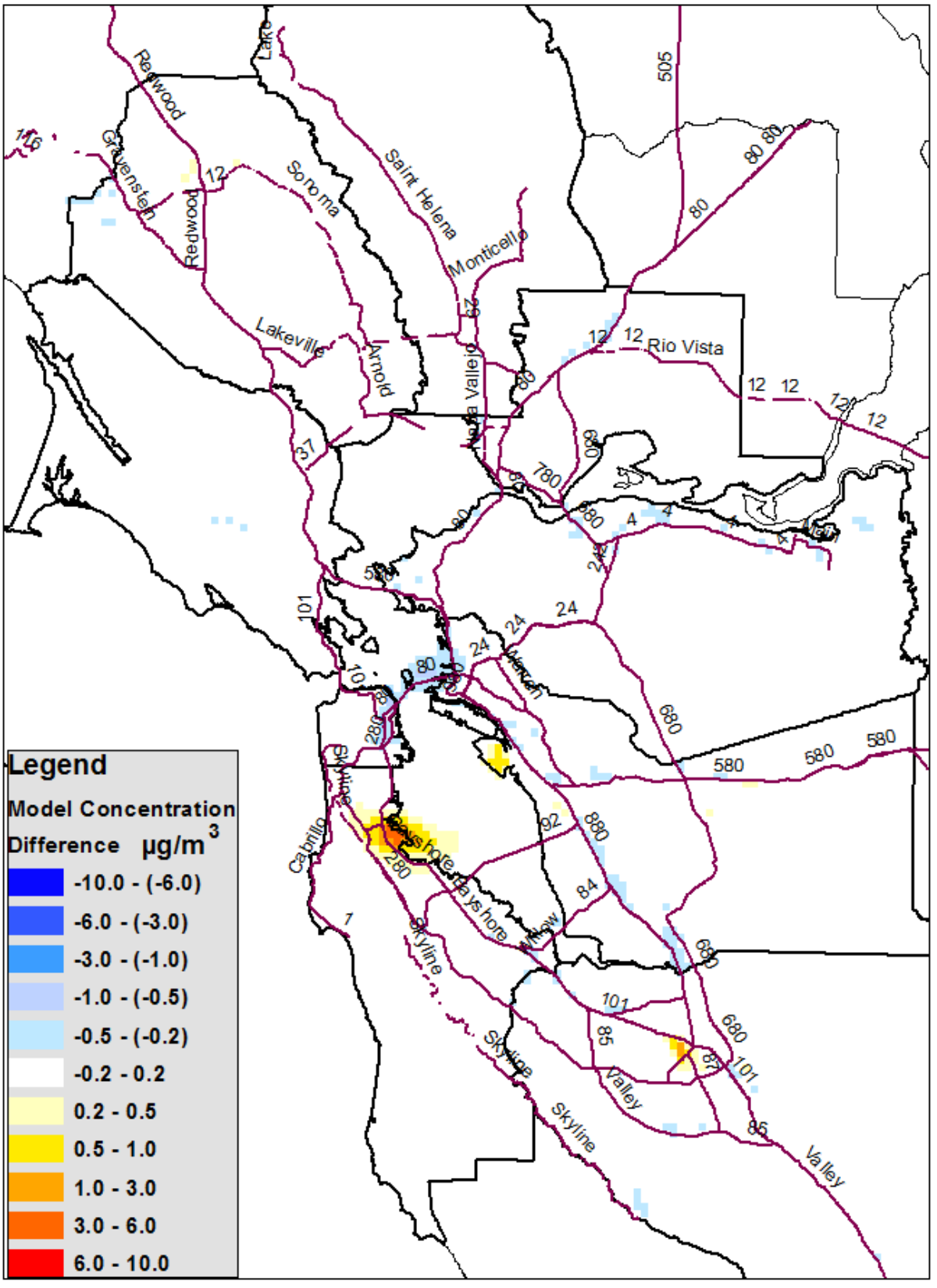

Figure C4: 2015-2005 annual average formaldehyde concentration difference.

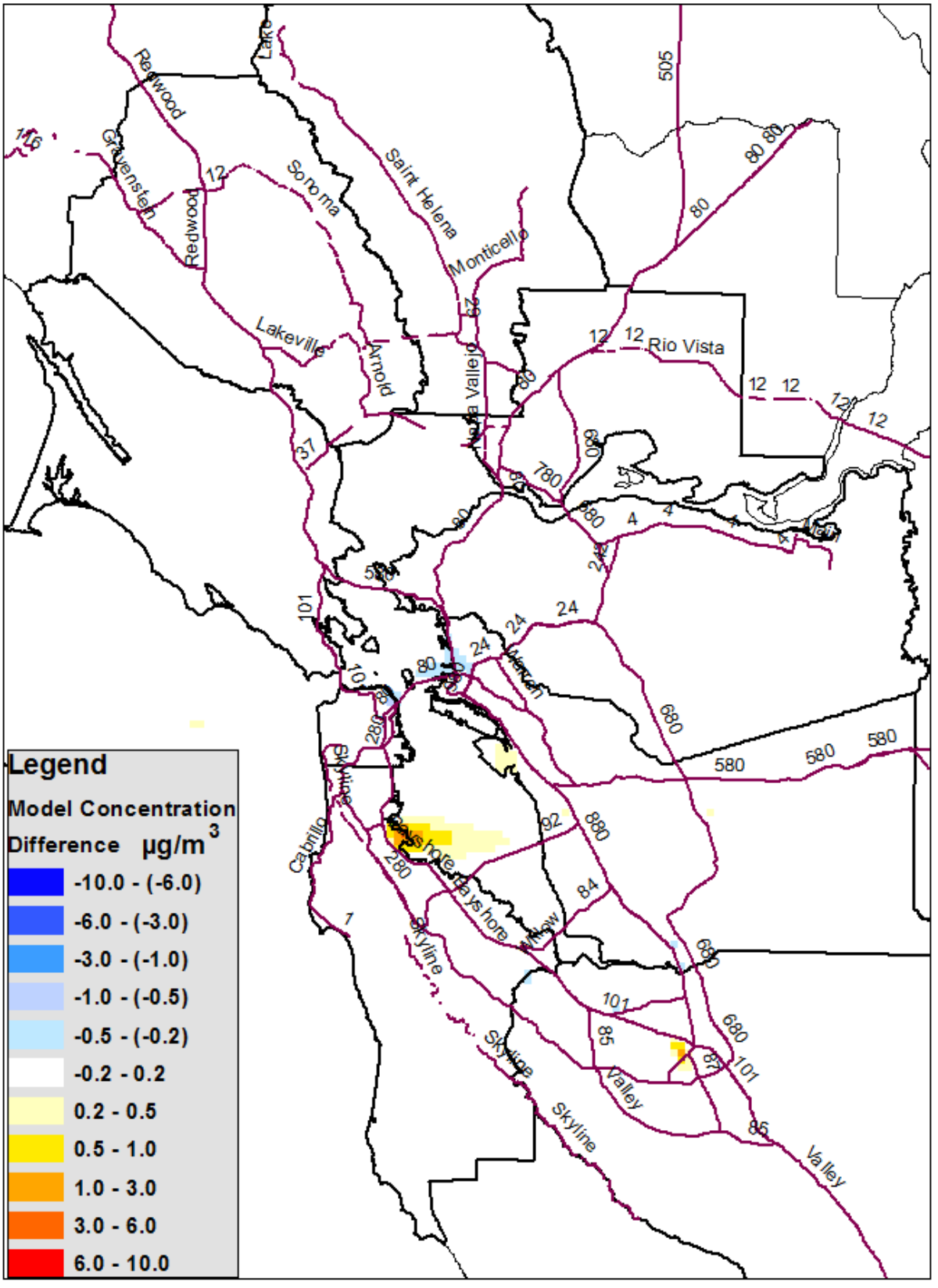

Figure C5: 2015-2005 formaldehyde concentration difference for July.

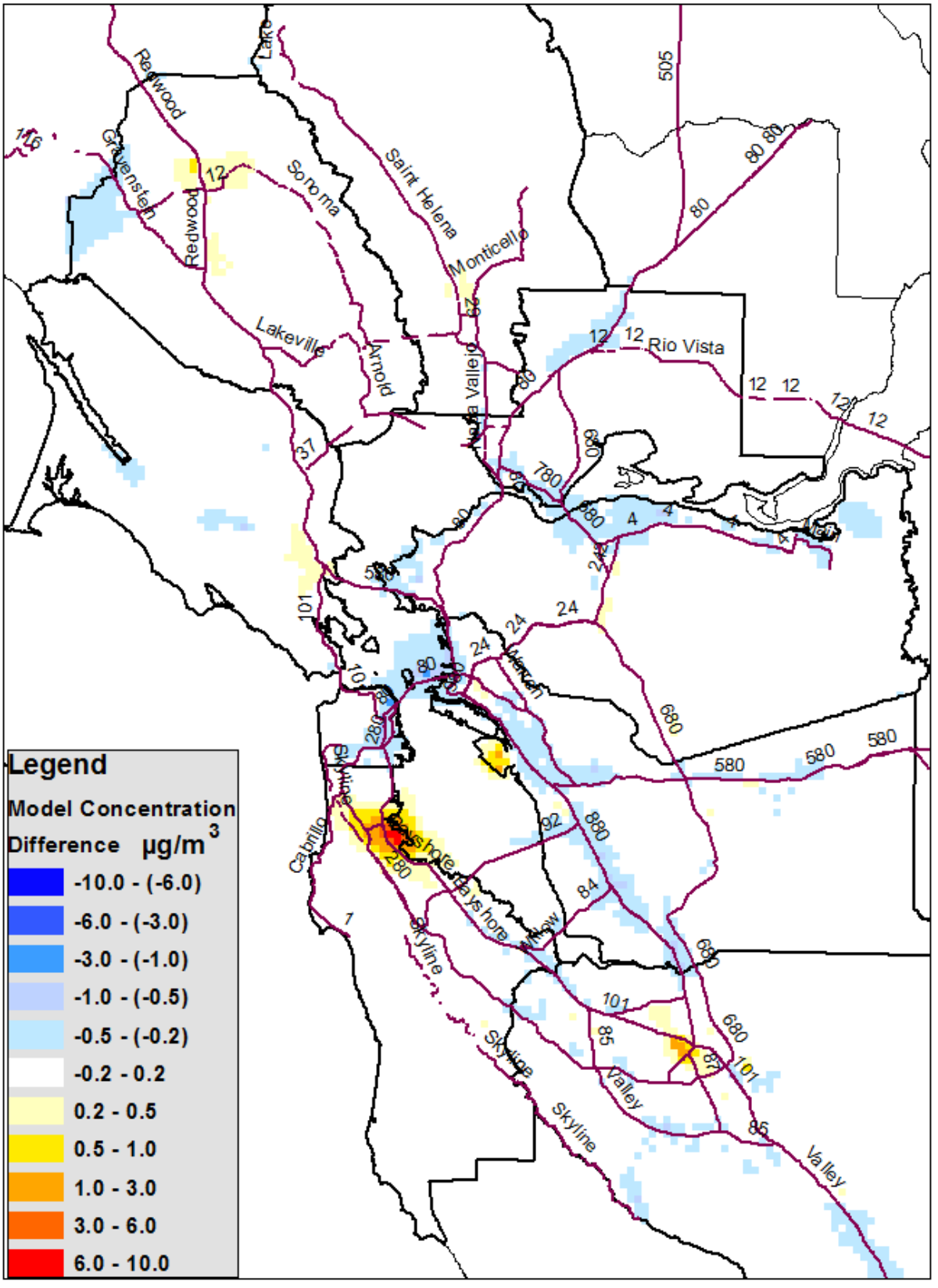

Figure C6: 2015-2005 formaldehyde concentration difference for December.

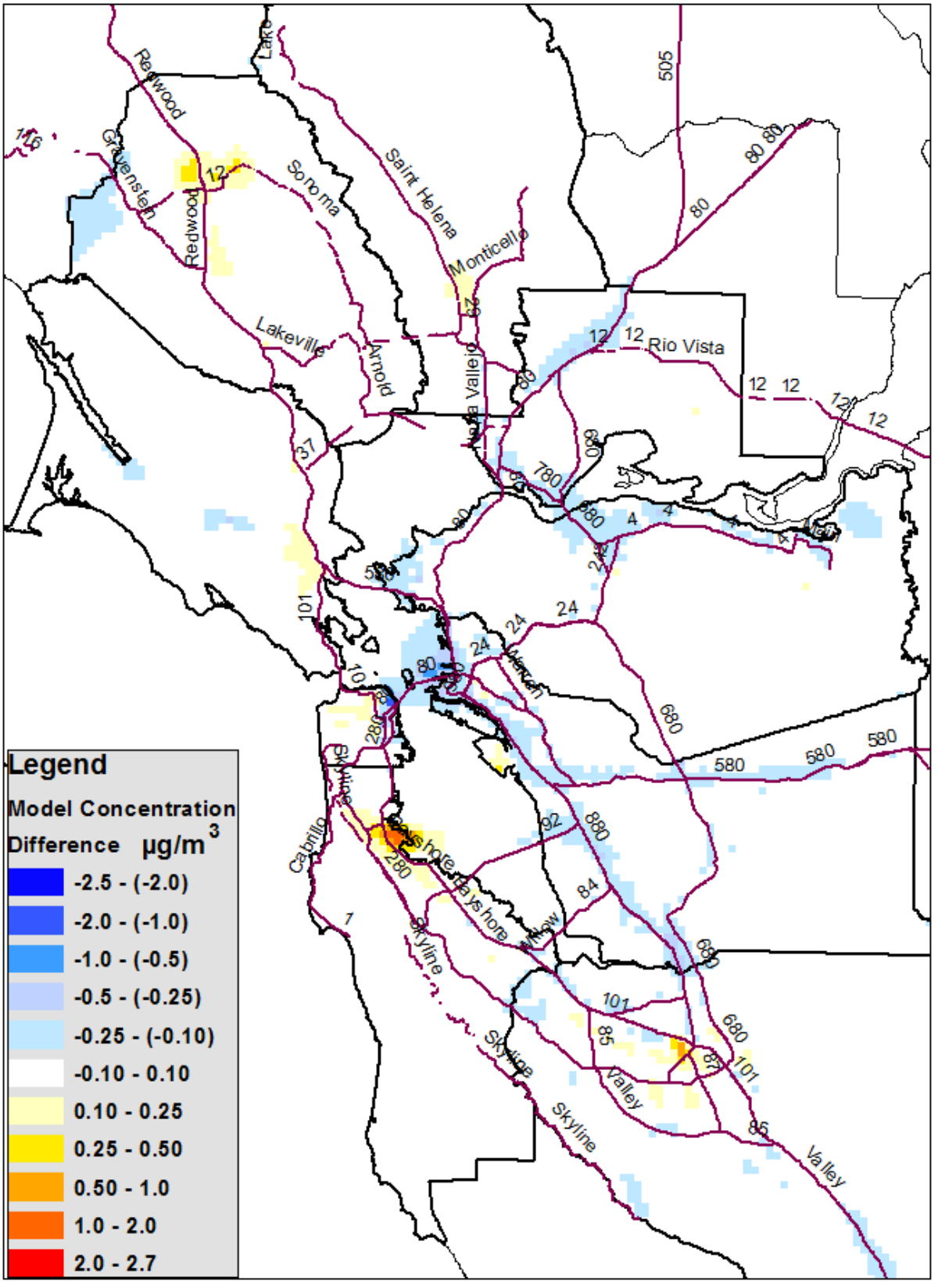

Figure C7:2015-2005 annual average acetaldehyde concentration difference.

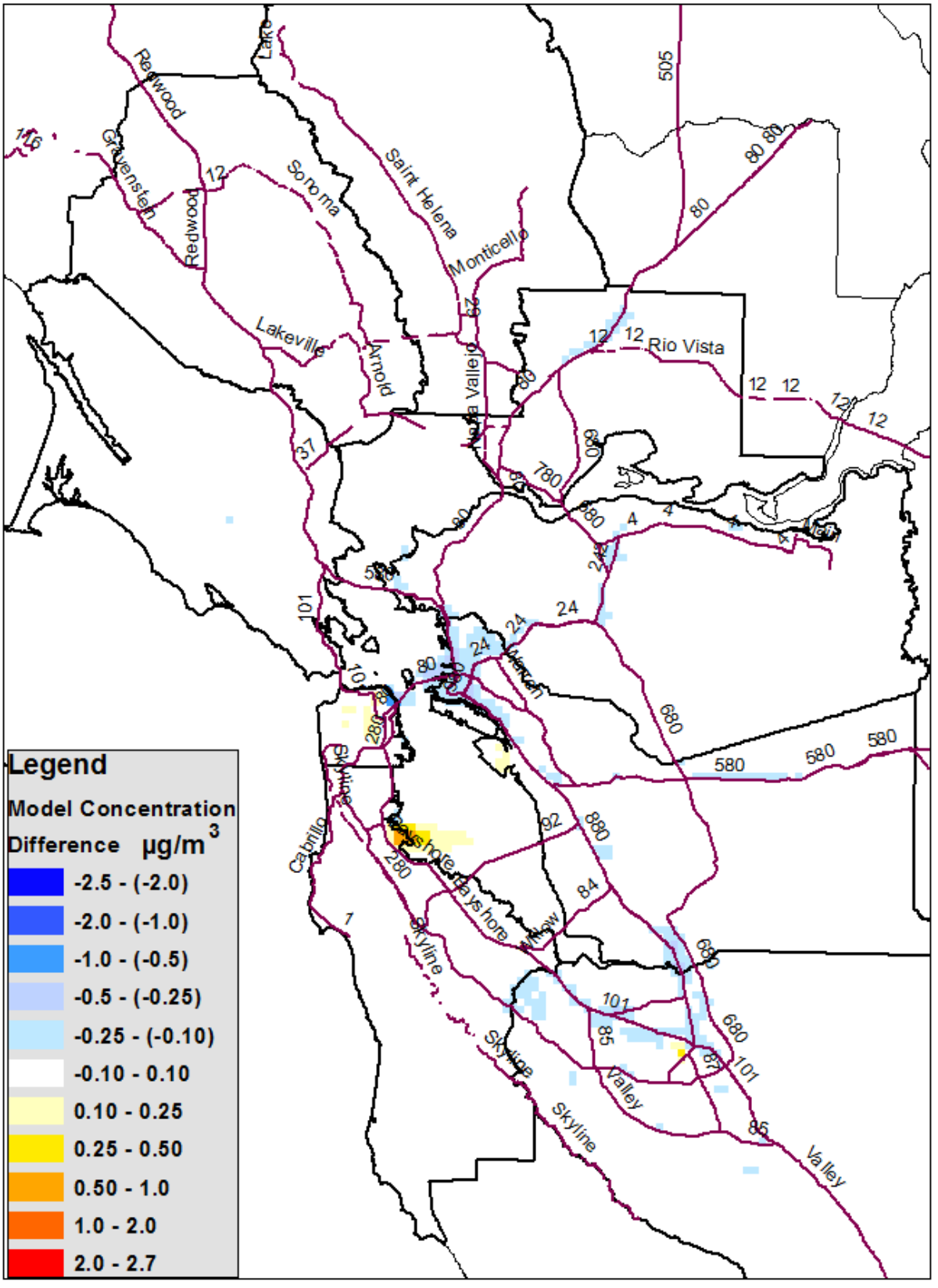

Figure C8: 2015-2005 acetaldehyde concentration difference for July.

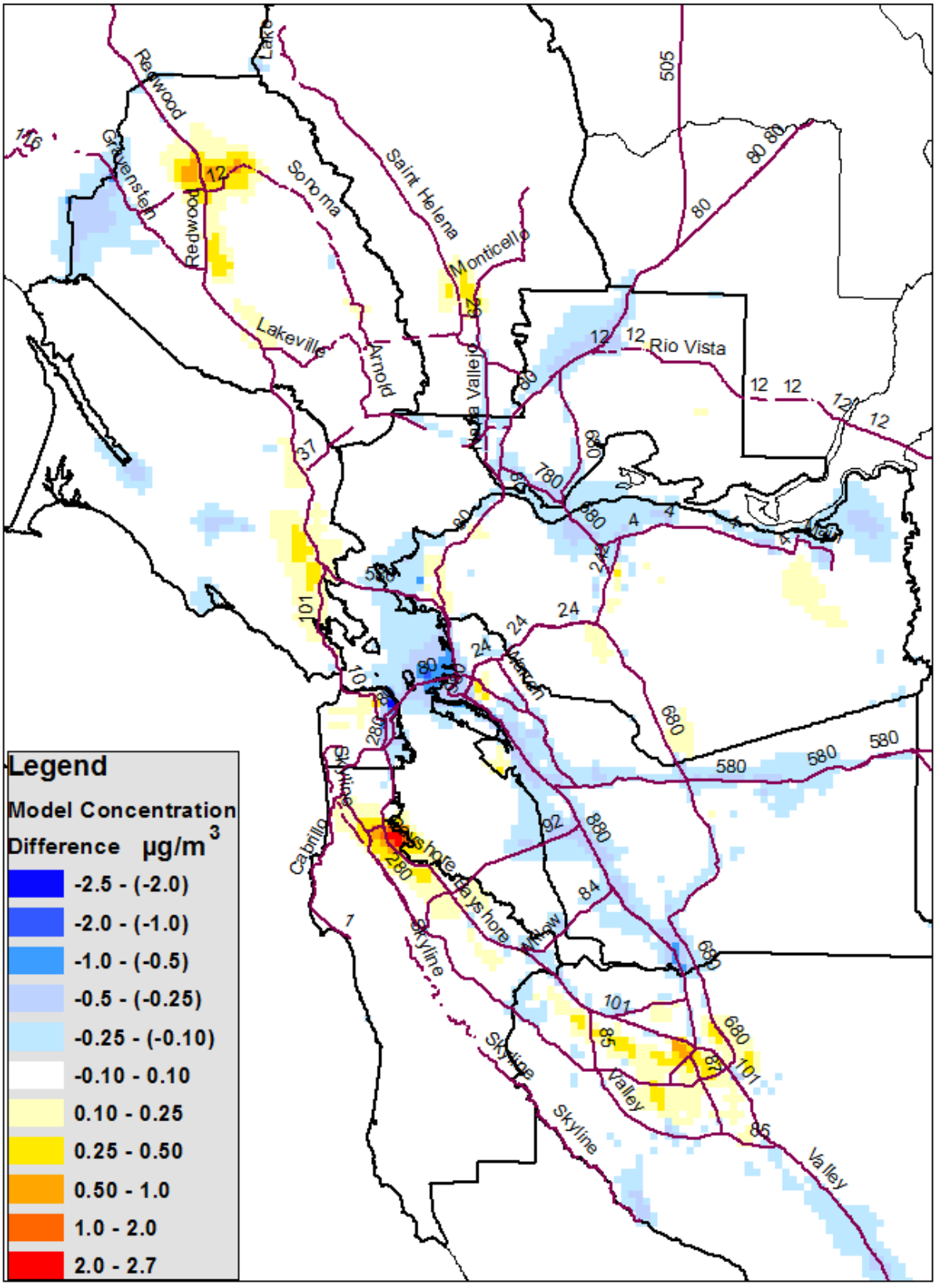

Figure C9: 2015-2005 acetaldehyde concentration difference for December.

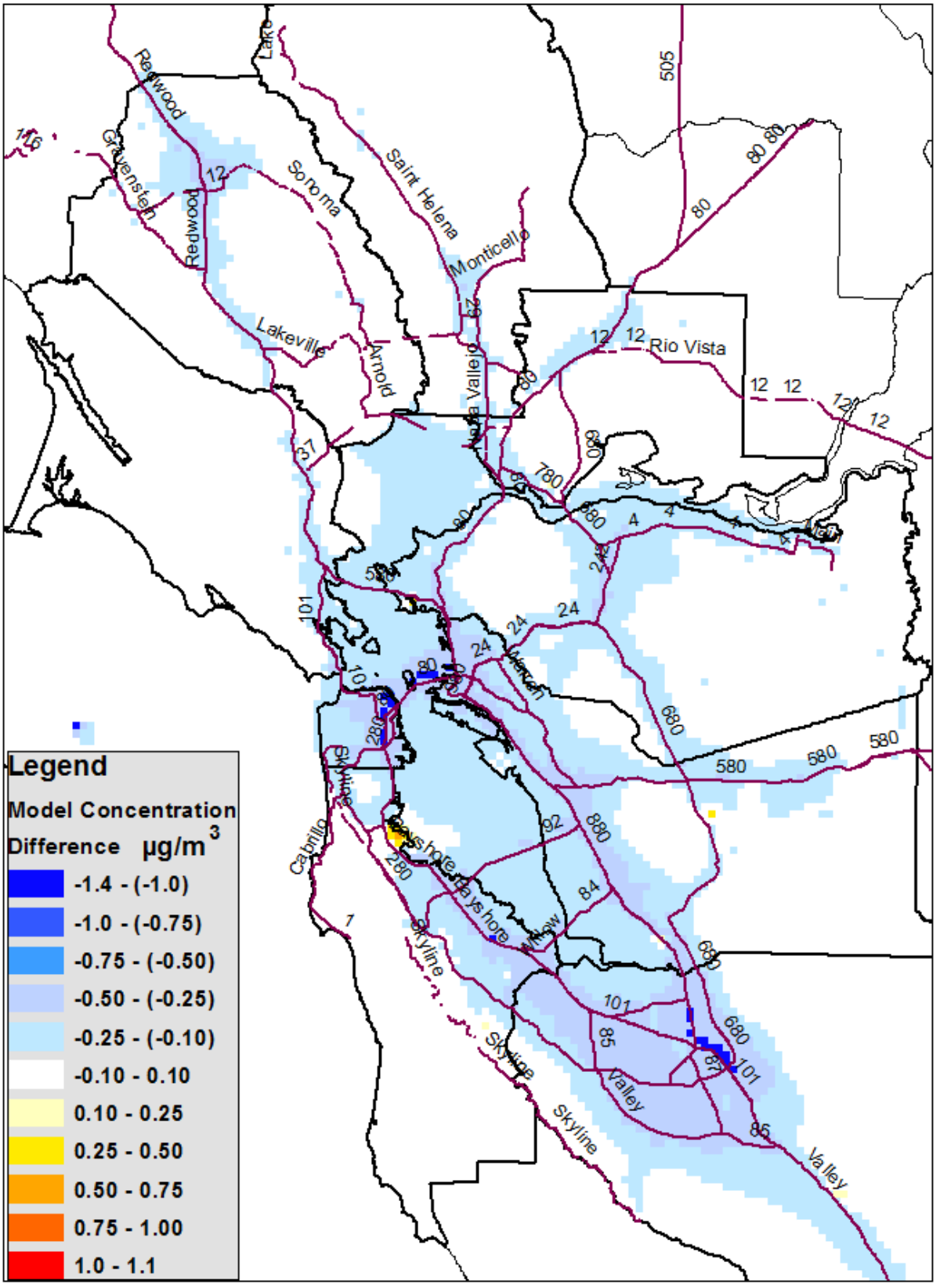

Figure C10: 2015-2005 annual average benzene concentration difference.

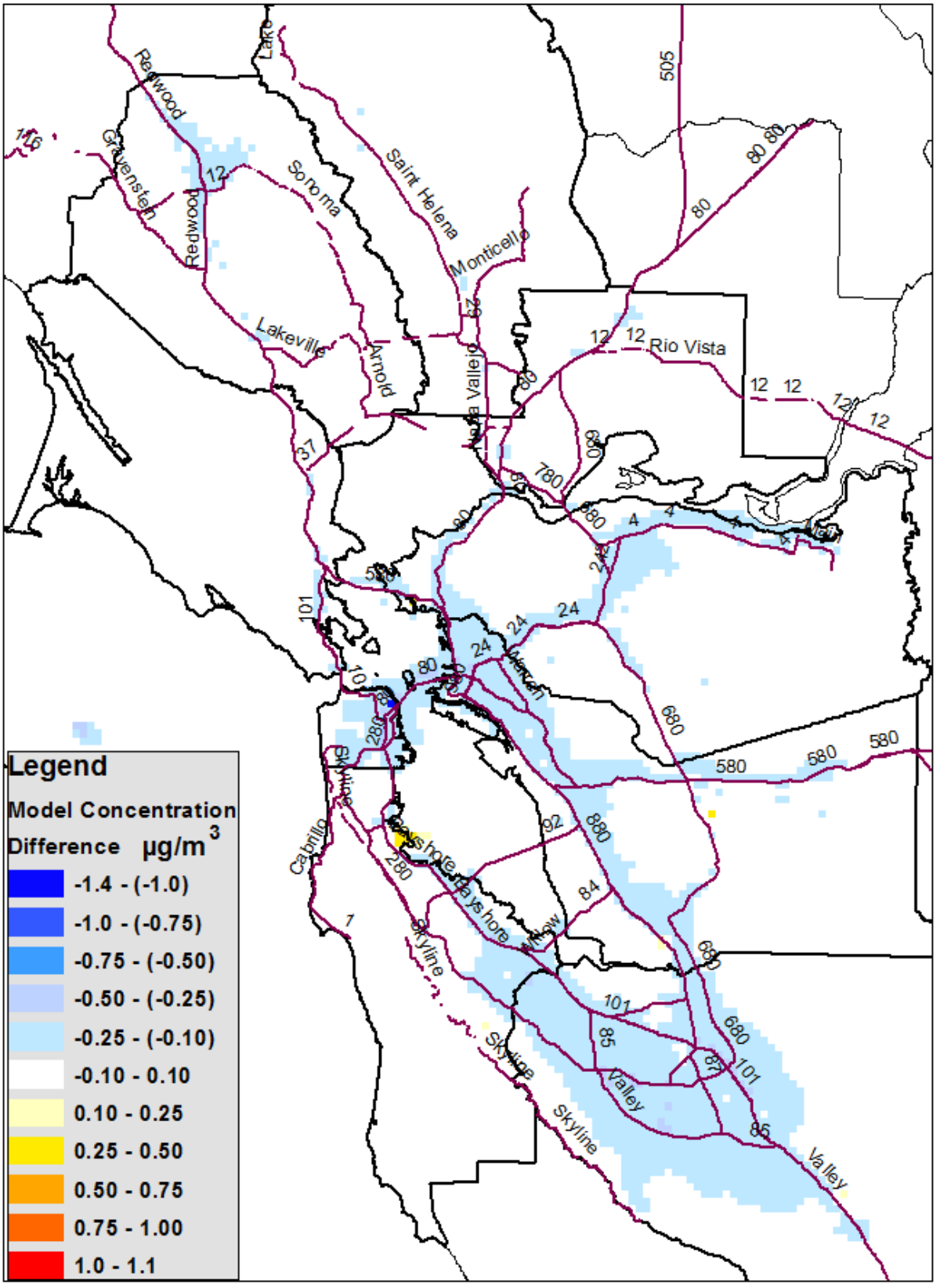

Figure C11: 2015-2005 benzene concentration difference for July.

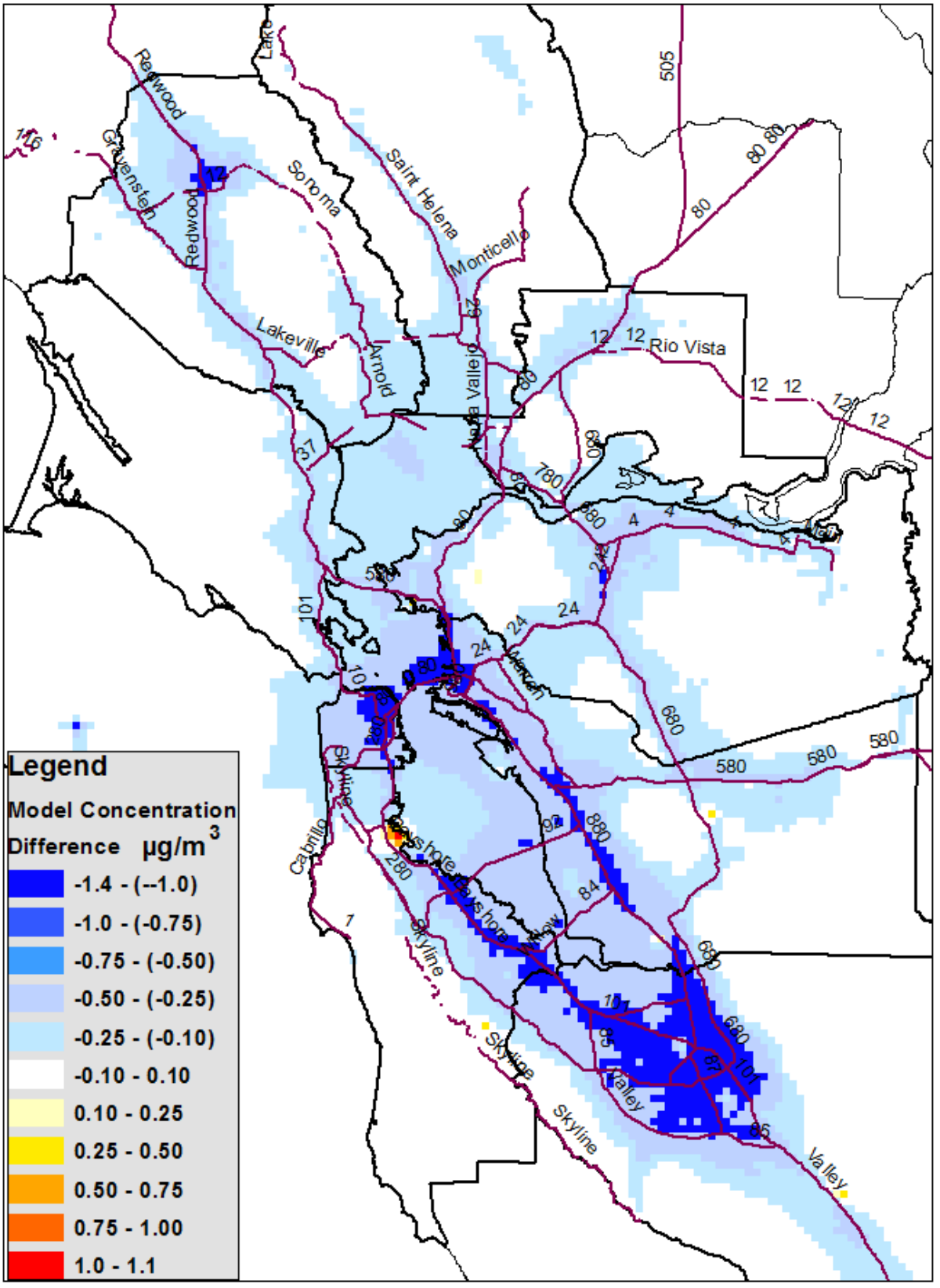

Figure C12: 2015-2005 benzene concentration difference for December.

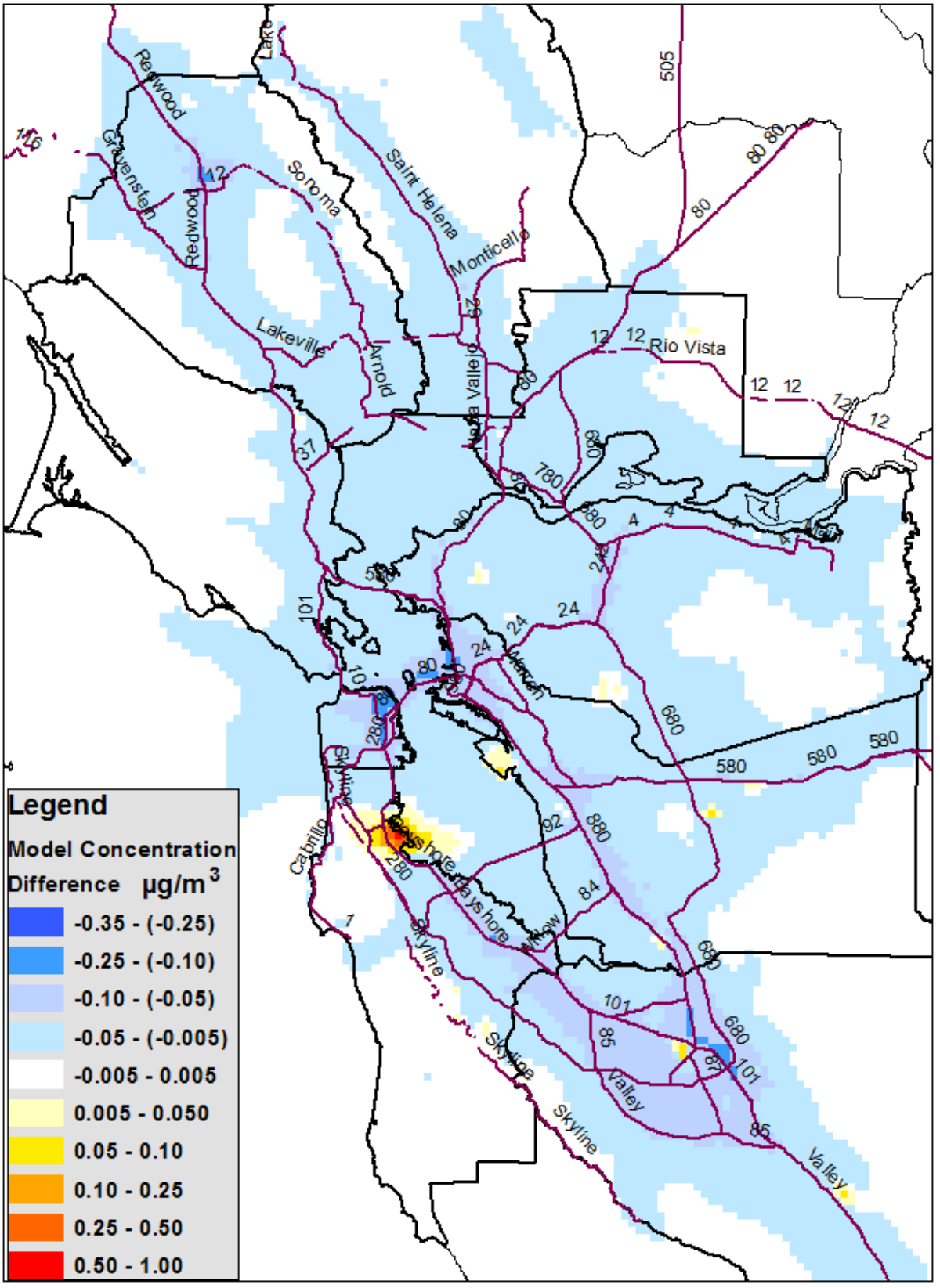

Figure C13: 2015-2005 annual average 1,3-butadiene concentration difference.

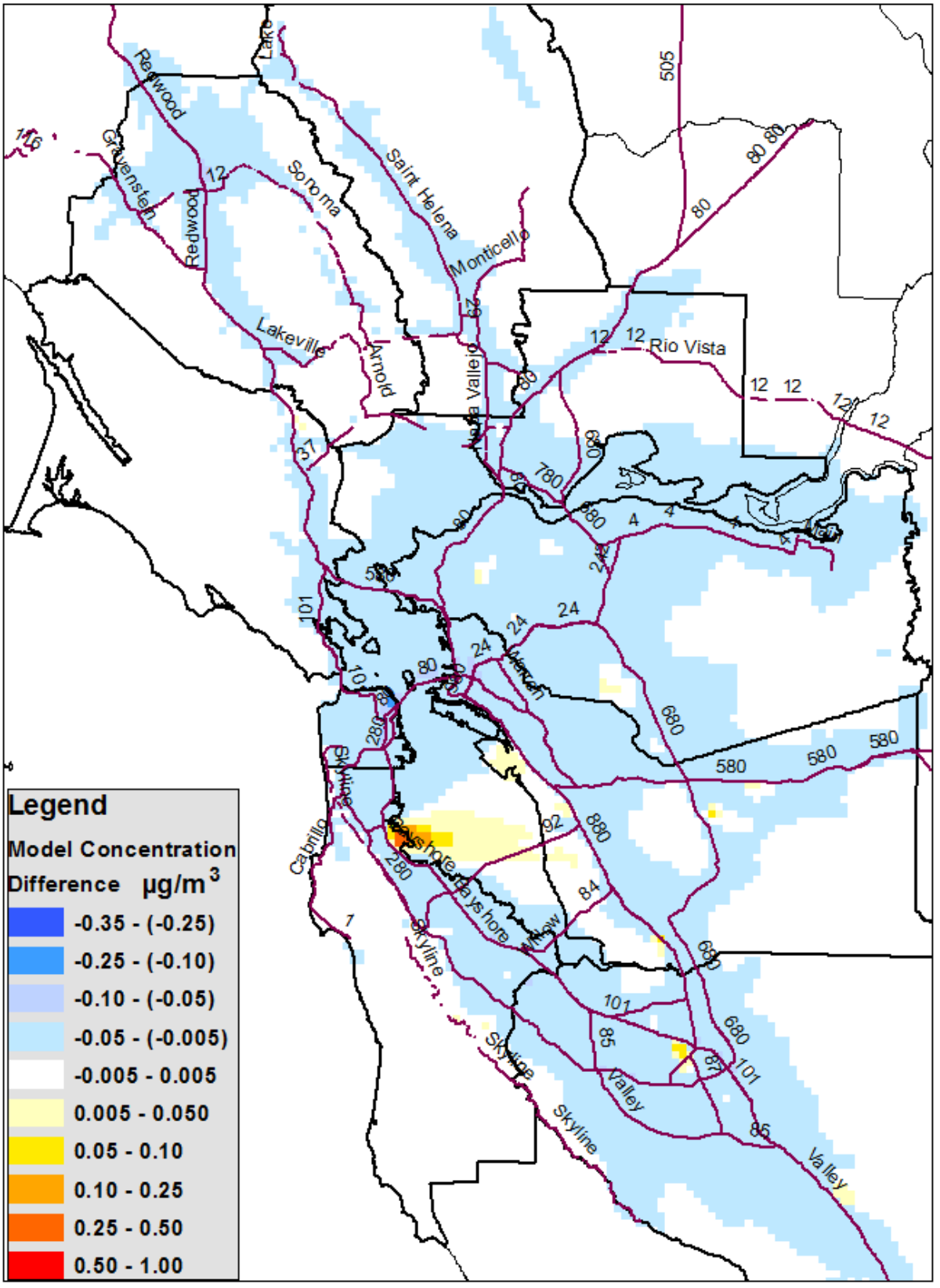

Figure C14: 2015-2005 1,3-butadiene concentration difference for July.

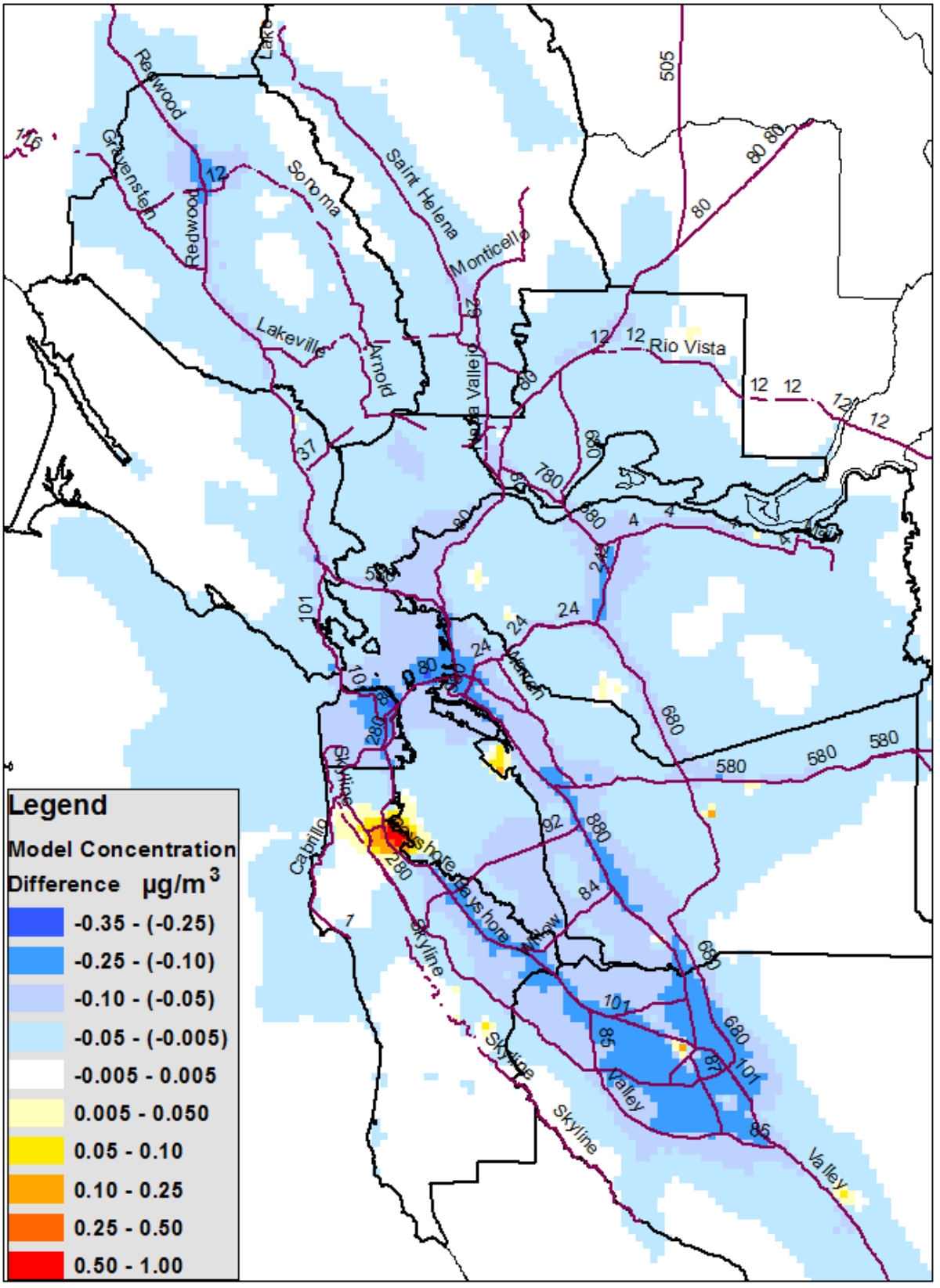

Figure C15: 2015-2005 1,3-butadiene concentration difference for December.

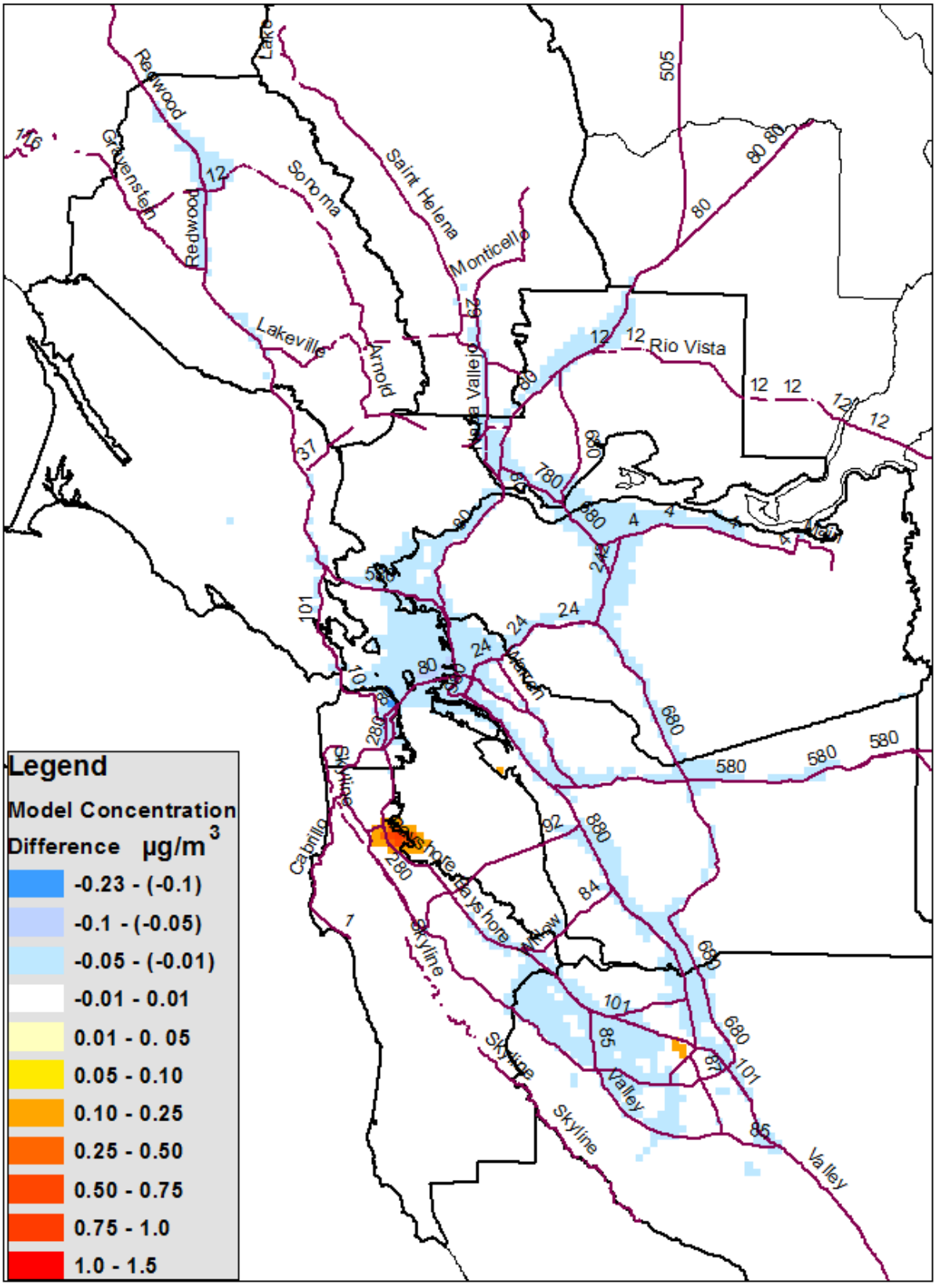

Figure C16: 2015-2005 annual average acrolein concentration difference.

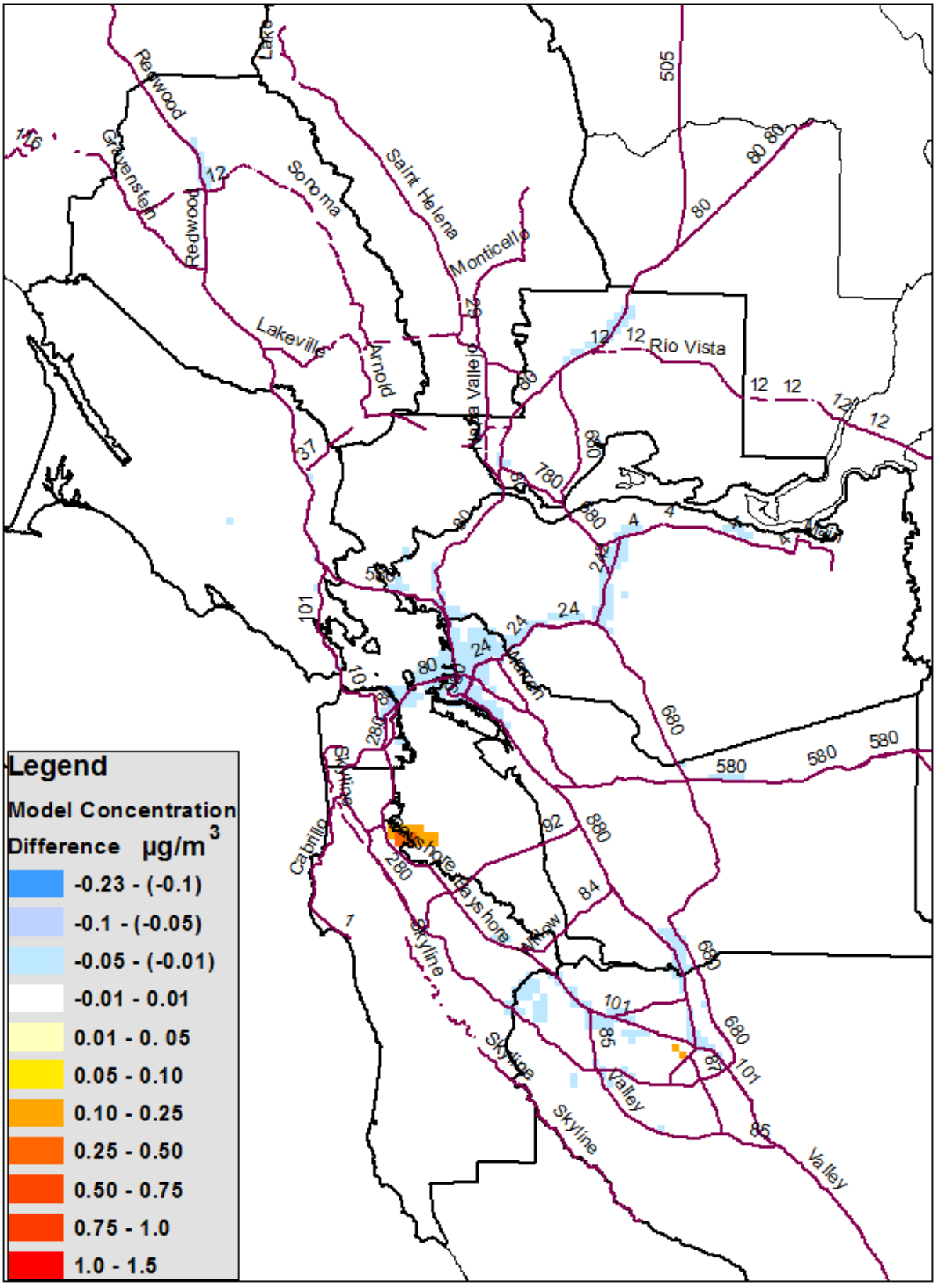

Figure C17: 2015-2005 acrolein concentration difference for July.

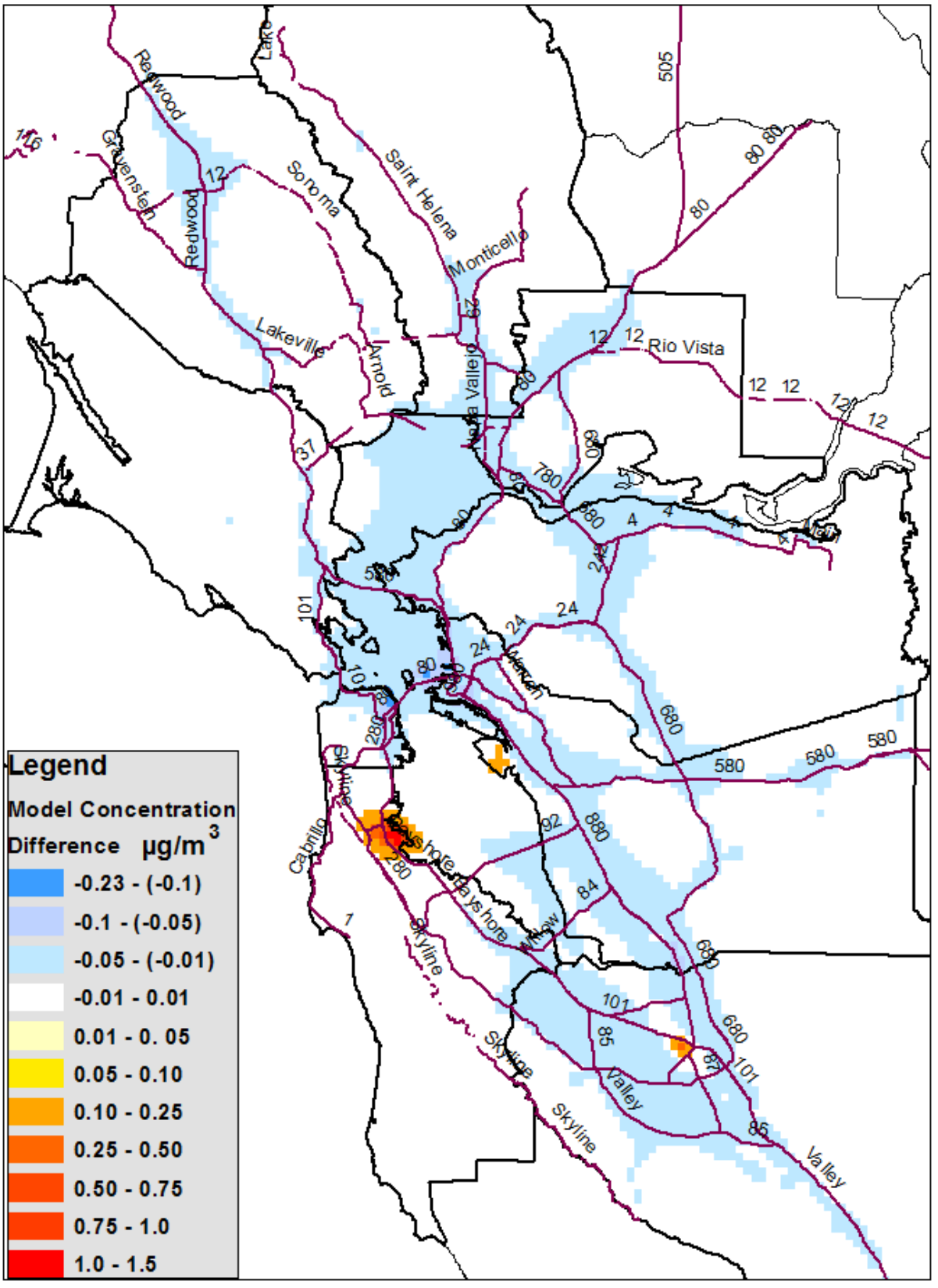

Figure C18: 2015-2005 acrolein concentration difference for December.

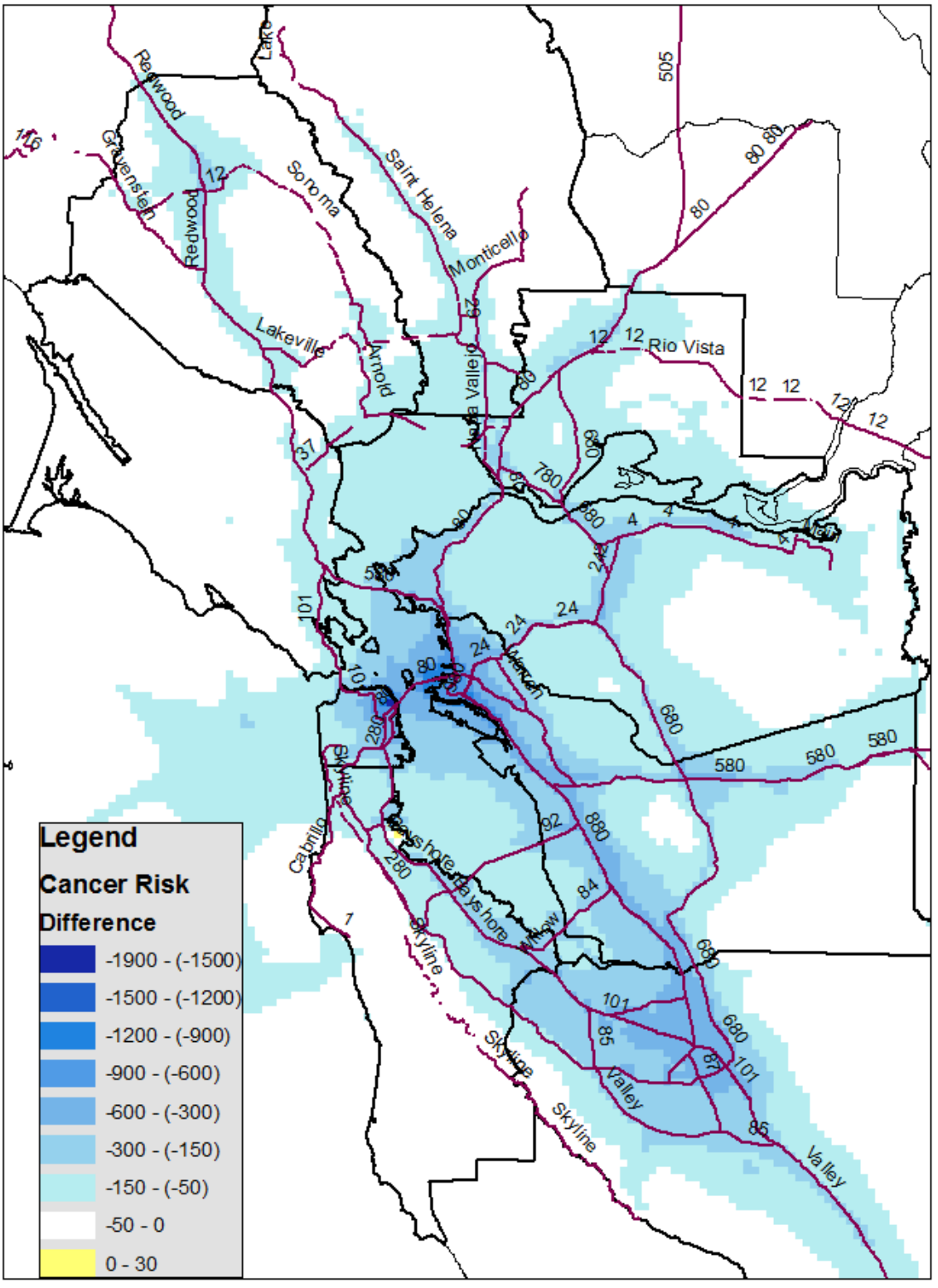

Figure C19: Estimated change in cancer risk (number per million) between 2005 and 2015 from changes in toxic air contaminants.

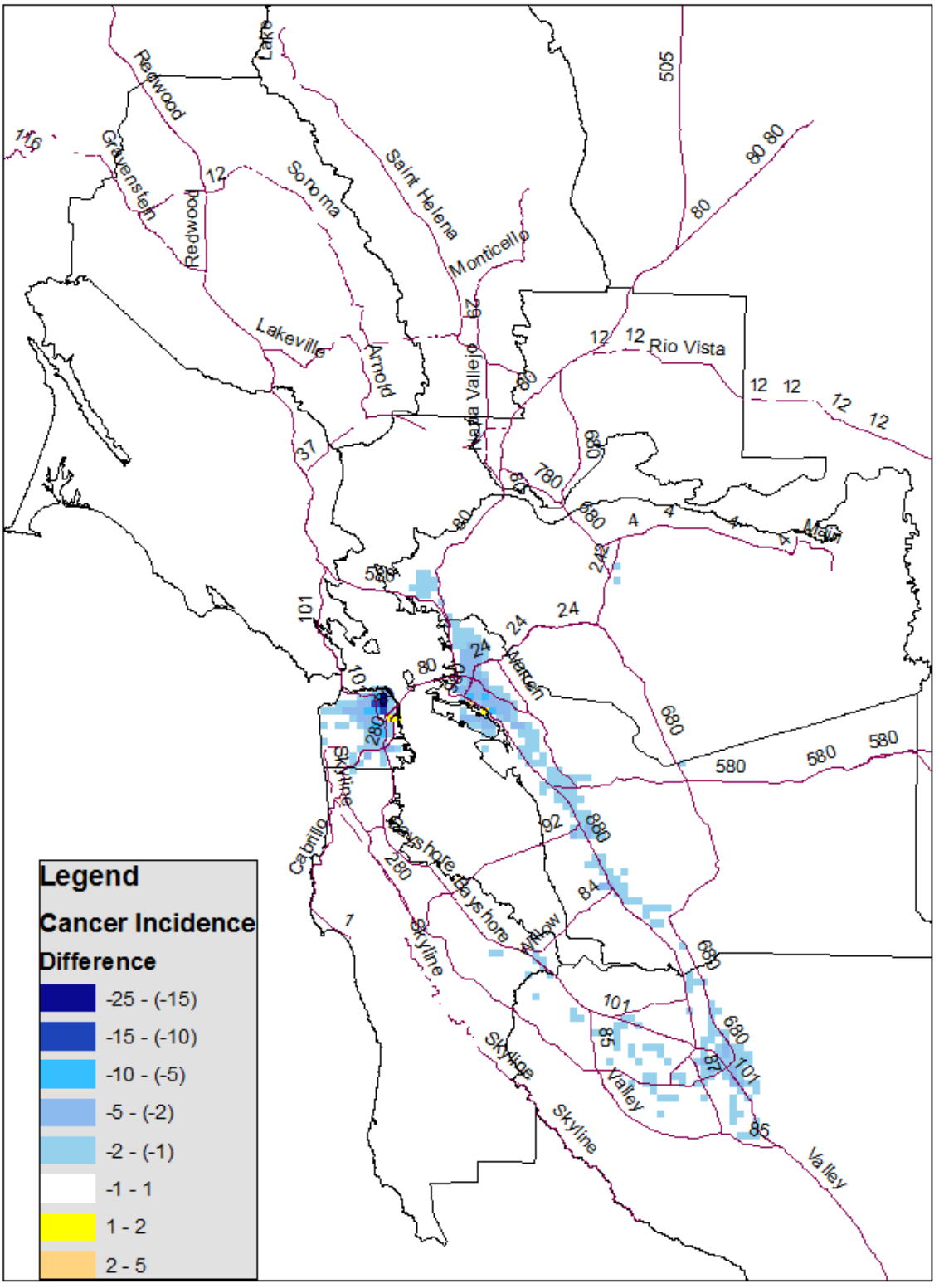

Figure C20: Estimated change in Bay Area cancer incidents between 2005 and 2015. Differences reflect both changes in modeled concentrations of toxic air contaminants and changes in population.

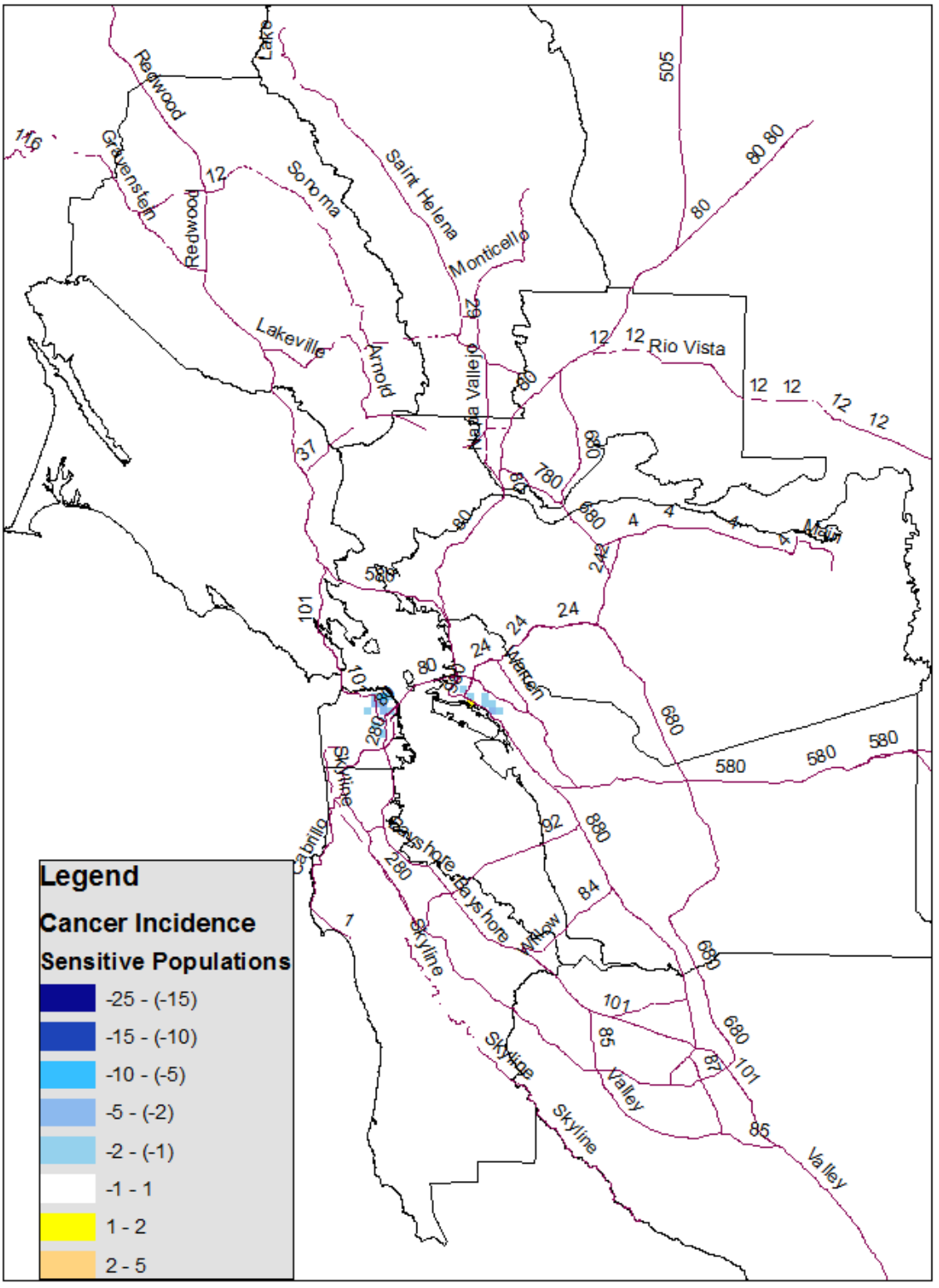

Figure C21: Estimated change in Bay Area cancer incidents between 2005 and 2015 for sensitive populations. Differences reflect both changes in modeled concentrations of toxic air contaminants and changes in population.

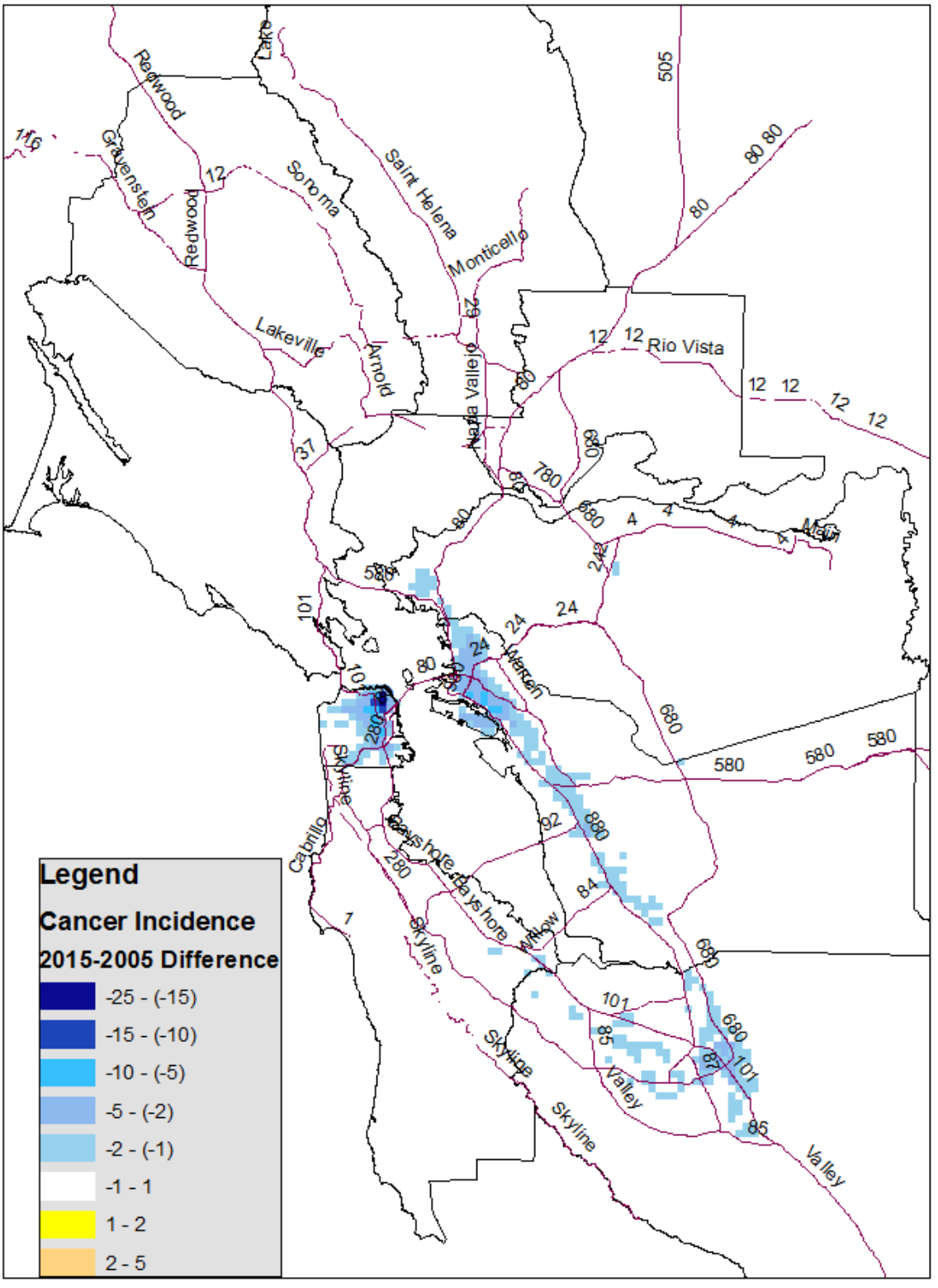

Figure C22: Difference in expected number of cancer incidents between 2005 and 2015, using the 2005 Bay Area general population for both years.

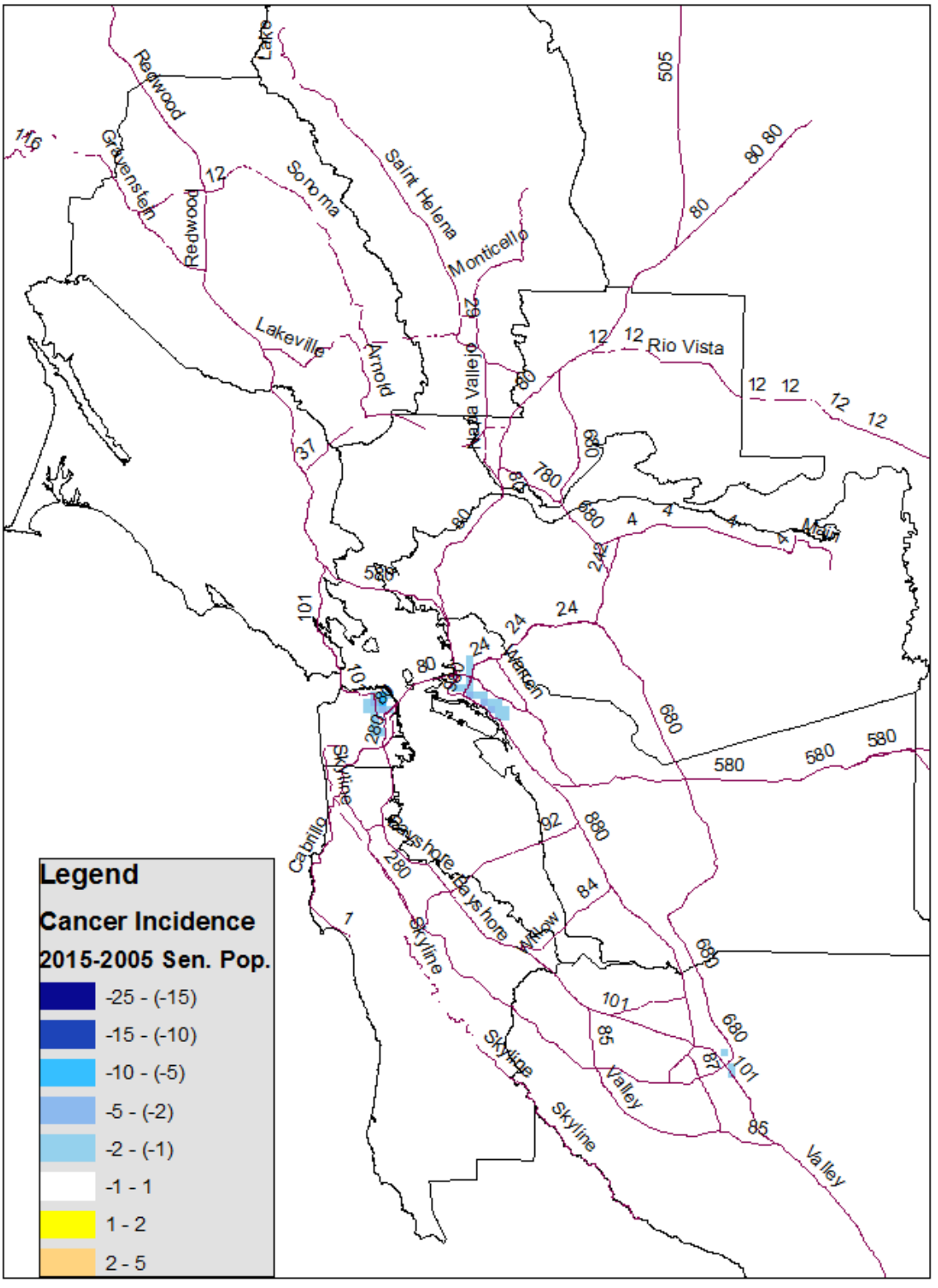

Figure C23: Difference in expected number of cancer incidents between the 2005 and 2015 scenarios, both using 2005 Bay Area sensitive population.